THE USE OF ENVIRONMENTAL ISOTOPES, SOIL WATER MEASUREMENTS AND SOIL WATER MODELLING TO UNDERSTAND TREE WATER USE OF AN *ACACIA MEARNSII* (BLACK WATTLE) STAND IN KWAZULU-NATAL

Andrew Watson

Submitted in fulfilment of the requirements
for the degree of MSc.

School of Agriculture Earth and Environmental Science
University of KwaZulu-Natal
Pietermaritzburg
January 2015

Supervisors: CS Everson, AD Clulow and HH Bulcock

ACKNOWLEDGEMENTS

The author would like to acknowledge the Water Research Commission (Project: K5/2022) and Department of Environmental Affairs, Working for Water Programme for funding of **The long-term impact of *Acacia mearnsii* trees on evaporation, streamflow, low flows and ground water resources. Phase II: Understanding the controlling environmental variables and soil water processes over a full crop rotation**, as well as the NRF for a student scholarship.

DECLARATION

I Andrew Watson declare that

(i) The research reported in this thesis, except where otherwise indicated, is my original work.

(ii) This thesis has not been submitted for any degree or examination at any other university.

(iii) This thesis does not contain other persons' data, pictures, graphs or other information, unless specifically acknowledged as being sourced from other persons.

(iv) This thesis does not contain other persons' writing, unless specifically acknowledged as being sourced from other researchers. Where other written sources have been quoted, then:

(a) their words have been re-written but the general information attributed to them has been referenced;

(b) where their exact words have been used, their writing has been placed inside quotation marks, and referenced.

(v) Where I have reproduced a publication of which I am an author, co-author or editor, I have indicated in detail which part of the publication was actually written by myself alone and have fully referenced such publications.

(vi) This thesis does not contain text, graphics or tables copied and pasted from the Internet, unless specifically acknowledged, and the source being detailed in the thesis and in the References sections.

Signed: AWatson

Supervisor:

Co-supervisor:

ABSTRACT

In Southern Africa commercial afforestation is an important agricultural activity and accounts for a large portion of the gross agricultural production, However, there are concerns regarding its possible detrimental impact on the hydrological system. Previous research in the Two Streams catchment by Clulow *et al*. (2011) showed that a commercial forestry species (*Acacia mearnsii)* was using more water than available through precipitation over a 30-month period (total evaporation was greater than rainfall) and they concluded that the trees were drawing water from another source.

In this study, field measurements of stable isotopes of rainfall, soil water, stream water and groundwater were collected and analysed in order to understand the deficit in the water balance identified by Clulow *et al*. (2011). Experimental apparatus was used to extract isotopes from soil water. Automated rainfall and streamflow samples were used to sample rainfall and stream water (evaporation seals were designed to prevent fractionation). A specific set of criteria was used to program the automated rainfall sampler to better differentiate between event samples. HYDRUS 1-D model outputs of simulated total evaporation and soil water fluxes were verified from total evaporation and soil water measurements at the site.

Rainfall varied in isotope signature throughout the year ranging from -150 to -15 permil (δ^2H) and -20 to 2 permil ($\delta^{18}O$), these values were largely dependent on rainfall volume. Groundwater isotope composition signature changed only slightly throughout the year ranging from -12 to -5 permil (δ^2H) and -4 to -1.5 permil ($\delta^{18}O$), with seasonality being the driving variable. The results from the isotope signatures showed that the main contributor to streamflow (-15 to -1.5 permil (δ^2H) and -4.5 to -1.5 permil ($\delta^{18}O$)) was groundwater. Soil isotope signatures varied with depth and season, ranging from -25 to -8 permil (δ^2H) and -1.5 to 4 permil ($\delta^{18}O$). Groundwater signatures were evident on three occasions within the soil horizon (2.0 m and 2.4 m on 23/08/2013 and 1.6 m on 13/0/2013), where water was moved by hydraulic lift or capillary rise and made available for uptake by rooting systems. This was confirmed by Watermark and TDR-100 measurements, where there were upward fluxes of deep soil water during the dry season. HYDRUS-1D results suggested that simulated total evaporation (1052 mm) was similar to measured actual evaporation (1095 mm) during the wet season and dry season.

The results conclude that the *Acacia mearnsii* trees extracted soil water or deep groundwater during the dry season, which allows for continuous growth throughout the year. This supports the conclusion of Clulow *et al*. 2011 and confirms that commercial forestry could have significant long-term impacts on catchment hydrology, particularly in dry season low flows.

TABLE OF CONTENTS

LIST OF ACRONYMS

FAO- Food and Agriculture Organisation of the United Nations
SFRA- Streamflow Reduction Activity
DWA- Department of Water Affairs
SPAC- Soil Plant Atmospheric Continuum
SMOW- Standard Mean Ocean Water
NBS1- US National Bureau of Standards
IAEA- International Atomic Energy Agency
VSMOW- Vienna Standard Mean Ocean Water
GMWL- Global Meteoric Water Line
LMWL- Local Meteoric Water Line
MAP- Mean Annual Precipitation
ASCE- American Society of Civil Engineers

LIST OF SYMBOLS AND CHEMICAL FORMULAE

T -	Absolute temperature
e_a -	Actual vapour pressure
σ -	Bulk electrical conductivity
Zc -	Cable impendence
Kc -	Crop co-efficient
δ-	Delta values (deviation from the international standards)
Ka -	Dielectric constant
α -	Factor related to the inverse of the air entry suction
C -	Velocity of signal in free space
S_e -	Effective water content
E-	Energy
z -	Gravitational Head
^{1}H-	Hydrogen-1
^{2}H-	Hydrogen-2 (Deuterium)
^{3}H-	Hydrogen-3 (Tritium)
ε-	Isotope enrichment factor
IRIS-	Isotope Ratio Infrared Spectrometer
IRMS-	Isotope Ratio Mass Spectrometer
LAI -	Leaf Area Index
LGR-	Los Gatos Research
M -	Molecular weight of water
m-	Mass
T -	Mean daily air temperature at 2 m height
^{15}N-	Nitrogen-15
R_n -	Net radiation at the crop surface
^{16}O-	Oxygen-16
^{17}O-	Oxygen-17
^{18}O-	Oxygen-18
OA-ICO	Off-Axis Integrated Cavity Output Spectroscopy
‰-	Parts per Thousand
l -	Pore-connectivity parameter
n -	Pore-size distribution index
Et-	Potential plant transpiration

Es-	Potential soil water evaporation
S_p -	Potential water uptake rate
Kp -	Probe constant
Ψ_{PLWP}-	Predawn Leaf Water Potential
h -	Pressure head
γ -	Psychrometric constant
k -	Radiation extinction (rExtinct)
x -	Rainfall intensity
La -	Real probe length
ρ -	Reflection coefficient
Hr -	Relative humidity
θ_r -	Residual water content
$\alpha(h)$ -	Root-water uptake stress function
ET_0	Reference evapotranspiration
K_{sat} -	Saturated hydraulic conductivity
e_s -	Saturated vapour pressure
$(e_s - e_a)$	Saturation vapour pressure deficit
θ_s -	Saturated water content
Δ-	Slope of vapour pressure curve
SCF -	Soil Cover Fraction
G -	Soil heat flux density
SCI-	Spectral Contaminant Identifier
LA/L-	Start distance and End distance
Sc -	Storage capacity
ΔT -	Travel time
TDR-	Time Domain Reflectrometry
R -	Universal gas constant
v-	Velocity
θ -	Volumetric water content
$\theta(h)$-	Water retention curve
L -	Waveguide length
μ_2 -	Wind speed at 2 m height

LIST OF TABLES

LIST OF FIGURES

1. INTRODUCTION

Commercial afforestation is one of the most important agricultural activities in South Africa as it is estimated that it accounts for approximately 6.3% of the country's gross agricultural production (FAO, 1998). Although commercial afforestation provides numerous benefits to the economy and society, it has negative impacts on the hydrological system (Scott *et al*, 2000). Presently, commercial afforestation is regarded as a streamflow reduction activity (SFRA) and is the only water-use activity to be given this status, according to the National Water Act of 1998 (NWA, 1998).

Previous research on tree water-use in the Two Streams Catchment has shown that the *Acacia mearnsii* stands were using more water than was available from precipitation (Burger, 1999; Clulow 2012). The trees are therefore able to access water from other sources within the catchment. This has raised concerns that the trees are accessing groundwater, bringing into the question the sustainability of commercial afforestation and its effect on water resources.

Groundwater and soil water are the available sources of water to the trees for growth. From the high water use results of the *Acacia mearnsii* measured by Clulow (2007) there is concern over the long-term sustainability of the water resources, particularly the groundwater, within the vadose zone. In literature, specific trees have been found to use groundwater as a source and therefore *Acacia mearnsii* might have this same ability (Lambs and Bethelot, 2002; Brunel *et al*, 1990; Thorburn *et al*, 1993). Therefore, the focus of this project was to determine whether the *Acacia mearnsii* are indeed using groundwater and whether this accounts for the deficit in the water balance identified by Clulow (2007). An environmental tracer (stable isotope) was used to determine whether the groundwater signature is the same as the soil signature in which the roots exist. If capillary rise is not considered, then the trees are able to use their roots and the hydraulic lift mechanism to transport water from deeper rooting systems to upper rooting systems.

Isotope techniques are useful and can be used to gather information from complex hydrological systems. They can determine different factors in hydrology, such as: the origin of water, the age, distribution, quality, occurrence, recharge characteristics, lithological data, as well as the porosity and permeability of the ground and other aquifer parameters. Isotope analysis can be used to determine the source of pollution, the

dynamics of water bodies (dams and lakes), water balances, evaporation/ evapotranspiration, recharge sources and areas, as well as the surface and groundwater interactions (Singh and Kumar, 2005).

In this study, isotope analysis was used to identify sources of tree water uptake and water movement through a small 1st order catchment. The isotope study at the Two Streams Research Catchment focused on environmental tracers and was supported by the modelling of root water uptake.

Root water uptake plays an important role in the soil-plant-atmosphere continuum (SPAC) of the water cycle and provides an understanding of the amount and seasonality of tree water use (Wang *et al.,* 2010). SPAC is the movement of water from the soil to the plants and into the atmosphere. The vadose zone plays an important role in many aspects of hydrology, such as soil water storage, evaporation, plant water uptake, groundwater recharge, erosion, runoff and infiltration. The vadose zone is a subsurface zone where water is contained at pressures below that of the atmosphere. In this zone, water and air is held by soil and rock pore spaces. In terms of identifying if groundwater is a possible water source for *Acacia mearnsii*, the vadose zone has been considered as the dominate pathway through which groundwater must move (capillary rise or hydraulic lift) to be redistributed near plant roots.

In the past, the only method used to understand root water uptake was by the excavation of roots (Dahlman and Kucera, 1965). Research by Dawson and Pate (1996) showed that plant root systems are not the only factor that have an effect on plant water and nutrient uptake. However, the excavation of a plant's roots is laborious, destroys the living environment of the plant and is thus not suitable for long-term research (Wang *et al.,* 2010). The use of stable isotopes, such as hydrogen and oxygen, can be used as a means to understand root water uptake (Zimmermann *et al.,* 1967). According to Zimmerman *et al*. (1967), there is no isotope fractionation during the root water uptake and the water that the plant takes up is a mixture of water from different sources. This means that the isotope composition of the water in the leaves and the stems is the same as the composition of the water in the roots. By using stable isotopes, such as the ratio between hydrogen and oxygen in the plant xylem, one can thus confirm the plant's source of water (Brunel *et al.,* 1995).

The objective of this study is also to use the HYDRUS to validate if soil water models can be used to determine water use impacts of tree species in poorly gauged catchments.

Many models have been developed to evaluate the computation of solute transport and water flow in the vadose zone. There are two different types, namely, numerical or analytical. Numerical models such as finite element models (HYDRUS), solve a set of differential equations that are used to describe a physical system. The model divides the groundwater system into a mesh of triangular, quadrilateral or other shapes, each of which is called an element. The groundwater water surface or head of each element is determined by the nodes at the corners of the element. A finite element model uses solvable equations to determine unknown groundwater heads at nodes by using basis functions (linear, quadratic or a combination of functions) to integrate the effects of areal recharge and storage change (ASCE, 1996). Analytical models do not calculate pressure heads on a grid, pressure heads are rather calculated at any point. Once the pressure heads are determined a gridded surface can be constructed from these points (Haitjema, 1995).

The most commonly used models make use of either the Richards Equation of variably saturated flow or the Fickian-based convection dispersion equation. HYDRUS is a physically based deterministic model, which uses physical measurements to understand a system, while making use of mathematical relationships to understand the linkages between various components in a hydrological system (Schulze, 2009). HYDRUS is a model that simulates water, heat and solute transport in one, two or three dimensions, using the Richards Equation for variably-saturated flow and the Fickian-based convection-dispersion equation for heat and solute transport (Simunek *et al*., 2009).

To understand the results that have been attained from the research catchment, it is important to understand the fundamentals behind the use of isotopes as environmental tracers. A review of the literature and previous case studies on the subject was used to source a methodology and to foresee any possible problems that might occur with the project.

2. LITERATURE REVIEW

2.1 Isotope Hydrology

2.1.1 Fundamentals of Isotope Hydrology

Isotopes are atoms of the same element, but which have a different number of neutrons. The difference in the number of neutrons means that the different isotopes have different masses. This is important, as variations of the masses in the composition of the isotopes in a sample will show if chemical reactions, physical changes or biological processes have occurred to the sample. Tritium is the heaviest of the hydrogen isotopes, with three atomic mass units, and it is a radioactive isotope, has a low abundance and therefore is not suitable for this study (Kendall and McDonnell, 1998). There are a large number of oxygen isotopes, some of which are radioactive (unstable) and some are stable. Radioactive isotopes are isotopes that decay and thus become depleted in abundance over time.

2.1.2 Standards Delta Notation

The composition of the hydrogen and oxygen isotopes is reported in terms of delta values (δ), which is the ratio of deviation from the international standards. δ is used to relate the ratios of a known international standard (Standard Mean Ocean Water) with the ratios of the collected sample.

The results of isotope readings are represented by δ where:

$$\delta^{18}(O‰) = (R_{\text{sample}} / R_{\text{standard}} - 1) \times 1000 \qquad (2.1)$$

R_{sample} is the ratio $^{18}O/O^{16}$ of the sampled water and $R_{standard}$ is the ratio $^{18}O/^{16}O$ from ocean water (Standard Mean Ocean Water: SMOW). This ratio is expressed in parts per thousand (‰).

In the past, the ratio between $^{18}O/^{16}O$ for average measured sea water was regarded as the Standard Mean Ocean Water (SMOW) (Mook, 2001). Epstein and Mayeda (1953) measured the ratio of $^{18}O/^{16}O$ for all the oceans across the world and an average

reference sample was determined, namely, NBS1 (US National Bureau of Standards). SMOW was defined by Craig (1961) as:

$$^{18}\delta_{NBS1/VSMOW} = -7.94\,permil(‰) \quad (2.2)$$

The International Atomic Energy Agency (IAEA) and the US National Institute of Standards and Technology have made sample batches of mean ocean water which are available for distribution as a standard reference for ^{18}O and ^{2}H. VSMOW (Vienna Standard Mean Ocean Water) has replaced SMOW for both $^{18}\delta$ and $^{2}\delta$, because VSMOW has fixed the zero point on the $^{18}\delta$ scale.

$$^{18}\delta_{NBS1/VSMOW} = +0.05\,permil(‰) \quad (2.3)$$

All measurements taken in this study are compared with those of the VSMOW reference standard.

2.1.3 Radioactive isotopes and stable isotopes

Isotopes that are radioactive are isotope-specific atoms that spontaneously disintegrate over time. While these atoms disintegrate, they emit alpha, beta particles and occasionally gamma rays. Stable isotopes are atoms that do not decay to form other isotopes over time, but can be produced by the decay of radioactive isotopes, in which case they are known as radiogenic atoms (Kendall and McDonnell, 1998).

2.1.3.1 Stable oxygen isotopes

Oxygen has three stable isotopes, ^{16}O, ^{17}O and ^{18}O, where ^{16}O is the most abundant, followed by ^{18}O and then ^{17}O (Nier, 1950). The isotope with the highest mass is ^{18}O, followed by ^{17}O and then ^{16}O. ^{17}O is rarely used in the analysis of the hydrological cycle as it provides little information. ^{18}O is more commonly used in isotope hydrology, as it provides information regarding streamflow, baseflow and groundwater recharge rates. The values of $^{18}\delta$ are high in saline lakes which are subject to a high degree of evaporation, while in cold climates and high altitudes $^{18}\delta$ values are low. Usually $^{18}\delta$ values in all environments do not exceed 30 permil (‰) (parts per thousand) (Mook, 2001).

2.1.3.2 Stable hydrogen isotope

Stable isotopes of hydrogen include ^{1}H and ^{2}H (Deuterium), ^{1}H being more abundant than ^{2}H, and ^{2}H weighing more than ^{1}H. Water that has undergone evaporation will contain more Deuterium than precipitation water and the same applies to ^{18}O (Mook, 2001). Low Deuterium levels will be found near polar ice (Mook, 2001).

2.1.4 Isotope composition of different water types

2.1.4.1 Isotope composition of ocean water

Isotopes in the ocean are unlike those in the hydrological cycle, as they are fairly homogenous. The isotope composition of ocean water is important as the composition of SMOW/VSMOW is used to compare the ratios of collected samples with those of standards. The values range within about 0.5 permil (‰) of the SMOW for $\delta\ ^{18}O$, while the δ for (^{2}H) can vary within a factor of 10, or larger (Gat, 2010).

Research done by Redfield and Friedman (1965), Craig and Gordon (1965), Dansgaard (1960) and Epstein and Mayeda (1953) has led to the development of a reference δ-scale of isotope composition in the water cycle. Research done by Anti and Gat (1989) has shown that there are larger isotope variations along the continental margins of the ocean, mainly in semi-enclosed marine basins or in bays and in the Arctic and Antarctic areas.

The isotope composition of seawater can vary, due to changes in salinity. Seawater that is subject to heavy trade winds is usually enriched with the heavier isotope species, as they have a high salinity content and thus reflect a negative water balance between evaporation and precipitation (E/P>1). Colder regions that are subject to the freezing and melting of seawater have varying isotope composition. The transition between the liquid and solid phase causes small isotope fractionation.

Another source of the changing isotope composition of oceanic water is believed to be from the melting of continental ice sheets. This isotope composition, which is given the term glacial increment, is estimated to be in the order of around -0.5 permil (‰) and +1.0 permil (‰) in $\delta(^{18}O)$, which is close to the value of SMOW for interglacial and glacial-maximum periods, respectively. The changing isotope composition of the hydrogen isotope, which is based on ice-cap composition, is termed the Global Meteoric Water Line

(GMWL), with values close to δ(^{18}O)= -30 permil(‰) and δ(^{2}H)= -230 permil (‰) (Gat, 2010).

2.1.4.2 Isotope composition of precipitation

The composition of the oxygen and hydrogen isotopes of rainwater varies in a 'semi-predictable' way. The correlation between δ^{2}H (D) and δ^{18}O in precipitation water worldwide corresponds to a best-fit line (Craig, 1961):

$$\delta D = 8\delta^{18}O + 10 \qquad (2.\ 4)$$

The line in equation 2.4 is known as the GMWL (Global Meteoric Water Line), where meteoric is known as rain, snow or hail water (Harris *et al.,* 2010). Although the majority of the precipitation that falls on the world is close to the GMWL, in some distinctive areas local meteoric water lines need to be established.

The new precise GMWL from the IAEA (2004) (based on Global Network of Isotopes in Precipitation) was used instead of the Craig (1961) line (Equation 2.5).

$$\delta^{2}H = 8.17(\pm 0.07)\delta^{18}O + 11.27(\pm 0.65)(‰)\ \text{VSMOW} \qquad (2.5)$$

There are five factors that affect the isotope composition of precipitation namely, altitude, climate (temperature), the amount of precipitation, continentality and the source region of evaporation to form clouds (Dansgaard, 1964).

The isotope composition of precipitation follows the Rayleigh Equation for an open equilibrium system under ideal conditions, which is when condensation takes place without reaching super saturation and when rainfall falls as soon as droplets are formed. However, in reality, the isotope composition of precipitation is governed by the rules of a closed system, in that there is a depletion or enrichment of heavier isotopes as the liquid water content in the clouds increases or dissipates. This process is dominated by equilibrium fractionation factors (Gat, 2010).

The isotope composition of precipitation's stable isotopes varies both spatially and temporally, due to climate variations. The isotope composition of precipitation is related to

the atmospheric circulation patterns, as it influences the sources and transportation of atmospheric vapour across continents (Liu *et al*., 2010).

2.1.4.2.1 Isotope composition of precipitation in Southern Africa

The isotope composition of rainfall needs to be looked at before interpretations of results can be made. The composition of oceanic water usually falls on the Global Meteoric Water Line (GMWL) shown as (a)(Figure 2.1). Local rainfall signatures were measured by Lorentz *et al*., 2007 in the Weatherly Catchment (Eastern Cape), these may fall below and above line (b). Rainfall that has a higher concentration of heavier isotopes falls on the lower end of the line. This type of rainfall usually occurs at higher elevations, inland locations and in cooler zones. Rainfall that falls at low altitudes, in warmer areas and near oceans usually falls at the higher end of the line (b). Rainfall that has undergone evaporation, prior to falling, may have concentrations along line (c). Rainfall that has undergone evaporation from soil or during flow over rock outcrops lies on line (e) (Lorentz *et al*., 2007).

It is expected that most of the rainfall that is received at the Two Streams Research Catchment during winter will be depleted in the lighter isotopes due to the influence of dominant frontal events, while summer rainfall will be enriched in lighter isotopes due to the influence of dominant convective storms.

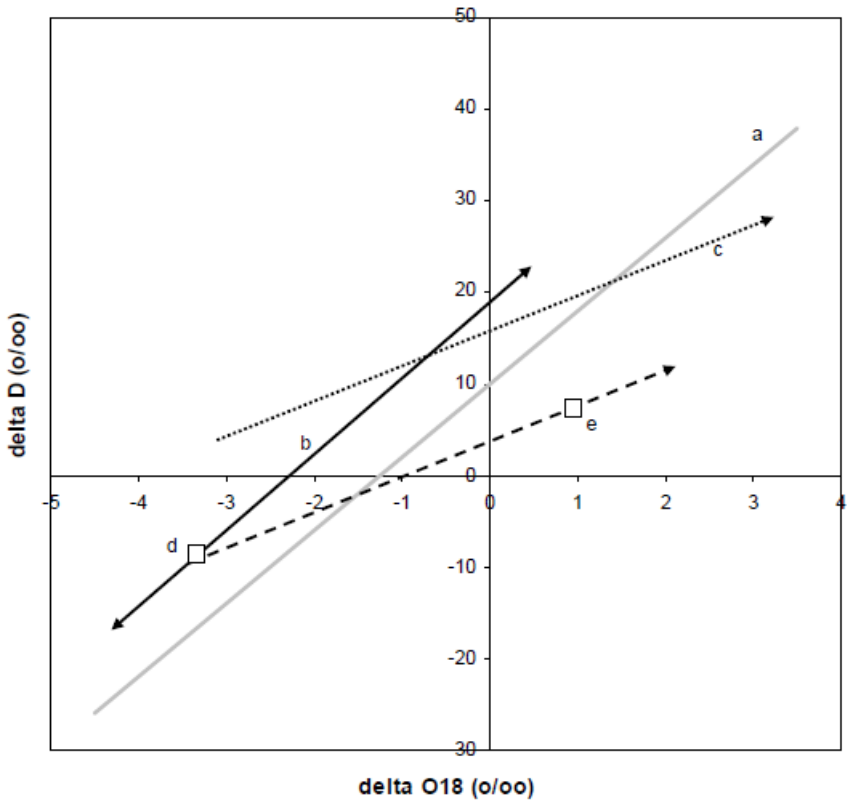

Figure 2.1 Composition of rainfall and runoff (after Aggarwal *et al*., 2002)

Point (d) on (Figure 2.1) above shows an isotope sample that has more $^{18}O/^{16}O$ and more $^{2}H/\ ^{1}H$, while the point (e) shows an isotope sample that has less $^{18}O/^{16}O$ and less $^{2}H/^{1}H$.

2.1.4.3 Isotope composition of water in plant tissue

The composition of water in plant leaves presumes that heavier isotopes will dominate, due to the evaporation of the lighter isotopes (Gonfiantini *et al.,* 1965). According to the Craig-Gordon evaporation model, on average there is a steady state relationship that is dominant for leaf isotope composition. For conditions when the transpiration flux exceeds the hold-up volume (interception capacity) of the leaf manifolds (canopy), the isotope composition of the transpiration flux should match that of the source water taken up by the plant. A comparison of the GMWL and the leaf water line shows that the slope is less than 8 (Gat, 2010). The isotope composition of the water in the leaf comes from the composition of the source water taken up by the plant. The slope for the leaf water is lower than that of surface water under similar conditions, as the evaporation of the leaf water occurs within the stomata and through an air pocket, whereas the fractionation that occurs in surface water is diffusive such that air with high humidity mixes with air of low

humidity. One of the main differences between leaf water and surface water is that leaf water is compartmentalised within stomata. Within different areas of the leaf, there is a variation in the isotope composition of water. This might result in the leaf water line not tracing back to the source water (Gat, 2010).

In the past, there was little understanding of isotope change and fractionation as water moved through the plant. Previously, roots were extracted and analysed to understand root water uptake (Dahlman and Kucera, 1965). Research by Dawson and Pate (1996) showed that plant rooting systems are not directly related to water uptake. The excavation of roots destroys the living environment of the plants and this method is thus unsuitable for long-term research (Wang *et al*, 2010). However, by analysing the ratios of hydrogen and oxygen isotopes, root water uptake can be better understood (Zimmerman *et al*, 1967; White *et al*, 1985; Thorburn *et al*., 1993). Zimmerman *et al*. (1967) discovered that there was no isotope fractionation during the uptake of water and that the water that the plant absorbs is a mixture of water from different sources. This means that the isotope ratio of the water in the tree stem and branches is the same as the ratio in the roots. Thus, by comparing the ratio of oxygen to the hydrogen isotopes of the water in the stem and branches, the different sources of water used by the tree can be determined (Brunel *et al*, 1995).

The isotope composition of water in the leaves of trees is not representative of the water source. This is due to the evaporation of water from within the leaves (Dawson and Ehleringen, 1991). Therefore, to extract water from plant material one needs to extract water from wood cores. Azeotropic distillation (Revesz and Woods, 1990; Busch *et al*., 1992) extracts sap out of wood cores by using an organic solvent, and then separating the aqueous phase. With quantitative freeze-drying technique (Cooper *et al*., 1989), the wood cores are distilled under high pressure and the sap is trapped in ice formation and removed. Neither of these procedures were used in this study due to the lack of availability of equipment and expertise.

2.1.4.4 Isotope composition of groundwater

Groundwater that usually is not exposed to extreme temperatures (higher than 60°C or lower than -80°C) can be used to characterise its origin. Groundwater that reaches temperatures of more than 80°C is known as geothermal water, the isotope composition of this water varies too much to characterise it's origin. Shallow groundwater that is not subject to high or low temperatures can be used to characterise meteoric water. In arid regions, or in regions where there are high temperatures, evaporation removes lighter isotopes during infiltration, which causes the composition of groundwater to be different from that of precipitation (Singh and Kumar, 2005).

2.1.4.5 Isotope composition of river water

Stream water or rivers have a varying isotope composition, which is dependent on the source water. Rivers water has an isotope composition of both surface water and sub-surface water (below surface water) (Singh and Kumar, 2005). As water drains over the surface, it interacts with antecedent soil water of the surface and topsoil and is furthermore exposed to evaporation. When the precipitation amount exceeds the infiltration capacity of the soil surface, runoff occurs, either on bare or fully saturated soil surfaces (Gat, 2010). Surface runoff is often more depleted in heavy isotopes than the amount-weighted average of the rainfall, due to the inter-action with rain drops (Ehhalt *et al*., 1963). Therefore, only the heavier and long-lasting rainfall events contribute to direct runoff (Gat, 2010).

2.1.4.5.1 Hydrograph separation

Baseflow and direct surface discharge are the response factors that cause the varying flow in a runoff stream. In semi arid regions which are under afforestation such as at Two Streams Research Catchment, the major streamflow contributor in winter is baseflow, whereas in summer there will be hyporheic exchanges and runoff will be the main contributor to streamflow.

The main principle in separating these two components is that base flow (groundwater) isotope composition, is steady and represents the average value of groundwater recharge over the recharge zone, while direct runoff, which is generated by rainfall event isotope composition, is modified by the flushing of accumulated surface and soil water residues. In temperate regions, direct runoff occurs by means of interflow and therefore its isotope composition is an average value of antecedent rain events (Gat, 2010).

2.1.4.6 Isotope composition of soil water

Water that is received by a catchment in the form of precipitation will eventually leave the catchment after some finite time. Water that is intercepted by vegetation or other non-porous surfaces may rapidly evaporate from the surface and thus has little effect on the isotope composition of remaining water in the catchment. A portion of the remaining water may fall on saturated areas, which are directly connected to stream networks and thus could form part of surface flow. The remaining water will infiltrate the soil and, depending on catchment conditions and other factors, will spend time as soil water or groundwater. Soil water will then leave the catchment via transpiration, evaporation, groundwater flow or streamflow (Kendall and McDonnell, 1998).

Research done by Zimmermann *et al*. (1967) (in contrast to that done in open water bodies) showed that soil effectively prevented turbulent vertical mixing, and the resultant steady-state isotope profile could be explained in terms of the balance between an upward convective flux and a downward diffusive flux of isotope (Kendall and McDonnell, 1998). Thus, evaporation from within a soil column is different to that of an open water body, in that the mixing of the isotope signature within the liquid and gas phase is restricted by the texture of the soil matrix (Gat, 2010). The isotope compositions of saturated and unsaturated soil are similar in terms of basic physical process, although there is a difference, namely, instead of all fluxes within the soil being in the liquid phase, there is a possibility of water and isotope movement in the vapour phase, and within the zone there should be an allowed isotope exchange between the two phases (Kendall and McDonnell, 1998).

In saturated situations, which occur immediately after a precipitation event, or in capillary-rise zones such as the vadose zone, there is an isotope composition gradient that is established between the water that is enriched with heavy isotopes at the evaporating surface and the water in the deeper soil layer, which is close to the mean composition of

input water. The soil texture and tortuosity has an influence on the diffusive dissipation of the enrichment at the surface. Above the evaporating surface, vapour is the dominant transport, while below the evaporating surface, liquid is the dominant form of transport (Gat, 2010).

Winter rainfall A, C, E (Figure 2.2) are enriched in δ_{18} (heavy isotopes) relative to Standard Mean Ocean Water (SMOW) due to the winter rainfall events (cold fronts) being more enriched in heavy isotopes (colder temperatures). In summer, D and B, temperatures are higher therefore isotopes are slightly depleted in heavy isotopes relative to SMOW.

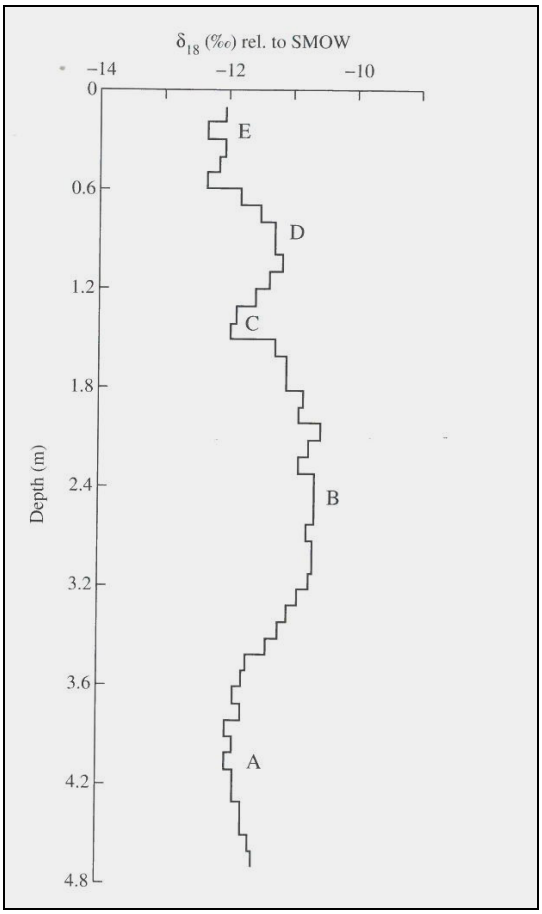

Figure 2.2 Soil profile depth with δ18O where the mean percolation rate is 260 mm/year. Points A, C, E correspond to winter precipitation, while D and B are related to summer precipitation (Gat, 2010)

2.1.5 Isotope Fractionation

In terms of hydrology, isotope fractionation occurs when water that is moving through the hydrological cycle undergoes a phase change, thus changing the abundance of a particular molecule with a particular isotope (Michener and Lajtha, 2007).

The chemical and physical properties of substances can be considered to be either mass- or non-mass dependent, depending on certain conditions. Different isotopes of the same elements have different masses because of their different number of neutrons. Non-mass dependent properties are determined by the nuclear interaction because of the structure of the nucleus and are not determined only by the mass difference of the nuclei. Thus, the different isotopes that make up an element will result in slightly different chemical and physical properties. These differences can be sufficiently large, so that when substances undergo a physical, chemical or biological process, the isotope ratio fractionates. The unique isotope composition of water can be used as a fingerprint of the biological, chemical or physical process that the water has been through (Kendall and McDonnell, 1998).

Isotope fractionation can be produced by two main processes, an isotope equilibrium exchange reaction or a kinetic process. In a well-mixed system that is closed, a forward and a reverse process can occur, using the chemical agents in the system. Equilibrium can be established between the forward and reverse processes, so that the two processes occur at the same rate. This equilibrium will also result in an isotope equilibrium being formed (Kendall and Mc Donnell, 1998). In an open system, for example, above a body of open water, the processes can be identified as the evaporation of the water and the condensation of that water vapour. The system is open because the water vapour formed by evaporation can be removed from the liquid gaseous interface by air currents. In such a case, equilibrium is not established and kinetic fractionation is the main process. Mass-dependent fractionation for isotopes is different for equilibrium and kinetic processes.

2.1.5.1 Equilibrium fractionation

Chemists discuss chemical equilibrium for reversible chemical reactions in terms of a chemical reaction written by convention, with reactants on the left and products on the right. Since this reaction is reversible, the term reactants and products are used to simply identify the substances on each side of the equilibrium. In a closed system, equilibrium is reached between the forward and reverse reactions, as described by the chemical equation, when the rates of both processes are equal. At this position, the concentrations of product and reactant remain constant at a particular temperature. In isotope equilibrium, the rates of the two processes are the same, with the concentration of the heavier isotope favouring the phase of lower energy. For example, if the two phases are water and water vapour, then the molecules with the highest kinetic energy in the liquid phase, will have enough energy to overcome the surface tension and enter the vapour phase. This will result in the ratio of heavy to light isotopes within the different phases changing, as the processes continue to occur. This means that the water phases will become enriched with molecules containing the heavier isotopes of oxygen and hydrogen, mostly ^{18}O and ^{2}H, while the vapour phase will become enriched with molecules containing the lighter oxygen and hydrogen isotopes, mostly ^{16}O and ^{1}H (Brown, 1964). Equilibrium is a dynamic process and the pathway or mechanism of the process does not affect the equilibrium ratio.

2.1.5.2 Kinetic fractionation

In open biological systems the processes are not reversible, as the one phase is removed from the interface of the two phases. These systems are unidirectional kinetic reactions and kinetic isotope fractionation occurs.

The kinetic process depends on:

- The masses of the isotope: the product of the process becomes enriched in the lighter isotope. If the reactant volume is limited, then the reactant becomes enriched in the heavier isotope.
- There are two explanations for this:
    - At any given temperature the molecules of a substance will have a certain average kinetic energy directly proportional to this temperature. Kinetic

energy is given by $E = ½ mv^2$, where m is the mass and v the velocity of the molecules. For a given kinetic energy, it follows that a molecule with a higher mass will have a lower velocity. Lower velocity molecules will not leave the liquid surface as readily as higher velocity molecules, as they will not collide with this surface as often.

- Molecules with higher mass will also have lower vibrational energy. Since a phase change from liquid to gas requires that the hydrogen bonds holding the water molecules together need to be broken, the higher mass molecules will require more energy to break the hydrogen bonds existing between them.

The Rayleigh Equation describes an ideal, open, kinetic fractionation system (Kendall and Mc Donnell, 1998) (Appendix I). Numerical values can be calculated that will describe the ratio of the reaction rates of the different isotopes in kinetic and equilibrium fractionation. An isotope enrichment factor, ε, can be calculated for a system. This factor depends on the climatic conditions and is an indication of the rate of reaction of the different isotopes (Kendall and Mc Donnell, 1998).

If the reversible reaction rate changes for example in increasing humidity conditions, then the system will approach the values for an equilibrium isotope system. In the water system the magnitude of kinetic fractionation is mostly bigger than the magnitude of the equilibrium fractionation for the same system under the same conditions.

2.1.5.3 Isotope prediction modelling

Craig and Gordon (1965) developed a model that is used for predicting the isotope fractionation for water bodies. This has led to the analysis of water for the heavy isotopes of ^{2}H (D) and oxygen-18(^{18}O) to trace the movement of water. The isotope predicting model suggests that isotope fractionation during evaporation does not only include equilibrium fractionation, but mainly kinetic fractionation, which is dependent on site conditions (Kebede *et al.,* 2009).

2.1.5.4 Case studies where isotope hydrology has been used

Isotope techniques can be used to monitor the movement of water with a high degree of accuracy, using either stable isotopes or radioactive isotopes. The isotopes that are analysed can be used as tracers (on aspects of the water cycle) in which different traced materials will have distinguishing signatures from those of the materials stream. Tracers can be injected into a study system, or as in this study, naturally-occurring tracers can be used. An example of the former is Nitrogen-15(^{15}N). The $^{15}NH_4Cl$ can be added to the soil, which allows for the monitoring of the physiological change (uptake of a tracer) in the vegetation (Ashkenas *et al*., 2002).

Isotope hydrology has been used widely to understand tree water uptake. For example, in France, Lambs and Berthelot (2002) used isotope ratios to monitor water from underground, to the trees on the riparian areas of a woodland.

In Australia, Farringto *et al*. (1996) used isotopes to trace water uptake by *Eucalyptus marginata* trees, using the abundance of Deuterium. They analysed tree water uptake by sampling twigs for xylem sap. Tree water use was analysed at three different sites in Western Australia, where there were different soils and varying depths of the water table. From the results of the study, there was no clear evidence that *Eucalyptus marginata* utilised water from groundwater more than 14 meters below the surface. They found that, in order to trace tree water uptake, there needs to be a difference in isotope composition between water in the soil profile and in the groundwater profile (Farringto *et al*., 1996). The results from the study showed that extraction from the soil of *Eucalyptus marginata* trees varies with season, which have an effect on rooting patterns.

At the Floreat Catchment, during summer and autumn the trees were extracting water from depths below 4 m, using sinker roots. During the months of May and June the trees were extracting soil water from above 1 m and below 3 m, this was due to winter rains which replenished deep soil water stores. As the soil horizons dried out during summer and spring, the trees became more reliant on water that was stored deeper down. At the Floreat Park Catchment, there was no evidence that the trees withdrew much groundwater. The water table was 14.6 m deep, suggesting that the sinker roots did not reach groundwater. At the Cordon Catchment, the results did not give a clear indication of where the trees were extracting water, especially over the summer period. At the end of

spring, the main source of water was above 5 m, where the winter rainfall was able to replenish the profile. By the end of summer, when the profile above 5 m had dried up, the water source for the trees using stable isotopes could not be identified with any certainty, because the δ^2H values of water samples from twig sap were more depleted than the values for soil water and groundwater. At the Bannister Catchment, the trees become more reliant on groundwater during summer because of shallower soil depth. In spring the δ^2H values in the twigs' sap water showed more enrichment than the groundwater, but by the end of summer the values between the trees and groundwater were similar (Farringto *et al*., 1996).

Thorburn *et al.* (1993a) confirmed that within eucalyptus trees, xylem sap obtained from core samples from the trunk and twigs, had similar isotope ratios. Water was extracted from *Eucalyptus* trees, using azeotropic distillation where three solvents were used in a laboratory. The results of this azeotropic distillation showed that there was no significant change in δ^2H values between the trunk and twigs. Thus, the least destructive sampling techniques were used, which was sampling from the twigs. Brunel *et al.* (1990) measured the stable isotopes from soil, groundwater and twigs of *eucalyptus*. The results showed that the trees were, using groundwater during summer.

Thorburn *et al.* (1993b) and Mensforth *et al*. (1994) showed that *Eucalyptus camaldulensis*, which was growing alongside a river above a shallow saline aquifer, tended to be opportunistic in the sources of water available, using less saline water, as fresh water from the river became available. Tree water sources were determined by comparing the concentrations of the stable isotopes of water in tree twigs to water in soil profiles and groundwater. Thornburn *et al*. (1993b) also confirmed that water from twigs was isotopically similar to that absorbed by roots. The concentrations of ^2H and ^{18}O were determined, using mass spectrometry. Water from twigs was extracted, using azeotropic distillation and a similar procedure was done for the extraction of water from soils. Trees that were positioned away from streams and which did not have access to stream water, used groundwater in summer and a combination of rainwater stored in the surface soil and groundwater in winter. Trees close to the rivers, extracted stream water directly in summer and from the soil storage in winter.

Kulmatiski *et al*. (2010) injected deuterium rich water into different soil depths to determine the vertical and horizontal location of water uptake by grasses and trees (*S. birrea* and *T. sericea*) in the Kruger Park, South Africa. The results showed that trees accessed most of their water from 20 cm depths, while grasses accessed most of their water from 5 cm.

Trees used little water below depths of 20 cm and during the dry season trees used stored water, therefore there was no evidence that trees were able to use large amounts of deep soil water.

In a South African study by Grellier *et al*. (2011), who researched the depth of water uptake of *Acacia sieberiana* in the sub-humid grasslands of KwaZulu-Natal. Soil samples and stems of *Acacias* were analyzed for isotopes ($\delta^{18}O$) along a catena in the wet and dry season. The water potential and $\delta^{18}O$ value were influenced by the season, size classes of *Acacias*, as well as the position in the catena (Grellier *et al*., 2011).

The study showed that small *Acacias* switched their water uptake depth between seasons from a depth of 40 cm to deeper soil layers, to avoid competition with grass species. Taller *Acacias* used deeper sourced water (>1 m depth). The difference between shallow and deep soil water isotopes can be used to discern the differences in root water uptake (Figure 2.3). The conclusions of the study were that the small *Acacias* competed with grass for water, but were able to access water at various depths, more so in the wet season when grass cover was dense. To avoid the competition with grass, *Acacia's* develop deep roots quicker, to allow for access to deeper water (Grellier *et al*., 2011).

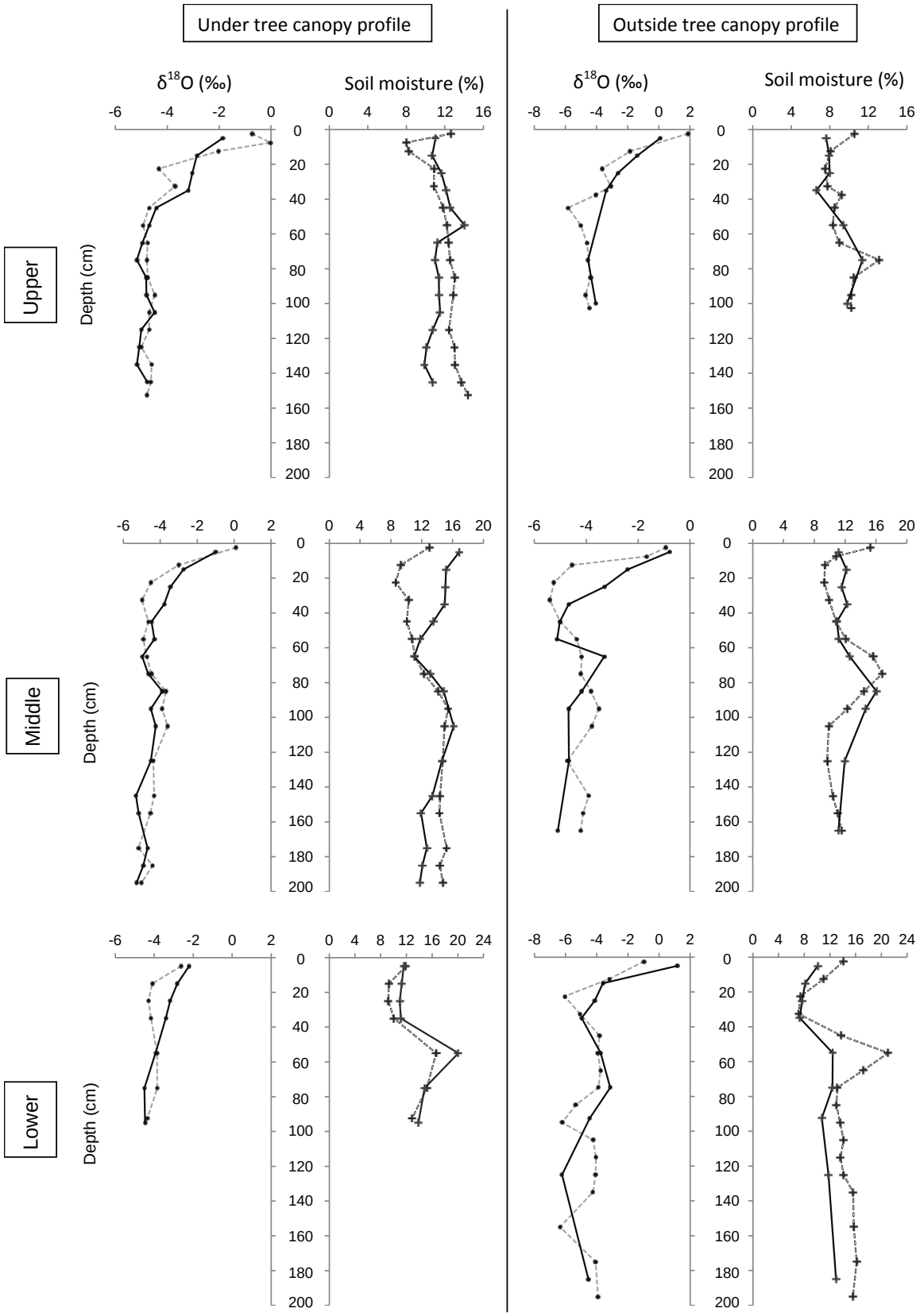

Figure 2.3 The $\delta^{18}O$(‰) and soil water content (%) for the three different positions in the catena outside and under the canopy of *Acacia* trees (Grellier *et al.,* 2011)

2.2 Root Water Uptake Modelling

The HYDRUS model is used to simulate the movement of water, heat and solutes in media which are variably saturated (Simunek, 2012). The model makes use of linear, finite elements to numerically solve the Richards Equation for saturated and unsaturated water flow (Simunek, 2012). A number of equations are available within the model interface to determine processes and describe properties such as the transportation of solutes, heat transfer, root water uptake during stress and unsaturated soil hydraulic properties (Simunek, 2012).

Water movement through soils depends not only on pore size distribution, but also on antecedent moisture conditions. Water movement through soils is therefore a function of soil properties and volumetric water content. The HYDRUS model numerically solves the Richards Equation for variable saturated conditions:

$$\frac{\partial \theta}{\partial t} = \frac{\partial}{\partial z}(K(\theta)\frac{\partial h}{\partial z}+1) \quad (2.1)$$

Where: θ-Volumetric water content (L^3L^{-3}), t is the time (T), h is the pressure head (L) and z is the gravitational head (L).

Plant root water uptake is an important process in subsurface and unsaturated flow and transport modelling. Root water uptake controls the actual plant evapotranspiration, water recharge and nutrient leaching to groundwater. The root water and nutrient uptake model provides for the improved integration of scientific principles, as is required for an interdisciplinary, ecological approach (Simunek and Hopmans, 2009).

There are two approaches that can be considered when simulating root water uptake in vadose zone hydrological models, on either a field scale or plot scale (Hopmans and Bristow, 2002). Early studies of water extraction by plant roots were based on a microscopic or mesoscopic (Feddes and Raats, 2004) approach that considered a single root to be a long cylinder of uniform radius with water-absorbing properties (Gardner, 1960). Water flow to the roots was based on the Richards Equation, in which water flow into the roots is driven by water potential gradients between the root and surrounding soil

and is proportional to the hydraulic conductivity of the soil that surrounds the roots (Mmolawa and Or, 2000). Recent modelling studies have applied the integration of the plant root-soil domain, where the total plant transpiration is computed from the solution of water potential, solving both root and soil water potentials (Doussan *et al.*, 2006; Javaux *et al.*, 2008).

HYDRUS is a widely applicable hydrological model that has been used extensively in agroforestry to perform water balance simulations (Schelgel *et al*., 2004). As water uptake is linked to nutrient uptake, modelling of the most important growth factor in the agroforestry system can be done using a hydrological model (Schelgel *et al*., 2004).

HYDRUS is well tested, reliable tool that can be used to optimize agronomic measures such as plant spacing, crop selection, fertilization and irrigation (Schelgel *et al*., 2004). HYDRUS has been extensively verified by Simunek *et al*. (1999) and has been used in a number of studies where root water uptake has been simulated. Schelgel *et al.* (2008) used HYDRUS-2D to model the effect that tree spacing has on root zone dynamics. The calibration showed that simulated data were in good agreement with observed data. Siliva *et al*. (2008), used the HYDRUS model to simulate root water uptake of a heterogeneous vegetation cover and although the HYDRUS model has not be tested too extensively on heterogeneous vegetation cover, it was found that the model performed well, where simulated and measured water levels were in good agreement with one another.

2.3 Soil water content analysis

2.3.1 Time Domain Reflectrometry

Time Domain Reflectrometry (TDR) makes use of soil probes that are inserted into a medium to measure the water content of the soil. The probes that are installed are a wave guide extension at the end of a coaxial cable. The reflections that occur from the signal move along the waveguide, which results in a change in impedance. The magnitude of the impedance is determined by the size and spacing of the probe and is inversely related to the dielectric constant of the surrounding soil. A change in the water content of the soil which is around the probe, causes a change in the dielectric constant. The change in dielectric constant causes a change in the impedance, which affects the shape of the reflection. The shape of the reflection is used to determine the water content of the soil (Campbell Scientific, 2010).

The travel time of the pulsed electromagnetic signal along the waveguide that is sent by the TDR 100 is dependent on the velocity of the signal and the length of the waveguide. The dielectric constant of the material surrounding the probe is directly related to the velocity of the signal (Campbell Scientific, 2010). The relationship can be seen below (Equation 2.6):

$$\frac{2L\sqrt{Ka}}{C} = \Delta T \tag{2.6}$$

Where: Ka is dielectric constant, C is Velocity of signal in free space, ΔT is Travel time and L is Waveguide length.

The changes in volumetric water content can be related to a change in dielectric constant of bulk soil material. Equation 2.7 is used to relate the apparent probe length La to the real probe length (Campbell Scientific, 2010), Where equation 2.8 relates the apparent probe length with the travel time and velocity of the signal.

$$La = C\Delta T / 2 \tag{2.7}$$

$$\frac{La}{L} = \sqrt{Ka} \tag{2.8}$$

The relationship between the dielectric constant and the volumetric water content (θ_v) has been described by Topp *et al*. (1980) in a polynomial equation (2.9) and by Ledieu *et al*. (1986) in a linear equation (2.10).

$$\theta v = -5.3\times10^{-3} + 2.92\times10^{-2} Ka - 5.5\times10^{-4} Ka^2 + 4.3\times10^{-6} Ka^3 \quad (2.9)$$

$$\theta v = 0.1138\sqrt{Ka} - 0.1758 \quad (2.10)$$

The TDR 100 generates a very fast time pulse that is sent to the connecting cable and probe. The reflections over a specified length of the transmission line are sampled and are digitized. Changes in the amplitude of the reflected signal are caused by discontinuities in the cable impedance. Distance information is obtained from the travel time of the reflected signal. The travel time from the probe to the TDR is determined by the soil water content, as water content increases the travel time of the pulse increases. The impedance transitions caused by the probe at the beginning and end are identified by the reflected waveform. Soil water content can then be determined (Campbell Scientific, 2010).

The amplitude of the reflected voltage is dependent on the electrical conduction of the applied signal between the probe rods. An attenuation of the applied signal will be caused by the presence of free ions in the soil solution. Giese and Tiemann (1975) determined an equation to measure the soil bulk electrical conductivity (Equation 2.11)

$$\frac{Kp}{Zc}\frac{1-\rho}{1+\rho} = \sigma \quad (2.11)$$

Where: σ is bulk electrical conductivity, Kp is probe constant, Zc is cable impendence (50ohm) and ρ is reflection coefficient

The measurements from TDR 100 probes were used to determine the accuracy of the simulation, where observed soil water content will be compared to that of the simulated results. Rubio and Poyatos (2012) used TDR 100 probes to determine the initial soil water content (%) for the HYDRUS-1D model in determining if HYDRUS-1D was applicable in modelling land use change in Mediterranean Mountains. Rubio and Poyatos used measurements of matric potential to calibrate the HYDRUS-1D model.

Verbist *et al,* (2009) installed twenty two TDR 100 (Campbell Scientific, Loughborough, Logan, USA) at depths between 7 and 45 cm below the soil surface. The equation proposed by Topp *et al*, (1980) was used to determine volumetric water contents. Verbist *et al*, (2009) estimated the soil hydraulic parameters by means of matching observed soil water content from TDR 100 to that of simulated soil water content from HYDRUS-2D.

2.3.2 Soil water potential

Watermark sensors (Irrometer Company, Riverside, California, USA) measure soil water tension by measuring electrical resistance. After installation of the sensor, the sensors stay in equilibrium with the moisture of the surrounding soil. When moisture is removed from the soil, the sensor will experience an increase in resistance and record the moisture change. The opposite is true for wetting. Watermark sensors are able to measure tensions ranging from 0 to 239 KPa. The advantage of using a Watermark sensor is that calibration does not have to be made for every installation as the sensor makes measurements of resistance within a defined consistent internal matrix material, rather than using the surrounding soil as a reference measurement.

2.4 Xylem Pressure Potential

Xylem Pressure Potential readings are important to this study as they give an indication of when *Acacia mearnsii* is under water stress. From previous research (done at Two Streams) discussed in Section 3, the assumption was made that *Acacia mearnsii* transpired freely and therefore it was important to use Xylem Pressure Potential as an indicator of plant water stress.

Predawn Leaf Water Potential (Ψ_{PLWP}) is assumed to represent the mean soil water potential next to the roots and is an indication of the relative transpiration rate (Ameglio *et al*., 1999). It has been shown to have a correlation with plant-water relation parameters, such as soil-available water (Stricevic and Caki, 1997), evapotranspiration (Meyer and Green, 1980), daily minimum stomatal resistance (Dwyer and Stewart, 1984) and relative transpiration (Valancogne *et al*, 1997). Xylem pressure potential can be used as an indication of trees switching their water source.

Pre-dawn leaf water potential has been used as an irrigation scheduling indicator. Schmidhalter (1997) used pre-dawn leaf water potentials for the irrigation of maize, sunflower, barley and wheat. Ameglio *et al*. (1999) used pre-dawn leaf water potentials for the irrigation of walnuts. Sato *et al. (*2005) used predawn leaf water potential as an irrigation timing indicator for wheat in northern Syria.

3. PROJECT OUTLINE

3.1 Research Questions

Previous research in a water-balance study by Clulow (2011) in the Two Streams Research Catchment found that a commercial forestry species (*Acacia mearnsii)* used more water than was available through precipitation over a 30-month period (i.e. total evaporation was greater than rainfall). Clulow *et al*. (2011) concluded that the trees were drawing the unaccounted water from another source. In this study, field measurements using stable isotopes were collected to identify the different sources of water used by the trees. Soil water measurements were used to populate the HYDRUS model in order to determine the distribution of soil evaporation to root water uptake (transpiration). In addition, the estimates of total evaporation from the model were verified by existing eddy co-variance measurements (and if not available surface renewal measurement were used). Figure 3.1 shows the sampling procedure followed and the samples that were collected during the study.

The research questions to be addressed in this study included:

- Are the trees using groundwater and how does their groundwater usage change between the dry and wet seasons?
- Is HYDRUS able to accurately model root water uptake and therefore transpiration?
- Can the HYDRUS model allow for the identification of depth from which the trees are extracting water?
- Does the HYDRUS model validate the use of soil water models to determine water use impacts of tree species in poorly gauged catchments?

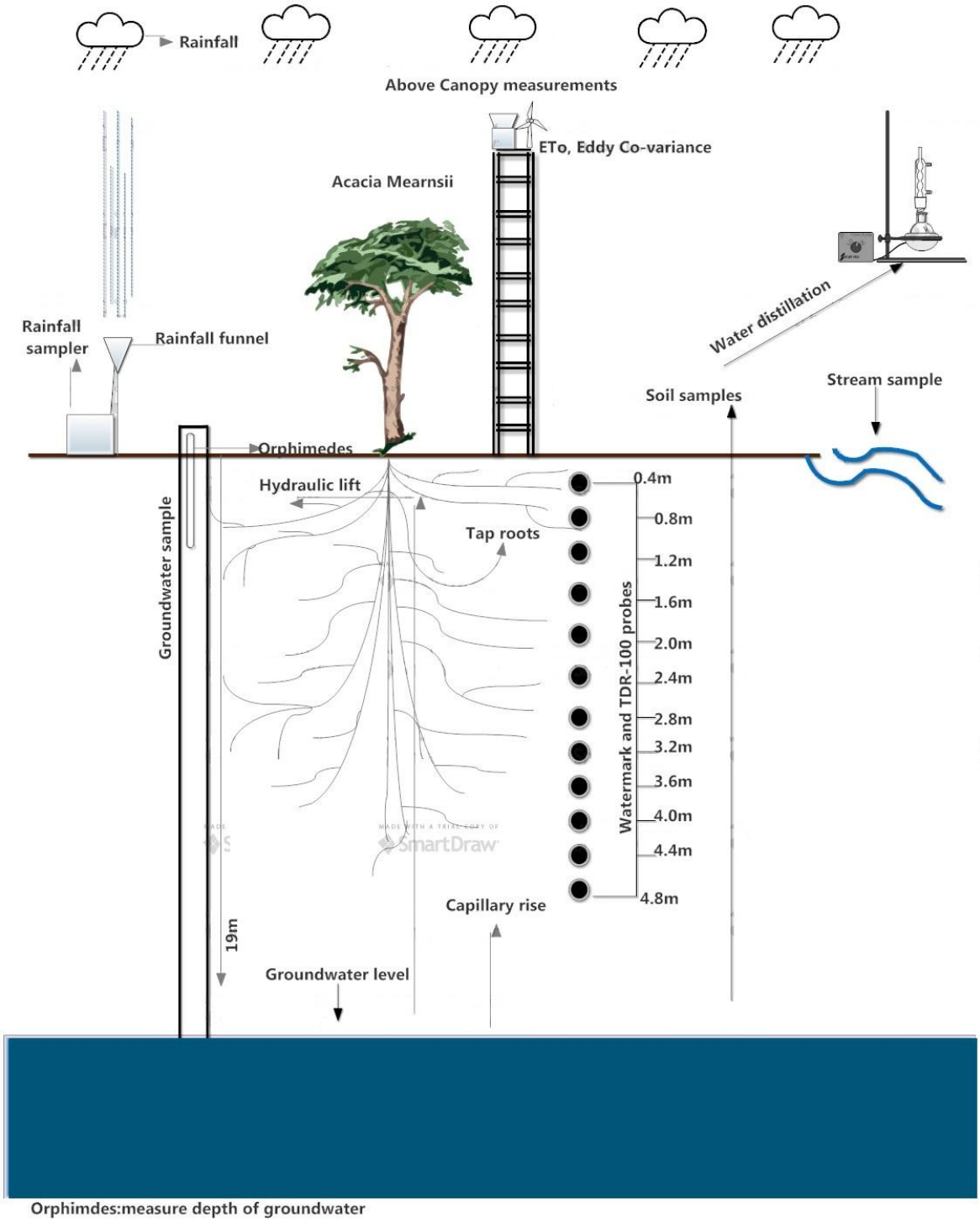

Figure 3.1 Conceptual representation of the measurement and samples that were taken at Two Streams Research Catchment.

3.2 Gaps in the literature

Literature on the possibility of *Acacia mearnsii* using groundwater as a source (in southern African conditions) is limited, as is the literature on the use of isotopes to determine the soil horizon from which trees extract water.

3.3 Hypothesis

Main Hypothesis:

If the total evaporation exceeds net rainfall, then either the seven-year-old *Acacia mearnsii* trees are able to extract groundwater, the measurement of total evaporation is flawed or soil water storage is depleted for a given period. The total evaporation measurement (surface renewal and eddy co-variance) takes into account all evaporation coming off a surface, even that of mist. Mist interception has not been measured at the catchment, which could be a source of extra moisture to the catchment.

Sub-Hypothesis 1:

If the isotope signature of soil water for a particular horizon is the same as groundwater and rooting matter has been found in this horizon, then the trees are able to access this water due to direct water uptake. If rooting matter has not been found in a particular horizon and the isotope signature of soil water is the same as groundwater, then trees are using groundwater as a source with the aid of capillary rise or hydraulic lift.

Sub-Hypothesis 2:

If the isotope signature of groundwater is the same as stream water in winter, then the majority of water leaving the catchment comes from baseflow.

Sub-Hypothesis 3:

If the isotope signature of rainfall is the same as stream water in summer, then the rainfall volume and intensity has to be great enough to cause surface runoff and therefore the majority of water leaving the catchment is from recent rainfall.

Sub-Hypothesis 4:

If HYDRUS is able to simulate total evaporation greater than that of rainfall, then the trees are able to use summer stored water to transpire freely during winter.

3.4 Study Site

The research that is presented in this document was undertaken in the Two Streams Research Catchment, in the Seven Oaks district of KwaZulu-Natal. The catchment is situated on the Greytown road, approximately 70 km north-east of Pietermaritzburg (Figure 3.2). The Two Streams Research Catchment is a hilly area that is dominated by "forb-rich, tall, sour *Themeda Triandra* grassland" (Mucina and Rutherford, 2006). The soil form that dominates the catchment is apedal and plinthic, belonging to the Ecca group of dolerite dykes and sills (Clulow *et al.*, 2011). The annual rainfall ranges from 659 to 1139 mm (Clulow *et al.*, 2011). The rainfall that the catchment receives is usually from summer thunderstorms or cold fronts, although mist is also a contributor to the precipitation that is received every year (Clulow *et al.*, 2011). Two Streams is at an elevation of roughly 1200 m.

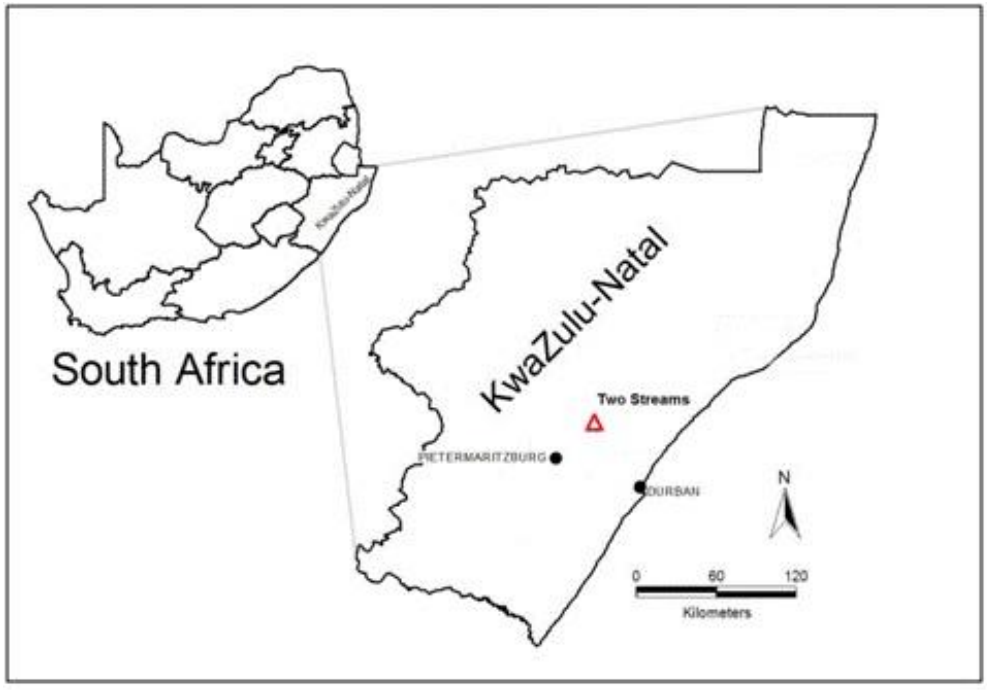

Figure 3.2 The Two Streams Research Catchment (Clulow *et al*., 2011)

3.4.1 Hydropedology

A conceptual hillslope hydropedological response model was constructed by Kuenene *et al*., (2013), using measured hydraulic properties and observed soil profile morphology (Figure 3.3)(Kuenene *et al*., 2013). The outputs of the hydropedological response model were used to confirm results from this study.

Rainfall that is received at the catchment will infiltrate and follow a vertical flow path (Arrow 1, Figure 3.3) to recharge deep weather saprolite. The hillslope soils are considered to be recharge types due to no periodic saturation being found in the solum. Overland flow can be expected when rainfall intensities are greater than the infiltration rate of the soil. The Katspruit soil in the valley bottom is frequently saturated with water, thus producing more overland flow during rain events. In the deep saprolite, water is expected to flow laterally at the transition, to less weathered and less permeable saprolite, and then to exit via the Katspruit valley bottom into the stream (Kuenene *et al*., 2013).

The research done by Kuenene *et al*. (2013) showed that *humic* A, re (light red) and ye (light yellow) horizons of the hillslope drain rapidly after a rainfall event, thus suggesting that these soils cause a recharge of water into deep saprolite, which is found at the valley bottom soils near the stream. Results from the deep neutron water meter showed that large amounts of water were stored in deep saprolite (Kuenene *et al*., 2013). The large amount of water stored in the saprolite is important for streamflow generation during the dry season and to provide water for *Acacia mearnsii* trees (Kuenene *et al*., 2013).

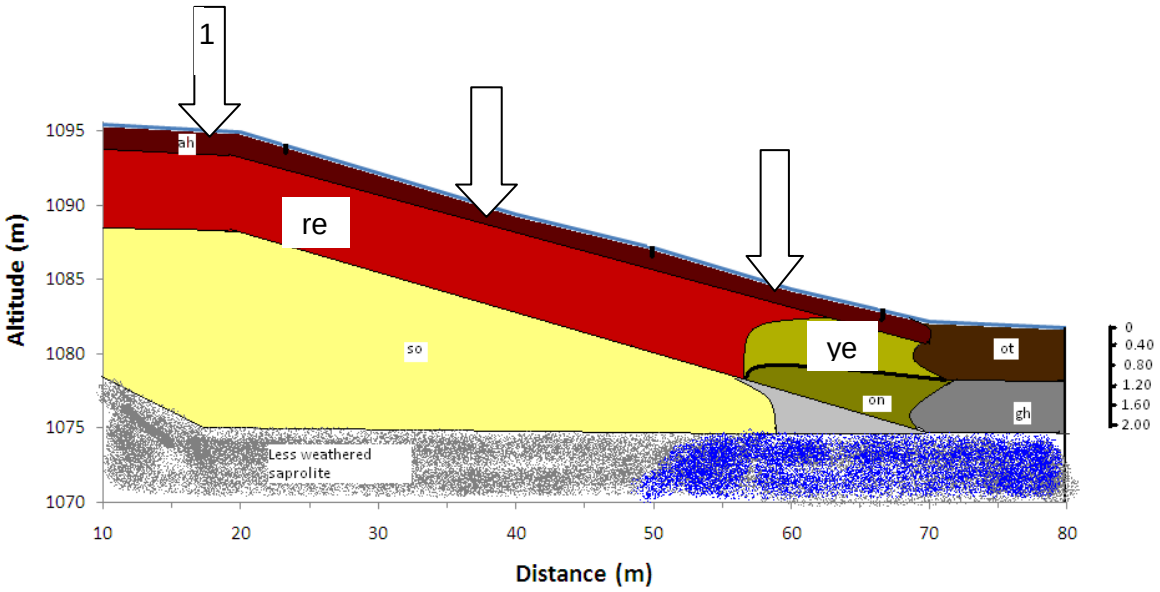

Figure 3.3 Conceptual model of a lower section of the model hillslope in the Two Streams Research Catchment (after Kuenene *et al*., 2013)

4. METHODOLOGY

4.1 Isotope analysis

When collecting samples for analysis with the isotope ratio laser spectrometry (4.5. Los Gatos Research DLT-100 Liquid Water Isotope Analyser), it is important that the during sampling process has not undergone isotope changes. If a sample has undergone isotope fractionation due to evaporation or condensation, then the sample will not be representative of the specific water being analysed. Isotope fractionation will alter the ratios between $\delta^{18}O$ and $\delta^{2}H$, which would make the tracing of source water impossible.

Therefore, fractionation was avoided during and after sampling. Bottles that were used for sample storage were placed away from sunlight, lids were tightly sealed and bottles filled with water, leaving no air spaces. The air space can cause sample phase change within the sample bottle, thus altering the signature. The machine used to analyse the water samples was a laser spectrometer, which has the capability of measuring $^{1}H/^{2}H(D)$ and $^{18}O/^{16}O$.The samples were collected from the following sources:

4.1.1 Rainfall (rainfall sampler)

Rainfall was collected using an automated sampler (ALCO), so that individual rainfall events could be differentiated and the mixing of rainfall prevented. The automated sampler was programmed so that after thirty minutes or more of no rainfall following a rain event, the sampler moved to a new bottle. A funnel was used so that there was a larger collection area to ensure that enough water was collected in each bottle during low volume events.

4.1.1.1 Development of a method to stop evaporation from occurring within sample bottles

A method was developed to stop evaporation from occurring within the open bottles of the ISCO (stream sampler) and ALCO (rainfall sampler). Weaver and Talma (2005) used a silicon oil layer as a seal to stop evaporation from occurring within their cumulative rainfall

sampler. Although silicon oils are ideal due to their temperature stability and low surface tension, concerns have been raised that by adding silicon oil, the viscosity of the sample would change, thus making the results inaccurate. Silicon oil could also contaminate the sample, giving an inaccurate reading.

The results shown below (Table 4.1 and Figure 4.1) showed that the addition of silicon oil did not contaminate the sample (although spectral analysis was not done) and that the addition of silicon oil did slow down the evaporation process by ±72% for δ^2H and ±56 % for $\delta^{18}O$. The silicon oil did not stop evaporation completely, possibly due to the insufficient quantity of silicon oil added (Table 4.1). Standard 1 (δ^2H of -61.3 permil and $\delta^{18}O$ of -8.12 permil) was used to determine if the evaporation was successfully stopped (Figure 4.1). As silicon oil was difficult to source, another solution was developed, i.e. a “U” seal. "U" seals are used by the plumbing trade as a continuously replaced air seal for drains. These results clearly showed the importance of preventing the evaporation of the samples. By preventing evaporation (fractionation) from occurring the determination of the isotope signature of incoming (rainfall) and outgoing (streamflow) water could be made accurately. The results showed that when Standard 1 was exposed to 4 days at room temperature the isotope signature changed from -61.30 (δ^2H); -8.12 ($\delta^{18}O$) to 0.20 (δ^2H); 1.47 ($\delta^{18}O$). Field samples were collected at two weekly intervals using "U" sealed bottles.

Table 4.1 Isotope results of Standard 1 showing the use of silicone oil to prevent water evaporation

Seal	Duration (days)	Temperature exposure	δ^2H (permil)	$\delta^{18}O$ (permil)
none	0	n/a	-61.30	-8.12
none	1	room temperature	-60.00	-8.16
silicone	1	room temperature	-61.29	-8.36
silicone	4	room temperature and 40◦C for 2 hours	-40.30	-4.42
silicone	4	room temperature	-43.90	-4.90
none	4	room temperature	0.20	1.47

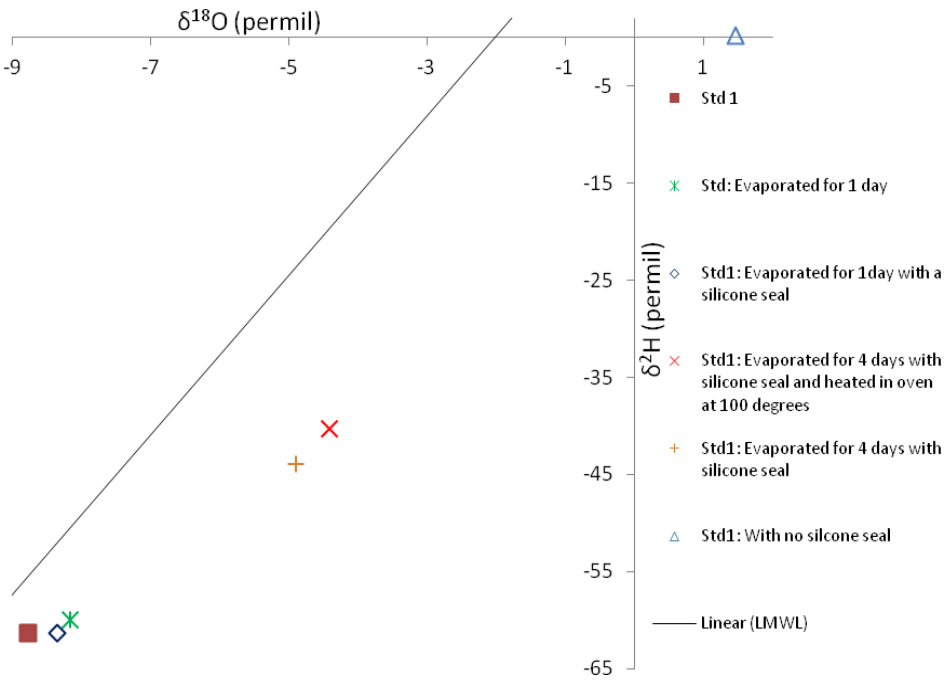

Figure 4.1 Testing of silicone seal to stop evaporation in ISCO and ALCO samplers

A “U” seal was used instead of silicon on all the gravity based systems, to stop evaporation within samples bottles (Table 4.2 and Figure 4.2). The “U” seal made use of “U” shaped glass tubing that was connected to a small funnel at the top of the U. A small hole in the lid allowed air to escape from the bottle to prevent air-locks. The water in the "U" sealed the main water sample from water that was exposed to the atmosphere in the "U". Thus further fractionation of the main water sample was prevented.

The problem with this apparatus was that the peristaltic pump delivered a faster flow rate than could be received by the “U” seal. Overflowing therefore occurred within the sampler, but this did not affect the quality of the sample in the bottle, as there was sufficient sample for analysis. The solution to this would be to install a bypass after the pump, to allow for a smaller flow rate to the “U” (Figure 4.4 and Figure 4.5). Testing of the stability of the isotope signature using a "U" seal was carried out over four days at room temperature (Table 4.2 and Figure 4.2). Since there was little deviation from Standard 1 (a deviation of 3.57 permil for δ^2H and 0.68 permil for $\delta^{18}O$ from Std 1), it was concluded that a "U" seal was a viable solution for limiting evaporation (fractionation) from the sample bottles (Figure 4.4 and Figure 4.5).

Table 4.2 Testing of the effectiveness of the "U" seal in preventing evaporation of Std1

Sample	δ^2H (permil)	$\delta^{18}O$ (permil)
Standard 1	-61.30	-8.12
U seal	-63.76	-8.80
Bottle	-65.59	-8.98

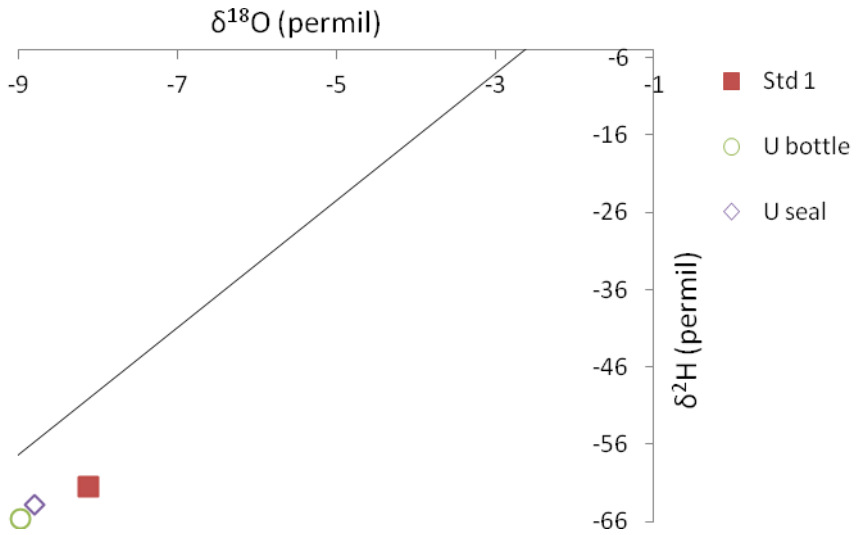

Figure 4.2 Testing of the "U" Seal to stop evaporation from occurring within sample bottles

Figure 4.3 Weather station with automated rainfall sampler and funnel

Figure 4.4 Automated rainfall sampler

Figure 4.5 Rainfall sampler bottles with "U" seal

4.1.1.2 Development of logger program for sampling of rainfall

The ALCO automated sampler was controlled by a CR200X logger and the program altered throughout the year to determine the best way to sample rainfall. The aim of using the ALCO[1] auto sampler was to be able to separate different events from one another, reduce wasteful sampling and allow for a longer time period until the sampler became full. The criteria for moving to the next bottle were based on the separation of isotope events and interception thresholds. The intercepted storage capacity of *Acacia mearsnii* at Two Streams Research Catchment ranges from 0.77-1.44 mm hr^{-1}, which is dependent on the rainfall intensity (Bulcock and Jewitt, 2012) (Equation 4.6, Section 4.4.6.2). A 2.0 mm hr^{-1} interception threshold was used, to simplify the program. The automated rainfall sampler therefore separated events that were greater than 2.0 mm (Figure 4.6). The ALCO control program was developed using Campbell Scientific Inc.'s LoggerNet, CRbasic logger development software. During sampling mode there are two sets of criteria that determine whether the sampler moves to next bottle: if rainfall received is greater than 2.0 mm plus the time since last rainfall is greater than 30 minutes and if rainfall received is greater than 16 mm.

[1] ALCO is a locally manufactured automatic rainfall/stream sampler

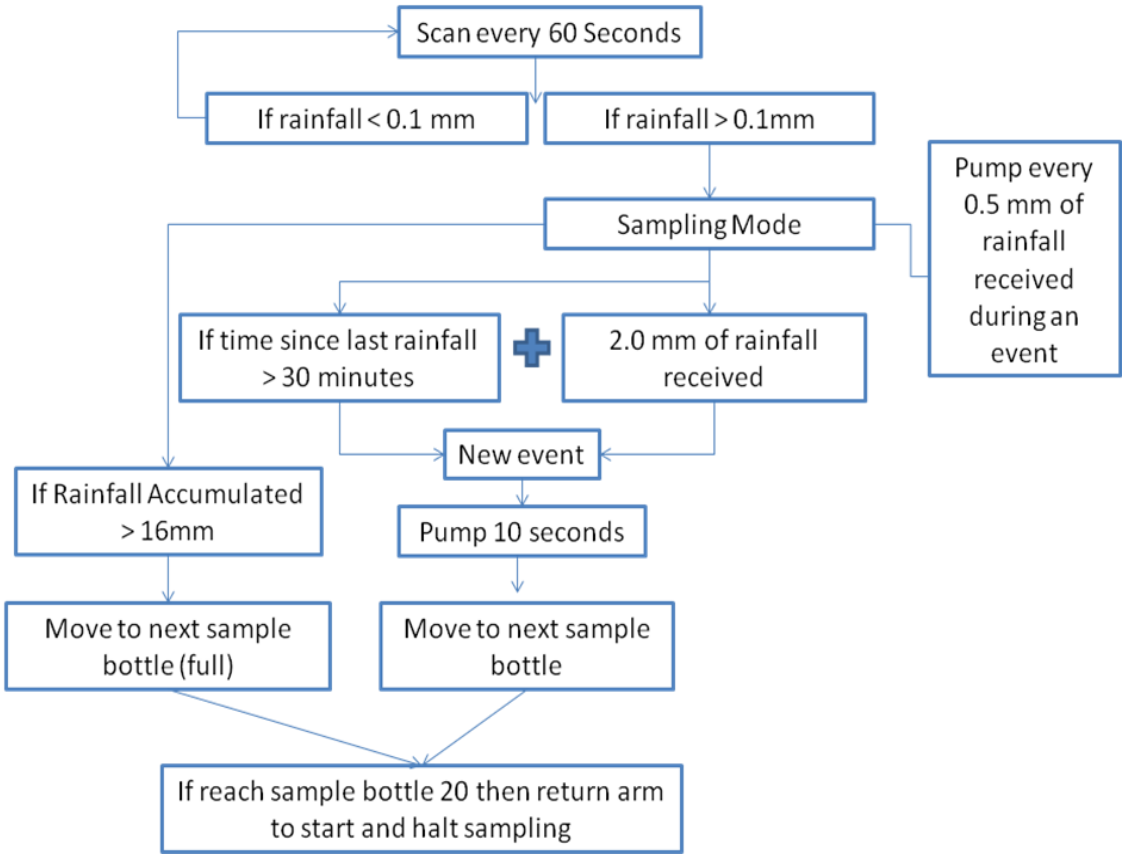

Figure 4.6 Criteria for the ALCO program to sample rainfall

4.1.2 Groundwater (boreholes)

Groundwater samples were collected at two locations from a borehole with a sealed lid, using a bailer. A bailer is a pipe with a one-way check valve at the top and the bottom. The top check valve allows air to be removed from the bailer, while the bottom one-way check valve stops the water coming out of the bailer (Sundaram *et al*., 2009). When collecting groundwater samples, nine samples were removed from the borehole and the tenth sample was used for analysis. Generally in groundwater sampling boreholes need to be purged and steady state chemical conditions, such as EC and pH need to be reached before sampling can commence, so that a representative groundwater can be collected (Mook, 2000). Although at Two Streams due to unavailability of suitable equipment (pump small enough to fit into borehole, EC and pH probe) and to limit the risk of causing a cone of depression where pumping may draw in water from other sources (Mook, 2000). Therefore, purging was manually performed using a bailer.

Samples were collected from two boreholes, namely, the centre borehole and the northern borehole, these boreholes (Figure 4.7). The water level in both boreholes was monitored

using an Ott Orphimdes level logger (OTT Hydrometrie, Germany), which recorded the depth of the groundwater at hourly intervals. The centre borehole had been drilled to 40 metres, while the northern borehole had been drilled to 60 metres (Clulow *et al*., 2011).

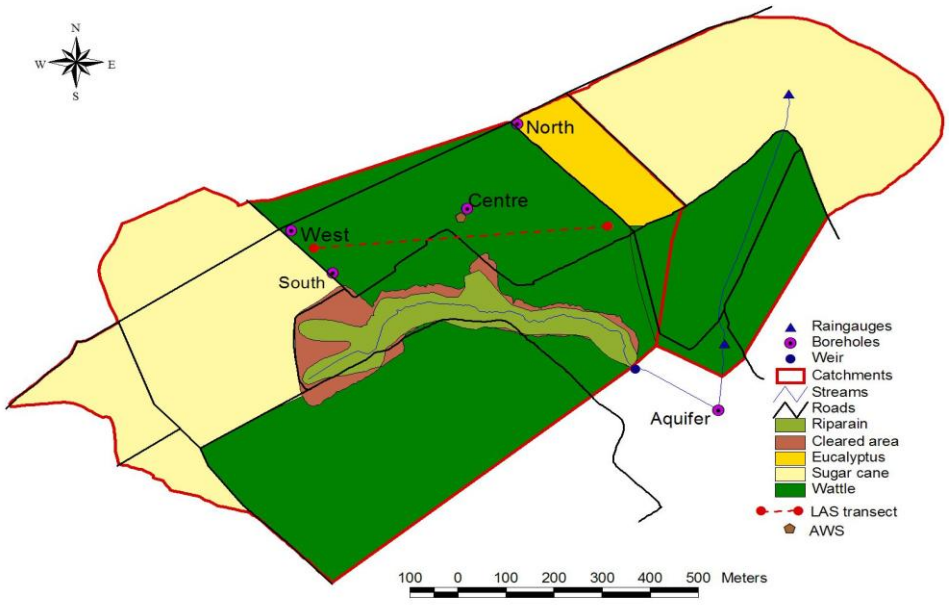

Figure 4.7 Two Streams Research Catchment showing borehole position (after Clulow *et al*., 2011)

4.1.3 Stream

Stream samples were collected using an ISCO automated sampler (Figure 4.8). The samples were collected based on event volume. The ISCO was triggered to sample during times of low flow and times of high flow. A "U" tube seal was used to stop evaporation from occurring within the bottle, as previously discussed under 4.1.1.1.

Figure 4.8 ISCO Streamflow sampler positioned at weir

4.1.4 Soil water sampling

The objective of soil water sampling was to identify the horizon in which the rooting system was able to extract groundwater from deep soil layers to drier shallow layers, due to hydraulic lift or capillary rise. Hydraulic lift is when there is a passive movement of water through roots from wetter, deeper layers to drier, shallow layers along a soil water potential gradient. Plant species that are generally able to make use of hydraulic lift are species with dimorphic root systems. Dimorphic rooting systems occur in trees that have a taproot that grows straight down to the water table and lateral roots where water can be redistributed back to the soil. Hydraulic lift allows for the redistribution of water to shallow layers, where it can be taken up to enhance transpiration (Caldwell *et al*., 1998). Hydraulic lift is an efficient mechanism to enhance transpiration rates and decrease water stress (Dawson, 1993).

In theory, cryogenic vacuum distillation is a suitable method to extract water from soil (Ehleringer and Osmond, 1989). Cryogenic vacuum distillation is a procedure that uses a cold trap, coupled with heating under a vacuum, to vaporise water from a sample and condense the sample into the cold trap (Figure 4.9). Cryogenic vacuum distillation needs to be run for 24 hours, so that all water in the sample is vaporised and so that both the light and heavy fractions are removed from the soil. Vacuum distillation needs to be air-tight, thus it is essential that no air enters the system.

When using cryogenic vacuum distillation to extract tree water/soil water, the isotope signature that is collected needs to be representative of the signature of the water in the vegetation and the signature of water that was in the soil. Thus, when collecting soil water, it is essential that both the heavy and light isotopes are removed from the samples and that not only the lighter isotopes (^{16}O and ^{1}H) are evaporated from the sample.

A check was run to determine the length of time that a sample must be run to get a representative sample from the soil. Standard 1 (Table 4.1) was added to dry soil and distilled for different time lengths and soil water contents.

Figure 4.9 Cryogenic vacuum distillation

The cryogenic vacuum distillation method was not used to extract isotopes from soils, due to the poor test results and the unavailability of equipment. Initially, the problem with the procedure was that the pump was unable to move the vapour from the sampling glass boiler into the cold trap. Another problem with the method was that liquid nitrogen sublimed before the entire sample could be collected. The liquid nitrogen also froze the tube, where vapour was moving into the cold trap, thus halting the collection of the sample (Figure 4.10). Other methods of cooling were tried, but were deemed unsuccessful, thus a new apparatus was designed to extract samples from soils.

Figure 4.10 Problem with Cryogenic Vacuum Distillation

A water distillation unit was used to extract isotopes from soils (Figure 4.11). The distillation unit uses water to cool down vapour and to collect the sample. A water distillation unit makes use of a heating mantle, a 5-litre glass bowl, a distillation unit and vacuum pump to extract water from the heated media. The vacuum pump was only used to remove the initial moisture from the system. A number of checks were run on the distillation procedure to determine if representative samples had been extracted (Figure 4.13).

Figure 4.11 Water distillation procedure

When samples that were near ground level were run in the distiller (0.4-1.0 m), the extracted water contained a substance that caused interference with the isotope machine. It was assumed that the distillation procedure extracted hydrocarbons from the rooting matter in this soil. These hydrocarbons caused the isotope machine to give false readings (Berman *et al*, 2009), similar to those of a highly evaporated sample (Table 4.3 and Figure 4.12). Hydrocarbon contamination was evident in the previous samples as the apparatus was not cleaned properly. Subsequently, the apparatus was cleaned in the furnace at 600 Celsius degrees, to burn off contaminants.

Table 4.3 Isotope composition of soil samples at various depths contaminated with hydrocarbons

Soil Depth (mm)	**$\delta^{2}H$ (permil)**	**$\delta^{18}O$ (permil)**
400	55.114	40.325
100	126.566	83.314

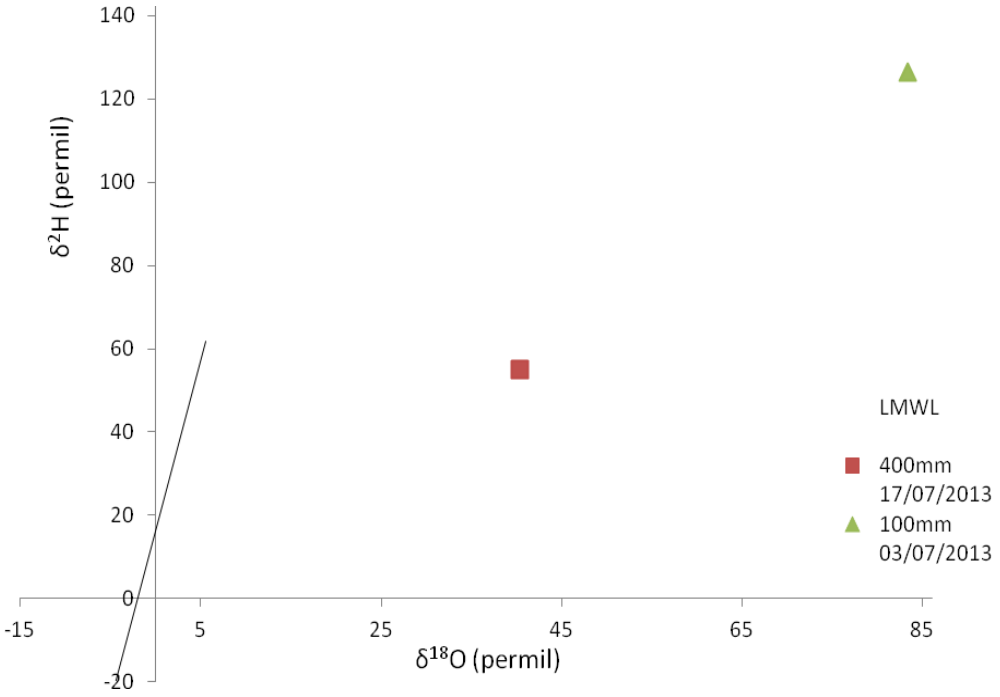

Figure 4.12 Isotope analysis of samples contaminated by burning of rooting matter

To check how accurate the distillation procedure was, Standard 1 (sample of bottled Evian water, French Alps) was added to silica sand to determine how close the isotope signature of the standard was to the distilled sample. Initially, it was perceived that the % water content was the most important factor that determined how much water was able to be extracted. Later, however, further investigation found that soil type had a larger effect on extraction volume.

Phase 1 of the system checks involved adding different quantities of Standard 1 to silica sand to determine how well the extraction process performed. The results showed that the extraction process was not feasible, as not all the water in the silica sand was extracted. The conclusion was that either heating was not long enough or the heating mantle was not hot enough to extract water.

Phase 2 of the system checks involved adding Standard 1 to dry soil from the Two Streams Research Catchment. This was done to determine the accuracy of the extraction procedure for that horizon of soil. Phase 2 of the system checks also looked at weighing masses of water and soil before and after extraction, followed by reheating in the oven to determine the amount of Standard 1 extracted. Results indicated that $\delta^{18}O$ was affected more than $\delta^{2}H$ by the amount of extraction percentage (Table 4.4 and Figure 4.13). It was

decided that results that did not have an extraction percentage higher than 85% would not be used as too much moisture was unaccounted for.

Phase 3 of the system checks involved the making of a new water distillation unit to increase the accuracy of soil isotope extraction. The new distillation unit was made bigger, to make extraction quicker. The connection between the 5-litre flask and the water distiller was changed from an "O" ring seal to a hermetic seal, to stop water being collected between the 5-litre flask and the water distillation unit. In this study the phase 3 extraction process was used to extract isotopes from soils that were taken from the Two Streams Research Catchment.

Table 4.4 System checks to determine accuracy of extraction using water distillation unit

Stage of check	Extraction amount (%)	Soil water content (%)	δ^2H (permil)	$\delta^{18}O$ (permil)
Standard 1	n/a	n/a	-61.30	-8.12
Phase 1	n/a	10	-79.84	-7.47
Phase 1	n/a	30	-76.76	-9.08
Phase 2	8	n/a	-66.63	-1.41
Phase 2	93	n/a	-58.01	-6.57
Phase 3	90	n/a	-63.81	-7.05
Phase 3	87	n/a	-56.53	-7.34

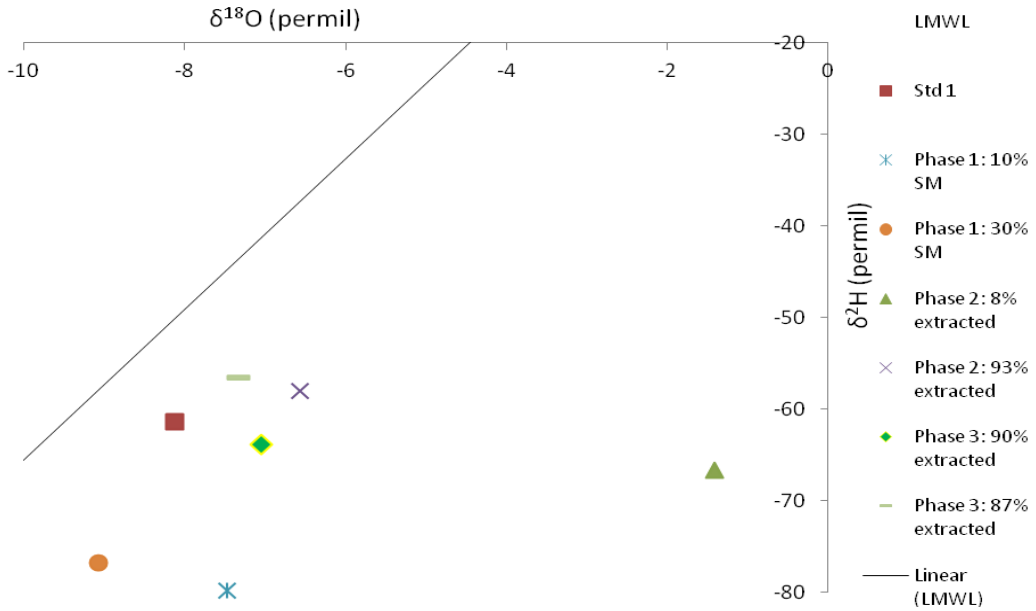

Figure 4.13 Phase 1, 2 and 3 of system checks

4.2 Soil water content analysis

Volumetric soil water content (UKZN CS 606) and soil water potential (Watermark 200, Irrometer Company, Riverside, California, USA) were monitored down the soil profile. UKZN CS 606 probes are equivalent to TDR100 probes (Campbell Scientific Inc., Logan, Utah, USA), although adjustment have been made to the shape so that they can be inserted into round augured holes (Figure 4.14).

Before the TDR 100 probes were installed, the TDR 100 probes were calibrated (against distilled water) to for the length from the TDR 100 to the SDMX 50 mulitplexers. The PC TDR program was used to determine the LA (apparent length of probe rods), LA/L (real rod length) start distance and end distance, window and temperature of the water (dielectric). Each probe was calibrated with a different probe offset. When connecting the TDR probes to the second multiplexer, there was a significant difference in probe offset. This was due to the increased length of the cable from the one multiplexer to the other in the calibration. The offsets for each probe were inserted into the CRBasic program.

The calibration of Watermark 200 sensors (Irrometer Company, Riverside, California, USA) was done using the following procedure that was entered into the logger CRBasic program:

The resistance of the sensors is calculated by assigned BRHalf instruction to the variable called KOhms.

$$kOhms = 1 \times (kOhms/1 - kOhms) \quad (4.1)$$

Where: The value of reference resistor in kOhms is given the value 1 and can be removed from the expression if desired.

Using soil temperature (Ts) and sensor resistance (Rs) the datalogger can calculate the soil water potential (kPa). There is a great need to measure soil temperature precisely as it is an important variable in soil water potential calculation.

Where soil water potential readings range from 0 to 200 kPa, the soil temperature and water potential responses can be assumed to be linear. The equation below is used to normalize the resistance measurement to 21°C.

$$R_{21} = \frac{R_s}{1-(0.018 \times dT)} \qquad (4.2)$$

Where: R_{21} is the resistance at 21°C, R_s is the measured resistance, dT is T_s - 21, T_s is soil temperature.

The water potential is then calculated from R_{21} using the following equation:

$$SWP = 7.407 \times R_{21} - 3.704$$

Where: SWP is soil water potential in kPa.

The TDR 100 probes were installed at depths of 0.4 m, 0.8 m, 1.2 m, 1.6 m, 2.0 m, 2.4 m, 2.8 m, 3.2 m, 3.6 m, 4.0 m, 4.4 m and 4.8 m. The Watermark sensors were installed at the same depths as the TDR 100 probes. Watermark sensors were installed in the same augured hole, while the TDR 100 probes were installed into different holes. Diatomatious earth was placed around each of the Watermark sensors, so that there was no shrinking and swelling of the soil around the sensor due to the drying and wetting cycles. The Watermark sensors were installed after first being submerged in water for 24 hours.

The results of the volumetric water content from the TDR 100 probes were compared to the gravimetric water content, to confirm the readings of the TDR 100 probes. Soil samples at different depths were taken 5 metres away from the TDR 100 system and oven-dried at 100°C to determine the gravimetric soil water content and not to damage cables of the TDR 100 system. The TDR 100 readings were on average, lower than that of oven dry soil. Therefore the TDR 100 under read the soil water contents of soils that were collected from Two Streams. However, because the samples had to be taken away from TDR 100 system probes, the variation observed is reasonable evidence to show the TDR probes were functioning correctly. Figure 11.1 (Appendix III) shows a comparison between TDR 100 readings and oven-dry mass readings.

Figure 4.14 Installation of UKZN CS606 probes

4.3 Xylem pressure potential

Xylem pressure potential (Shaolin Pressure Bomb, Mari Mosler-Makinose, Berlin, Germany)(similar to Scholander pressure bomb) readings were performed. A fresh branch with leaf tissue was placed inside a sealed chamber so that most of the tissue was inside and only a small amount extended outside through the chamber (Boyer, 1995). An airtight seal formed a barrier between the interior and the atmosphere. This allowed for the tissue to be pressurized inside, forcing water towards the outside. The pressure of the chamber that causes xylem to be released from the tissue is known as the water pressure potential in the tissue. The more dehydrated or stressed the tissue is, the more pressure is required to displace water. The pressure bomb makes use of the concept that the water potential in cells creates a negative pressure (tension) in the cell walls that pulls water toward the cells from the root cells, xylem and the soil. By applying a pressure to the tissue, the cell water potential rises and forces water out and into the xylem which is open to the atmosphere outside the chamber. When the applied pressure fully opposes the pressure in the sample, xylem solution appears at the surface (Boyer, 1995). The pressure in the chamber is a direct measure of the tension in the xylem because of continuous liquid phase extending into the cell walls (Scholander *et al*. 1965). Pressure potential readings were taken once a month over a winter and summer period. Pre-dawn measurements were taken at around 5.30 am while, post-dawn measurements were taken at 7.30 am. Many samples were taken and a median was determined, to exclude outliers. Pre-dawn leaf water potential readings were used as an indicator of plant stress and to identify when trees were using groundwater as their source based on the change in plant stress throughout the year.

4.4 HYDRUS

The HYDRUS model (PC-Progress) was used to determine the root water uptake of a cylindrical column of soil. HYDRUS was run with input data obtained from the measurements in the Two Streams Research Catchment (CD Appendix IV, 1-4700; 4700-8700, Input data, ATMOSPH.IN). The inputs of potential transpiration/potential evaporation were collected from surface renewal and eddy co-variance data (CD Appendix IV, 1-4700; 4700-8700, Output data, Eddy co-variance).

The HYDRUS 1D model (Pc-Progress) was used to estimate the transpiration rate from the *Acacia mearnsii* stand Catchment (CD Appendix IV, 1-4700; 4700-8700, Output data, T_Level.out, vRoot- cumulative actual transpiration). The model was set up with data that had been gathered from the Two Streams Research Catchment. The HYDRUS model was used to determine if *Acacia mearnsii* trees were using more water than was available through precipitation and the soil water balance.

HYDRUS was run using input data from the centre tower at Two Streams (section 4.4.8/9). Eddy Co-variance data was used to validate HYDRUS. Reference evaporation (grass reference) was used as potential evaporation and was proportioned into transpiration and soil water evaporation, using Beers' Law (equation 4.9, 4.10 and 4.11).

Initially, it was decided to perform inverse modelling to determine soil hydraulic parameters, but as there were only two measurements to compare with simulated soil water content, TDR (soil water content) and Watermark (tension at which water is held in the soil in KPa), it was decided that calibrating the model would lead to equifinality i.e. that similar results may be achieved with different initial conditions and in many different ways. (Refer to section 4.4.4 for hydraulic parameters)

The modelling procedure that was followed was based on research done by Hachmann (2011) in the Kruger National Park, where the objective was to determine plant available water and hydrological fluxes for two contrasting soils and vegetation types.

4.4.1 Modelling period and temporal resolution

The modelling time step was broken up into two different periods: December 2012 - July 2013 (December included as a warming up period) and July 2013 - December 2013. The

model was run in an hourly time step (to prevent numerical instability in the model iterations). When the model was run in a daily time step, it was unable to infiltrate the large rainfall events that were received and would thus "crash".

4.4.2 Modelling domain

The domain of the simulation was a rectangular column of soil, where the depth of the soil was limited to the depth at which the roots were found in the soil. The node density was set higher at the top of the column and decreased in density towards the bottom. This was done to allow for the infiltration of the large quantity rainfall events and represented the system realistically. The top boundary condition was set as an atmospheric boundary condition, which allowed for the input of time variable boundary conditions, which were potential evaporation, soil evaporation and transpiration. The bottom boundary condition was set as free drainage, to allow for water to freely drain the soil profile.

4.4.3 Material distribution and Hydraulic properties

Steady state distribution parameters for the HYDRUS run include soil hydraulic properties. Measured data from Two Streams Research Catchment were used as input data into soil hydraulic and pore size distribution models.

The soil hydraulic parameters were determined by Kuenene *et al*. (2013) for the Two Stream Research Catchment (Appendix II Table 10.1). These measurements were used as inputs into the HYDRUS model.

The Van Genuchten predictive equation for unsaturated hydraulic conductivity in terms of water retention parameters is presented below:

$$\theta_h = \begin{cases} \theta_r + \dfrac{\theta_s - \theta_r}{1 + (\alpha h)^{n})^m} & h < 0 \\ \theta_{\bar{s}} & h \geq 0 \end{cases} \qquad (4.2)$$

$$k(h) = K_{sat} S_e^l \left[1 - (1 - S_e^{\frac{1}{m}})^m \right]^2 \qquad (4.3)$$

$$m = 1 - \frac{n}{1}, n > 1 \quad (4.5)$$

where: $\theta(h)$-water retention curve (L^3L^{-3}), h - matric pressure head (L), θ_r -residual water content (L^3L^{-3}), θ_s -saturated water content (L^3L^{-3}), α - is related to the inverse of the air entry suction α > 0 (L^{-1}), n - is a measure of pore-size distribution index n > 1 (dimensionless), K_{sat} -saturated hydraulic conductivity (LT^{-1}), l -pore-connectivity parameter (dimensionless) and m is pore size distribution model.

4.4.4 Initial conditions

The initial conditions required were soil water content and soil water tension derived from TDR and Watermark probes respectively. These TDR probes and Watermarks were installed late in February 2013. The initial conditions that were selected were those of lowest soil water content at which the HYDRUS model would run (Q_s-Q_r >0) so that HYDRUS would be run in its driest state (to not overestimate total evaporation), where residual water content (Q_r) is greater than, or equal to, initial soil water content (Q_s).

4.4.5 Time dependent variable boundary conditions

4.4.5.1 Rainfall

HYDRUS was run on an hourly time-step in mm dimensions. All input parameters, including rainfall were calculated per hour (mm/hr). HYDRUS has a limited ability to separate runoff from rainfall. When rainfall exceeds the infiltration capacity of the soil, HYDRUS removes water from the soil surface, this residual value becomes the modelled runoff (Rassam *et al*., 2004).

4.4.5.2 Interception

HYDRUS does not account for interception within the model framework. Therefore interception was subtracted from rainfall before it was entered into HYDRUS. In forestry catchments such as Two Streams, interception can account for a large proportion of the rainfall. Bulcock and Jewitt (2012) measured the litter and canopy interception of *Acacia*

mearnsii at the Two Streams Research Catchment. The following equation was used to determine the gross precipitation that was received at Two Streams:

$$Sc = 0.659x^{-0.28} \quad (4.6)$$

Where Sc is the storage capacity (mm) and x is the rainfall intensity (mm hr^{-1}). The storage capacity ranges from 0.77-1.44 mm. Therefore equation 4.6 was used to determine the storage capacity of an event and if the storage capacity of consecutive events were greater than 1.44 mm, it was assumed that the canopy was fully saturated. It was assumed that after two hours of no rainfall, the canopy was dry and storage capacity was at its maximum.

Table 4.5 Intercepted rainfall at Two Streams for HYDRUS runs

	Time Step	Precipitation (mm)	Gross precipitation (mm)	Total intercepted (mm)
2013/01/01-2013/12/31	1-8759	758	571	187

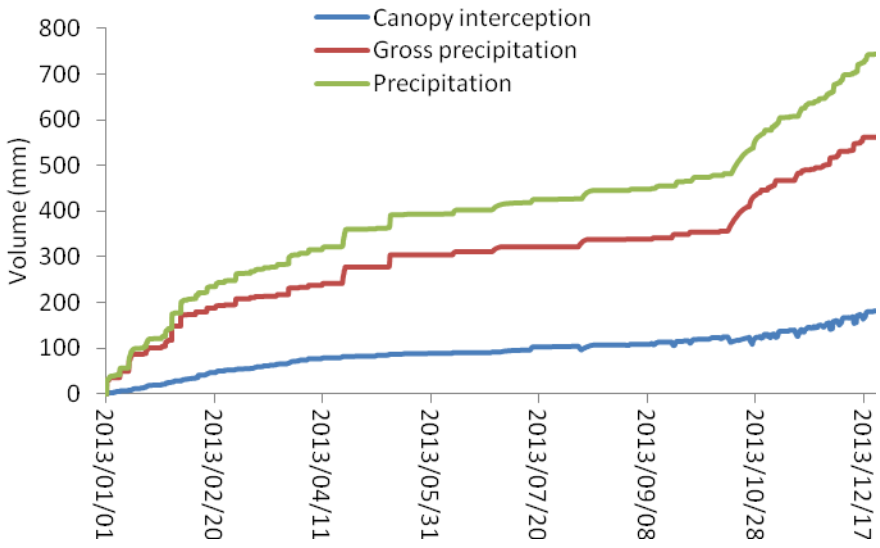

Figure 4.15 Intercepted rainfall at Two Streams for the HYDRUS runs

4.4.5.3 Surface runoff

Surface runoff can be separated in two different ways, namely, Horton-Overland Flow or Saturated Overland Flow. Horton-Overland Flow is when the rainfall intensity exceeds the infiltration rate of the soil, thus water flows horizontally on the surface, while infiltrating the soil. Horton-Overland Flow is dependent on various soil parameters and the antecedent soil water content. Dry soil has a large suction potential and thus can take up water more rapidly. However, when the soil is saturated, but not waterlogged the rate of infiltration is constant and the infiltration capacity of the soil is equal to the saturated hydraulic conductivity (Hachmann, 2011). Under conditions where water is unable to infiltrate to the deeper depth, surface runoff is described as saturated overland flow. For saturated overland flow conditions to occur, no water infiltrates the soil profile and the surface runoff that is generated is at full potential (Hachmann, 2011). At Two Streams there is a thick litter layer (20 mm) (Bulcock and Jewitt, 2012), therefore little surface runoff would occur.

4.4.5.4 Total Evaporation

The FAO56-Penman Monteith method was used to determine the reference evaporation for a short grass surface. The extension of reference evaporation from daily estimates to hourly estimates was recommended (Allen *et al*., 2006). Reference evaporation was estimated using Savage MJ, (2010) equations. The ET_0 equation was used to determine reference evaporation for hourly intervals.

$$ET_0 = \frac{0.408\Delta(R_n - G) + \gamma \frac{C_n}{T + 273} \mu_2 (e_s - e_a)}{\Delta + \gamma(1 + C_d \mu_2)} \quad (4.7)$$

Where: ET_0 is reference evapotranspiration in mm day^{-1} for 24-h time steps and mm h^{-1} for hourly time step , R_n is net radiation at the crop surface in MJ m^{-2}day^{-1} or MJ m^{-2}h^{-1}, G is soil heat flux density in MJ m^{-2} day^{-1} or MJ m^{-2}h^{-1},T is mean daily or hourly air temperature at 2 m height in °C, μ_2 is wind speed at 2 m height in m s^{-1}, e_s is saturation vapour pressure in kPa, e_a is actual vapour pressure in kPa, $(e_s - e_a)$ is saturation vapour pressure deficit in kPa, Δ is slope vapour pressure curve in kPa °C^{-1} , γ is psychrometric

constant in kPa °C^{-1}, C_n is 900 for 24 hour time step and 37 for hourly time step in K mm s^3 mg^{-1} day^{-1} and K mm s^3 mg^{-1} h^{-1} respectfully and C_d is 0.34 for 24 hour time step and for hourly time step during the day 0.24 and during the night 0.96 in s m^{-1}.

$$Kc = ETc / ET_0 \quad (4.8)$$

Kc - Crop co-efficient, ET - Reference evaporation for short grass crop, ETc - Crop evapotranspiration.

The crop factor (Kc) was determined by first plotting eddy co-variance data against FAO 56 Penman Monteith Reference evaporation (Figure 4.15). A crop factor was determined by plotting eddy co-variance data against FAO 56 Penman Monteith Reference evaporation and fitting a best-fit straight line to the data points. The crop factor was then determined from Day 335 of 2011 to Day 335 of 2012, so that the eddy co-variance data for 2013 could be used as a comparison (between HYDRUS simulated total evaporation). An average crop factor for each month was used to determine an estimate of actual evaporation.

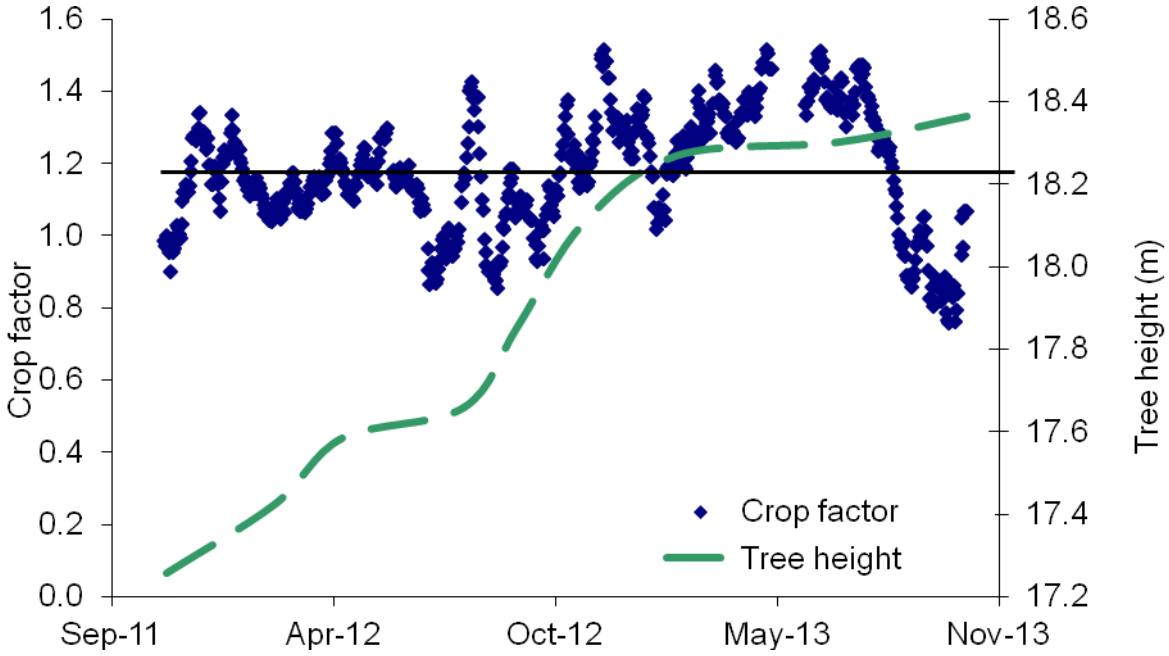

Figure 4.16 Crop factor used to determine actual ET

4.4.5.5 Partitioning root water uptake and soil water evaporation

Soil water evaporation and transpiration were separated within HYDRUS, using Beer's Law:

$$b = 1-\exp(-k \times LAI) \quad (4.9)$$

$$Et = E \times SCF \quad (4.10)$$

$$Es = E \times (1-SCF) \quad (4.11)$$

where: k - radiation extinction (rExtinct=0.463), LAI - Leaf area index ($L.L^{-1}$)(measured using LiCor LAI-2000 Plant canopy analyzer), Et - Potential plant transpiration, Es - Potential soil water evaporation and SCF - soil cover fraction defined as constant b.

The input parameter hCritA is the minimum allowed pressure head at the soil surface. The value can only be activated by evaporation. As long as the pressure head at the soil surface is higher than hCritA, the actual evaporation rate will be equal to the potential evaporation rate. Once the pressure head at the soil surface reaches that of hCritA, the actual evaporation rate decreases from the potential evaporation rate, because the soil is too dry to deliver this rate (Šimůnek, 2008). hCritA can be determined using equation 4.12 and substituting constant values from the HYDRUS manual (CD Appendix IV, 1-4700; 4700-8700, Input data, ATMOSPH.IN).

$$Hr = \exp(hMg / RT) \quad (4.12)$$

where: *Hr* is the relative humidity, h is the pressure head, M is the molecular weight of water [M/mol] (=0.018015 kg/mol), R is the universal gas constant [$ML^2/T^2/K/M$] (= 8.314 kg $m^2/s^2/K/mol$, J/mol/K), and T is the absolute temperature [K]. It was decided to use a constant from the manual, instead of the equation above to allow for maximum transpiration (simulate trees' high water use).

4.4.6 Root water uptake

Root water uptake that is simulated by HYDRUS, takes into account two parts: rooting distribution and root stress function (Feddes *et al*., 1978). The Feddes' model makes use of parameters to determine characteristics of root water uptake. This model makes use of a sink term (S) to define the volume of water that is removed from a unit volume of soil per unit time to plant uptake. The S-term is defined as:

$$S(h) = \alpha(h)S_p \quad (4.13)$$

where: $\alpha(h)$ is the root-water uptake stress function, which is a dimensionless function of the soil water pressure head $0 \leq \alpha \leq 1$ and S_p is the potential water uptake rate (T^{-1}). When soil is at saturation (wetter than h_1) and at wilting point pressure head ($h<h_4$), water uptake is assumed to be close to zero (Figure 4.17). Water uptake is at its optimal between pressure head h_2 and h_3. When the pressure head is between h_3 and h_4, water uptake decreases, while the pressure head between h_1 and h_2 water uptake increases linearly with h. S_p is a variable that is equal to the water uptake rate during periods of no water stress when $\alpha(h)$=1 (Simunek, 2012).

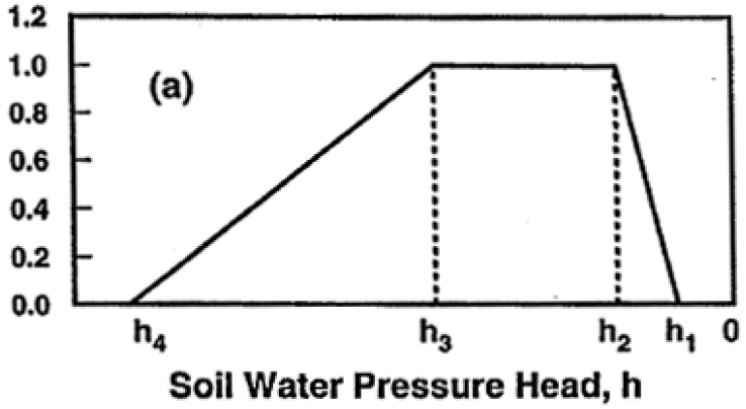

Figure 4.17 Plant water stress response function α(h) (Y-axis) vs soil water pressure head (x-axis) (Feddes *et al.,*1978)

Due to the limited number of studies done by Feddes *et al*. (1978) on the root stress function for different species, the parameter values for *Acacia* mearnsii were estimated (Appendix II, Table 10.2). The input root distribution function was graphically represented in HYDRUS, using root masses that were measured at the Two Streams Research Catchment (Clulow *et al*., 2010) (Appendix II, Table 10.3).

4.4.7 Validation

Simulated soil water content was validated using TDR 100 and previously installed soil water probes (CS 616) as discussed under 4.1.4. Simulated total evaporation (HYDRUS) was compared with actual total evaporation (eddy co-variance) (CD Appendix IV, 1-4700; 4700-8700, Output data, Eddy co-variance). Where eddy co-variance data and surface renewal data was not available, data was patched using Priestley and Taylor (1972). Priestley and Taylor (1972) was found to be accurate at Two Streams with an R^2 of 0.94.

4.4.7.1 Eddy Covariance

The eddy co-variance system makes use of high frequency measurements of CO_2 and water vapour above vegetation canopies. High frequency measurements describe gas concentrations in eddies of air that are the drivers of gas exchange above aerodynamically rough vegetation. In fully turbulent air flow, the mean vertical flux *F* is given by:

$$F = \overline{\rho_a w s} \qquad (4.14)$$

S- Entity per unit mass of fluid, ρ_a-density of air and *w*- vertical wind velocity. The over bar denotes that the measurements are averaged over a suitable period of time.

Wind velocity, air density and entity per unit mass of fluid exhibit short-period fluctuations about their mean values in the surface boundary layer. Their instantaneous values can be expressed by:

$$w = \overline{w} + w', \qquad s = \overline{s} + s', \qquad \rho_a = \overline{\rho_a} + \rho_a' \qquad (4.15)$$

The prime symbol (') denotes the departure from the mean. The expressions in 4.15 can be substituted into equation 4.16 and if fluctuations are ignored the mean vertical flux is:

$$F = \overline{\rho_a w s} + \overline{\rho_a w' s'} \qquad (4.16)$$

or by writing ρ_a for $_a$

$$F = \rho_a \overline{ws} + \rho_a \overline{w's'} \quad (4.17)$$

The first term on the right-hand side of the Equation 4.17 ($\rho_a ws$) represents the flux due to the mean mass transfer or vertical flow. The second term ($\rho_a w's'$) represents flux due to eddy motion. The mass transfer or vertical flow term may arise from the divergence or convergence of air due to the sloping surface. Over a long period of time and over horizontally uniform terrain, the total quantity of ascending air is approximately equal to the quantity descending and the mean value of the vertical velocity will be negligible. Therefore, equation 4.17 can be reduced to

$$F \approx \rho_a \overline{w's'} \quad (4.18)$$

Based on the above equation, the sensible heat flux (H) and water vapour flux (E) can be expressed as:

$$H = \rho_a C_p \overline{w'T'} \quad (4.19)$$

and

$$E = \frac{\varepsilon}{P} \rho_a \overline{w'e'_a} \quad (4.20)$$

where w′, *T′*, and $e_{a'}$ are the instantaneous departures from the mean horizontal velocity, air temperature and vapour pressure, ε is the ratio of molecular weights of water vapour and air and *P* is the atmospheric pressure.

4.5 Los Gatos Research DLT-100 Liquid Water Isotope Analyser

Water samples were analysed using the Los Gatos Research DLT-100 Liquid Water Isotope Analyser. The Isotope Analyser uses infrared absorption spectroscopy to quantify the measurement of $^{2}H/^{1}H$ and $^{18}O/^{16}O$ ratios of water samples in an optical cell. The advantages of the laser-based water isotope analyser are that it does not require extensive consumables or sample conversion and that it runs on low power, thus cost per sample is low. The disadvantage of the machine is that samples need to be clean and should not contain dissolved organic matter or alcohols (Berman *et al*, 2009). Figure 4.18 below shows the configuration of the Los Gatos Research DLT-100 analyser and how measurements are made by the LGR (LGR, 2010).

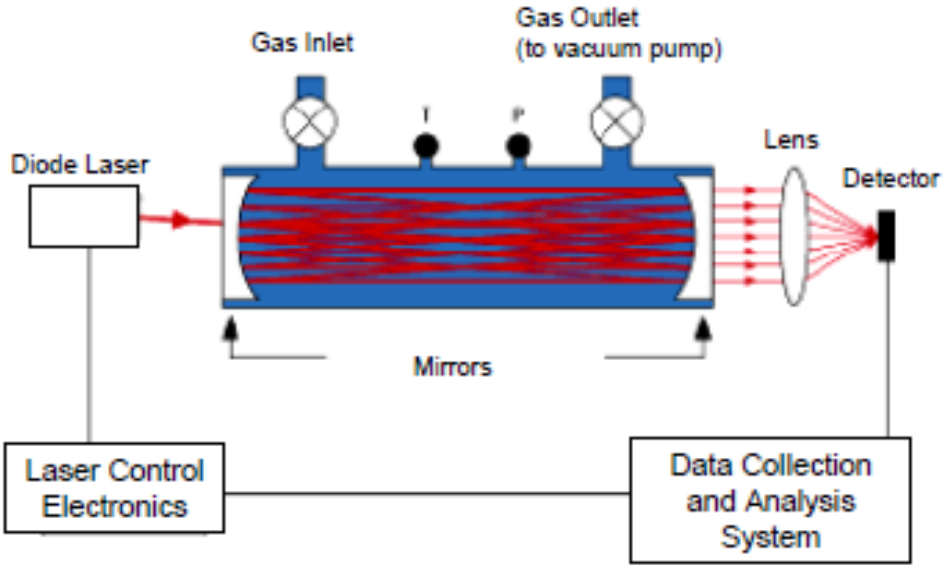

Figure 4.18 Diagram showing LGR configuration (after LGR, 2010)

4.6 Standards and References for Isotope Analysis

The sample preparation, sample measurement and sample analysis were carried out in the isotope laboratory at UKZN using the following procedures:

4.6.1 Sample Preparation

Samples were shaken to equilibrate before, being removed from the bottles. A volume of 1.5 ml of each sample was pipetted into marked autosampler vials with fresh pipette tips.

The samples were then capped with septa and stacked in the autosampler trays. Three standards were placed in the trays before every five samples and after ever five samples, to allow the machine to calibrate and to clean the needle, as samples may contain contaminants (Pretorius, 2012).

Table 4.6 Standards used for isotope analysis (after Pretorius, 2012)

Standard	Name	$\delta^{2}H$	$\delta^{18}O$
1	LGR2	-117.00	-15.55
2	VSMOW2 (IAEA)	0.00	0.00
3	IARO53 (IAD)	-61.97	-10.18

4.6.2 Sample Measurement

Each sample was sub-sampled six times, using the Los Gatos Research (LGR) DLT-100 Liquid Water Isotope Laser Analyser (Pretorius, 2012).

4.6.3 Sample Analysis

The LGR DT-100 analyser reports $^{2}H/^{1}H$ and $^{18}O/^{16}O$ ratios and not δ values on a VSMOW scale. Post-processing required the determination of the ratios for the standards and the development of a relationship between known VSMOW δ values and the measured ratios of the different standards. A relationship was applied to determine the ratio of each of the measured sub-sample ratios.

The post-processing checks that were implemented in this research included (after Pretorius 2012):

- The temperature variation of rate of change of less than 0.3°C/hour or a standard deviation for each sample less than 0.004°C,
- The sub-sample density between 2 to 4x 10^{16} molecules cm^{-3} and standard deviation between measurement less than 1000 times smaller than the injected density,
- The deviation of $^{2}H/^{1}H$ less than 1000x smaller than the measured ratio and $^{18}O/^{16}O$ less than 3000x smaller than the measured ratio, and

- The results of each sub-sample were reported as an average and the standard deviation of the six injections. The standard deviation of ^{2}H results should be less than 2 permil (0.002%) and ^{18}O less than 0.3 permil (0.0003%).

5. SOURCES OF ERRORS

5.1 Isotope ratio infrared spectroscopy

The machine that was used to analyse isotope samples was an Off-Axis Integrated Cavity Output Spectroscopy (OA-ICO) Los Gatos Research DLT-100 Liquid Water Isotope Analyser (IRIS).

Measurements from Isotope Ratio Infrared Spectrometer (IRIS) are comparable with measurements from the Isotope Ratio Mass Spectrometer (IRMS). Methods of removing organic contaminants from the samples prior to analysis have not been fully developed or validated, although post-data processing software has been developed to flag samples that contain organic contaminants. Research done by the University of California on sap samples that have been collected by means of cryogenic vacuum distillation, showed samples that should be treated with activated charcoal to remove organics and make samples clear and odourless. This method reduces errors in measurement when using the IRIS. The post-data processing software for off-axis integrated cavity output spectroscopy is Spectral Contaminant Identifier (SCI) software (West *et al*., 2011). The SCI software was used to determine the interference metric that was recorded by the spectra (West *et al*., 2011). The metric was compared with that of known standards and good or bad flags were used to indicate the reliability of the measurement. From the research done at the University of California on sap samples, the results showed that the IRIS gives less error when compared to those from IRMS. Spectral interference can only be used to determine if there are contamination problems and errors in the measurement (West *et al*., 2011).

6. RESULTS AND DISCUSSION

6.1 Isotope results

6.1.1 Rainfall signatures

In theory, the isotope composition of precipitation should follow the Rayleigh Equation for an open equilibrium system under ideal conditions, which is when condensation takes place without reaching super saturation and when rainfall falls as soon as droplets are formed. However, in reality, the isotope composition of precipitation follows the rules of a closed system, in that there is a depletion or enrichment of heavier isotopes as the liquid water content in the clouds increases or dissipates. The process is dominated by equilibrium fractionation (Gat, 2010).

Rainfall isotope signatures were collected using an automated sampler (ALCO). The rainfall isotopes are the incoming isotope signature into the catchment. The rainfall signatures from the catchment were used to determine a Local Meteoric Water Line (LMWL), which was used to interpret samples collected at different locations (Figure 6.1). The LMWL shows a slight deviation ($y=8.2503x + 19.323$, R^2 of 0.96) from the Global Meteoric Water Line (GMWL) ($y=8.17x + 11.27$, R^2 of 1), suggesting that samples from the catchment contain more δ^2H than international standards. The slope of the GMWL and the LMWL are similar (±0.1), although the y intercept is different (±8.5 permil).

The local rainfall isotope signature at Two Streams is similar to that at Weatherly, Eastern Cape, (Lorentz *et al*., 2007) Line b (2.1.4.2.1, Figure 2.1, below Figure 6.1 and in Appendix I, Table 9.1). The rainfall at Two Streams generally falls in the middle (-5 to 0 permil ($\delta^{18}O$) and -25 to 25 permil (δ^2H)) of the LMWL. Rainfall signatures that ranged from -150 to -70 permil (δ^2H) and -20 to -10 permil ($\delta^{18}O$) reflect rainfall that was received from cold events, when super cooled temperatures were reached in the atmosphere, causing the signature to be close to that of snow melt water (EVIAN, STD1, -61.43 permil (δ^2H) and -8.12 permil ($\delta^{18}O$)). According to Lorentz *et al*. (2007), rainfall that occurs at higher elevation, inland locations and in cooler zones falls on the lower end of the LMWL, while rainfall that falls at low altitudes, in warmer areas and near oceans, usually falls at the higher end of the LMWL. Therefore, one can presume that, due to Two Streams being

inland and at a relativity high altitude (1500 m), the rainfall signatures should fall on the lower end of the LMWL.

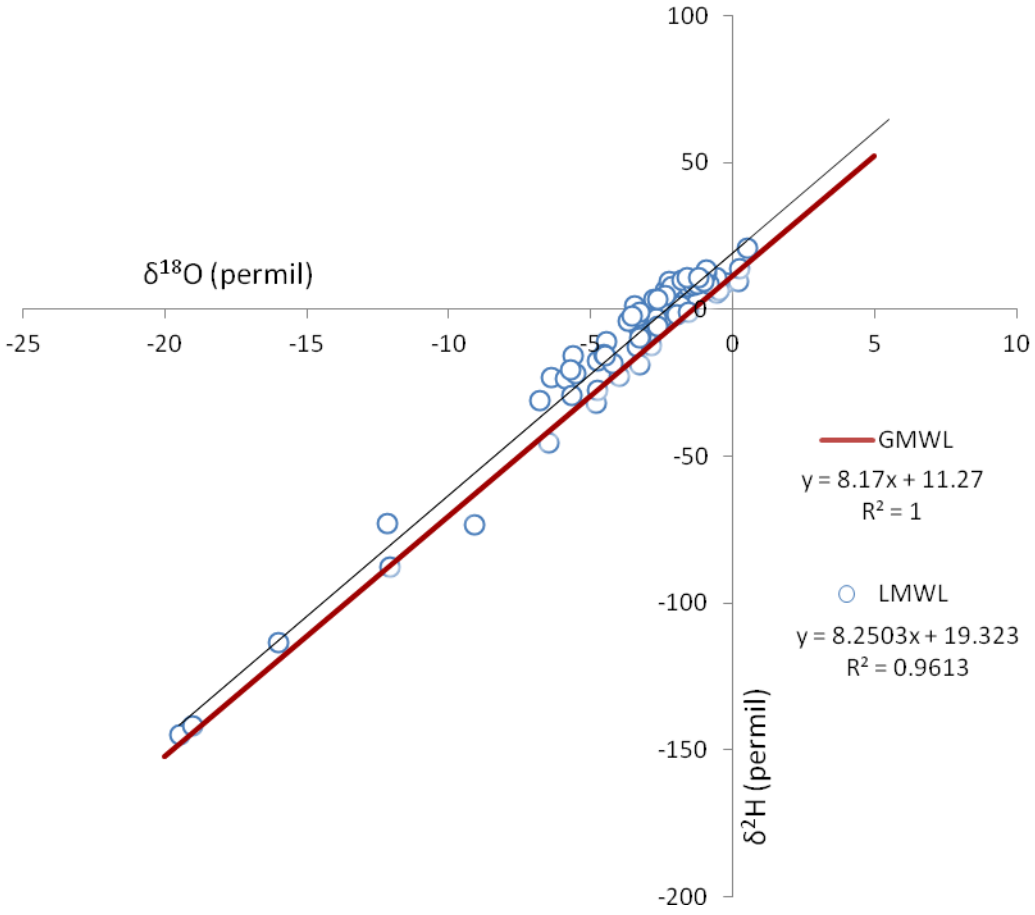

Figure 6.1 Rainfall isotopes showing the LMWL for Two Streams for 2013

Isotope fractionation occurs when water evaporates and loses mass in its lighter isotope fractions. When rain falls, water is subject to evaporation within the atmosphere. According to Dansgaard (1964), there are five factors that determine the composition of precipitation. These are, namely; altitude, temperature, the amount of precipitation, continentality and the source region of evaporation to form clouds. Due to the installation of an FAO-56 Automatic Weather Station that is positioned opposite the automated rainfall sampler (Figure 4.3) at Two Streams Research Catchment, it was possible to plot rainfall isotope signature with air temperature and the amount of precipitation. There was no trend observed between rainfall isotope signature and ground air temperature (Appendix I, Table 9.1).

There was no evident trend when plotting rainfall isotope signature with rainfall volume, although it was noted that there was a weak relationship (R^2=0.08). Generally, it would be

expected that the large events in winter (greater than 5 mm) would yield a more negative signature δ^2H (DH), as they are cold fronts and therefore less evaporation will occur (Figure 6.2). On occasions, large events have a more negative signature, but in July during the sampling of multiple events, it was evident that rainfall volume is not directly related to isotope signature (Figure 6.2). Throughout winter the δ^2H isotope signature fluctuated between -30 permil and 10 permil (‰). Rainfall events greater than 5 mm yielded δ^2H isotope signatures ranging from 0 permil to -30 permil. During summer, the δ^2H rainfall isotope signature varied from 15 permil to -45 permil, where the majority of the events that were received were greater than 5 mm.

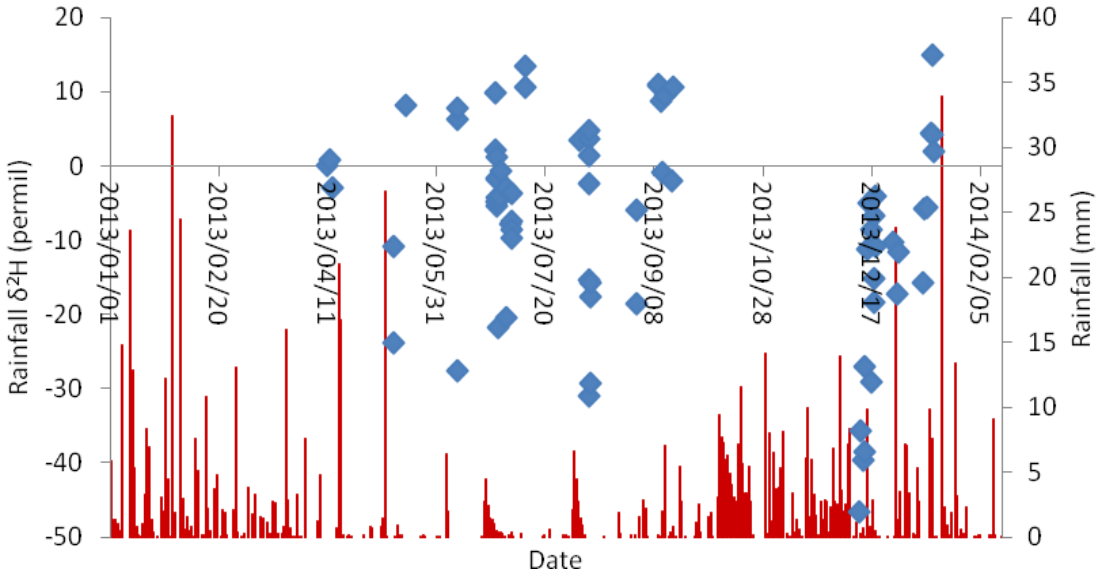

Figure 6.2 Relationship between rainfall volume and isotope signature

6.1.2 Streamflow and Groundwater

Shallow groundwater is not subject to high and low temperatures and thus is similar to meteoric water (High temperatures cause evaporation to occur quicker, therefore making heavier isotopes more abundant). In regions where there are high temperatures, the isotope composition of rainfall is different to that of groundwater, due to the removal of lighter fractions during infiltration (Singh and Kumar, 2005). During convective rainfall events, rainfall is subject to high temperatures at Two Streams, thus there is a difference between rainfall composition and groundwater composition. At Two Streams the groundwater signature (-5 to -12 permil (δ^2H) and -2 to -4 permil ($\delta^{18}O$)) generally lies in between the stream (-3 to -17 permil (δ^2H) and -4 to -2 permil ($\delta^{18}O$)) (Figure 6.3) and the rainfall signature (70 to -180 permil (δ^2H) and -20 to -15 permil ($\delta^{18}O$)) (Figure 6.2).

The main contributor to streamflow at the Two Streams Research Catchment is groundwater (Figure 6.3 and Appendix I, Table 9.2, Table 9.3). On a few occasions, the isotope signature of streamflow does not match (δ^2H value of -15, -20 and -25 permil) that of groundwater and therefore the stream is fed by overland flow or direct rainfall (where isotope signature of the stream is between -15 and -4.5 permil (δ^2H), -25 and -5 permil ($\delta^{18}O$) (Figure 6.4).

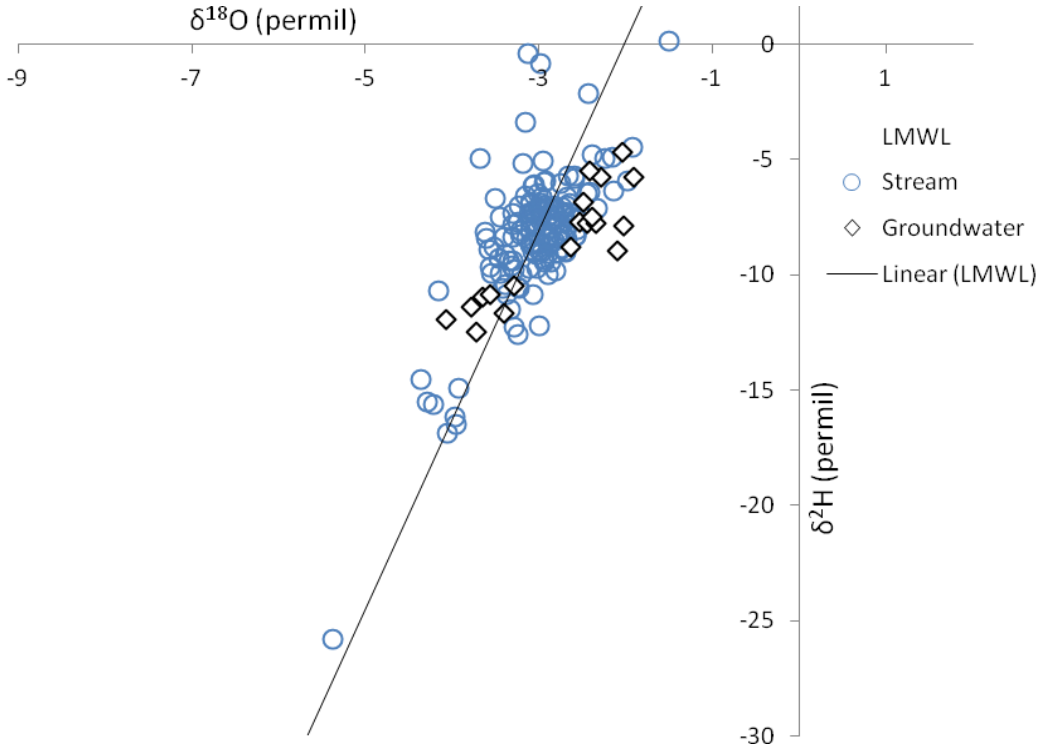

Figure 6.3 Stream signature with groundwater signature

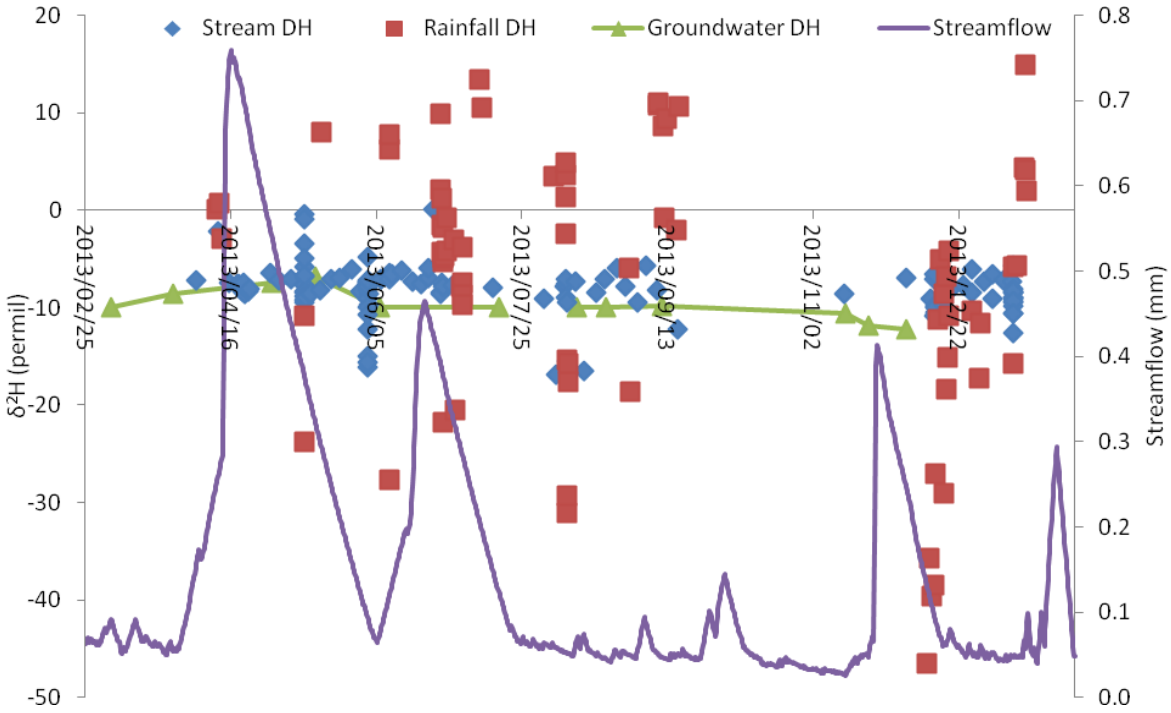

Figure 6.4 Isotope signatures of rain, groundwater and stream water with streamflow record

In South Africa there is a large variation in the rainfall isotope signature because of the vast variation in the type of rainfall events (cold front/convective events) that are received. Therefore the isotope signature of rainfall varies significantly throughout the year. From 2013/09/22 to 2013/11/11 there were a few malfunctions in the automated samplers that halted sampling during this time (Figure 6.4). The groundwater isotope signature generally lies in the middle (δ^2H of -10 permil) of the average rainfall signatures (δ^2H of 10 and -15 permil) and the stream water signature (δ^2H of -8 permil) (Figure 6.4). The stream water signature varies throughout the year (δ^2H ranges from 0 to -17 permil), where the main source leaving the catchment comes from groundwater (δ^2H value of -10 permil). A factor to this could be due to a groundwater ridging pressure wave that causes pre-event water to appear in large quantities in stormflow hydrograph. Research done by Waswa *et al*. (2013) at the Weatherly Catchment has shown that groundwater ridging pressure waves can occur at low-lying wetland zones and when capillary fringe is close to the ground surface.

Generally during the year, the stream signature is similar to that of groundwater (δ^2H of -8 to -10 permil), but there were occasions that the stream signature was the same as that of rainfall (on the 23/08/2013, δ^2H of -17 permil), suggesting overland flow or direct rainfall.

Stream δ^2H was predominately more positive (δ^2H of -8 permil) than groundwater (δ^2H of -10 permil) and rainfall (δ^2H of 10 and -15 permil), which is due to the evaporation of water.

Throughout the year there was a slight fluctuation in the δ^2H groundwater isotope signature which varied from -11 permil to -6 permil (Figure 6.5). During the period 2013/02-2013/05 there was an increase in δ^2H from -10 to -6 permil; this could be due to recharge of the groundwater by means of water enriched in δ^2H and $\delta^{16}O$ signature. (Figure 6.2 and Figure 6.5). During the period 2013/06-2013/09 the groundwater δ2H signature did not vary much (-10 permil); this is due to limited recharge as there is little rainfall (Figure 6.5). During the period 2013/11-2013/12 there is a change in groundwater δ^2H from -10 to -12 permil, caused by the recharge of groundwater by rainfall that has been subject to little evaporation (cold fronts) (Figure 6.4 and Figure 6.5).

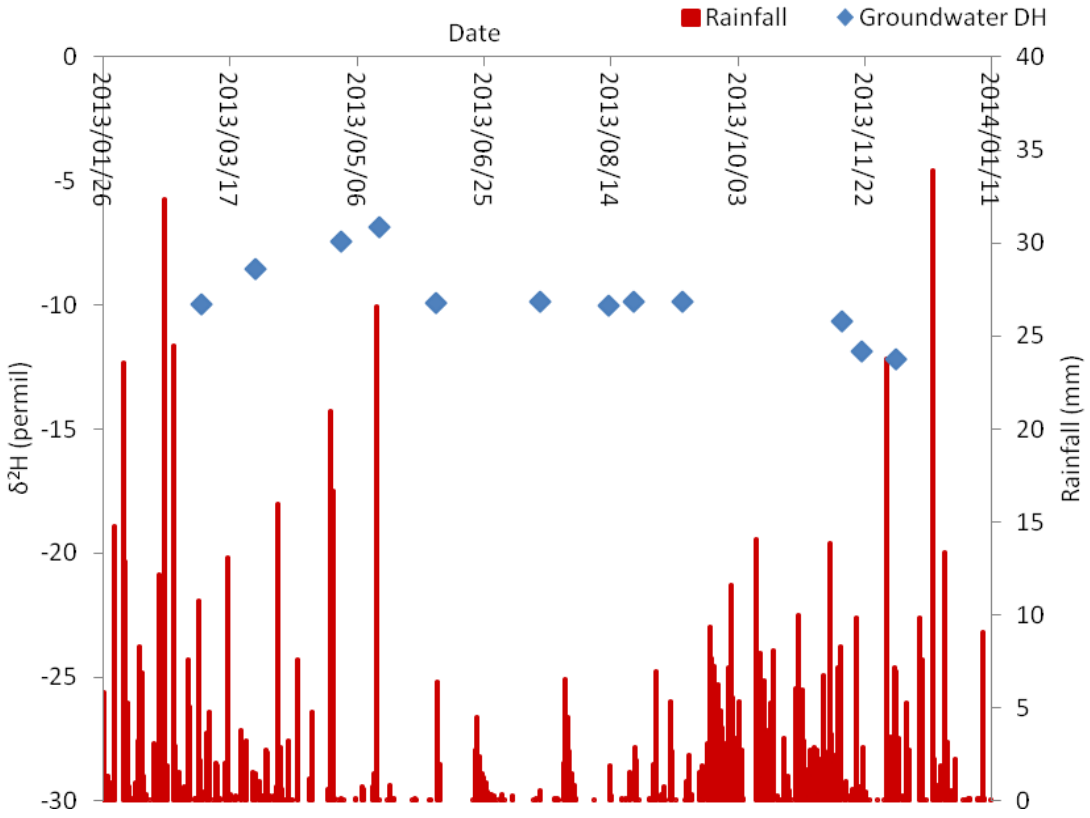

Figure 6.5 Changes in groundwater δ^2H with observed rainfall

6.1.3 Soil Isotope signature

In theory, after rainfall events, or in capillary rise zones there is an isotope composition gradient that is established between the water at the evaporating surface which is enriched with heavy isotopes and the water in the deeper soil layers which is similar to that of input water. Above the evaporating surface, vapour is the dominant transport, while below the evaporating surface, liquid is the dominant form of transport (Gat, 2010).

The literature suggests that there is an isotope composition similarity between soil water and Standard Mean Ocean Water (SMOW) for a site with mean percolation rate of 260mm/year. At soil depths of 0.3, 1.4 and 4.0 m the $\delta^{18}O$ permil relative to SMOW is -12.2, -12, respectively, while in winter, while in summer at depths 1 and 2.4 m the $\delta^{18}O$ permil relative to SMOW is -11 and 10.8 respectively (Figure 2.2)(Gat, 2010). Research done by Grellier *et al*. (2011) on *Acacia sieberiana* in the KwaZulu-Natal grasslands showed that the $\delta^{18}O$ soil isotope signature under the tree canopy at 1 m was between -4.8 to -3.8 permil, while at 1.6 m it was -5 permil and at 2 m was -5.2 permil (Figure 2.3).

The $\delta^{18}O$ soil isotope signatures that were collected at Two Streams are more positive compared to those in the literature (Figure 6.6 and Appendix I, Table 9.4). At a soil depth of 1.6 m the $\delta^{18}O$ isotope composition was -0.20 permil in winter and 2.0 permil in summer, a significant difference to the findings of Grellier *et al*. (2011). At a soil depth of 2.0 m the $\delta^{18}O$ was -1.0 permil during winter, which is different to that of -5.2 permil shown by Grellier *et al*. (2011). The differences between the two catchments areas are vast and therefore comparison is speculative.

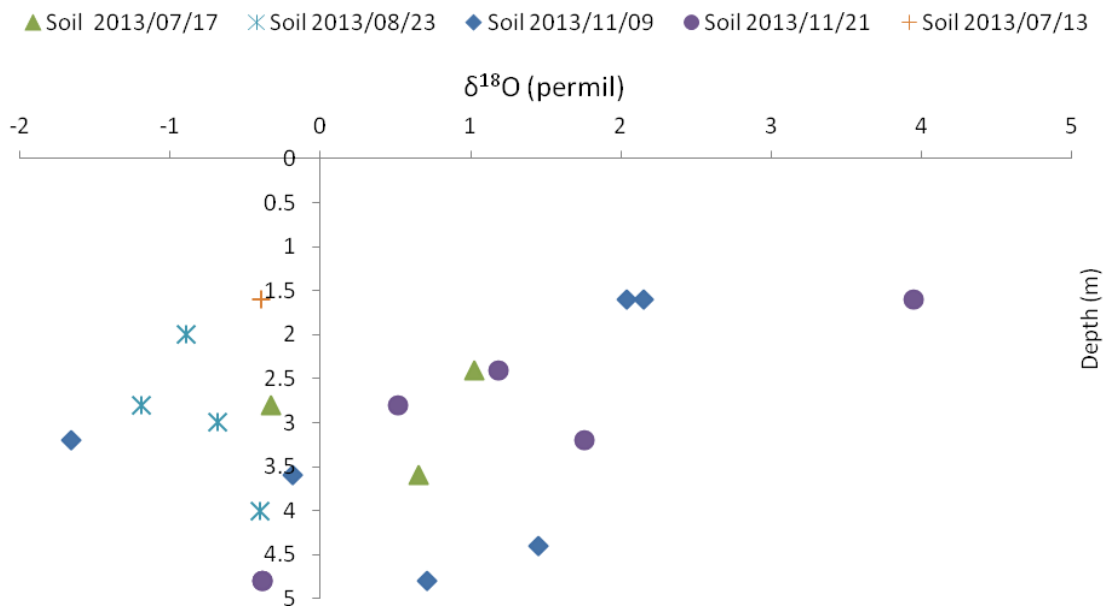

Figure 6.6 Isotope signature ($\delta^{18}O$) with soil depth

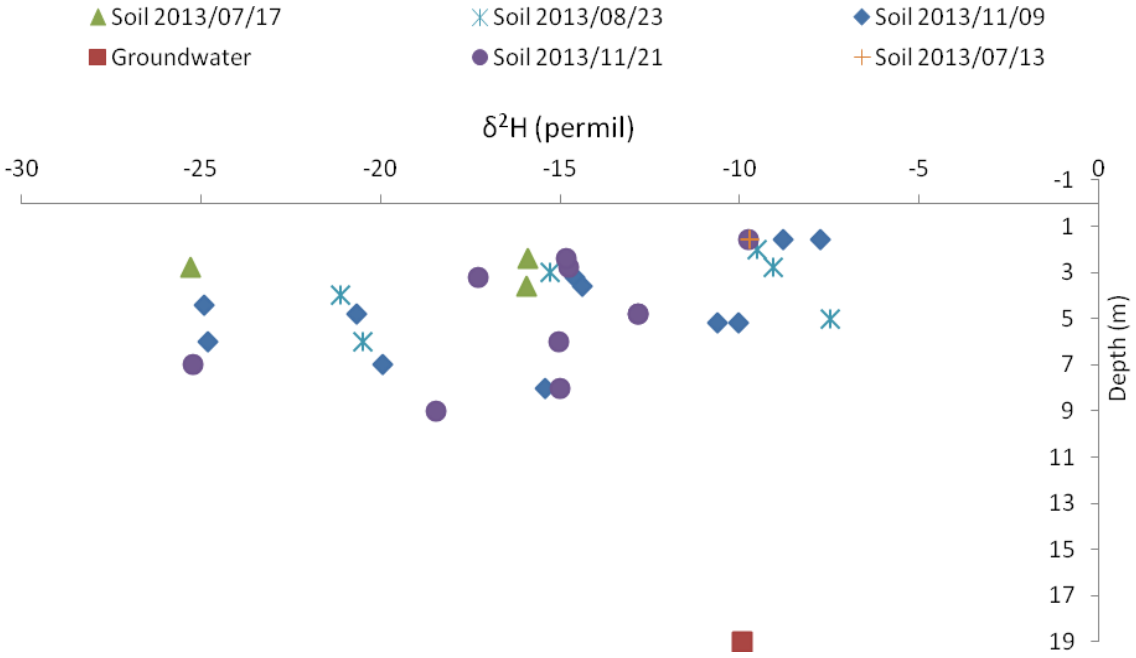

Figure 6.7 The isotope signature of soil and groundwater with respect to their depths ($\delta^{2}H$)

It is generally accepted that the deeper down the soil horizon, the heavier the isotopes. Large rainfall events are able to induce infiltration past the rooting zone more readily than smaller and less intense rainfall events. The isotope composition of soil water at Two Streams varies with depth down the soil profile. The rainfall at Two Streams generally lies around the GMWL, while groundwater lies lower down on the GMWL (Figure 6.8). The soil isotope signatures lie to the right of the GMWL, suggesting there are more ^{18}O to ^{16}O and

more ^{2}H to ^{1}H, which suggests that evaporation has taken place (Figure 6.8). The isotope composition of soil lies from -25 to 9 permil ($\delta^{2}H$) and -4 to -2 permil ($\delta^{18}O$).

On two occasions in winter, 13/07/2013 and 23/08/2013, the 2, 2.4 and 1.6 m soil horizons have the same isotope signature as groundwater (Figure 6.9) suggesting that hydraulic lift or capillary rise has moved groundwater from deeper horizons to this depth for root water uptake (see measured rooting massed, Appendix II, Table 10.3 for rooting masses). Samples collected from 09/11/2013 to 21/11/2013 showed that from 1 to 2 m the soil isotope signature had become more positive due to the replenishment of soil water by evaporated rainfall (Figure 6.9). However, between 4 and 5 m the soil isotope signature is similar to that of groundwater, suggesting that rainfall did not replenish the soil water store down to 4 m.

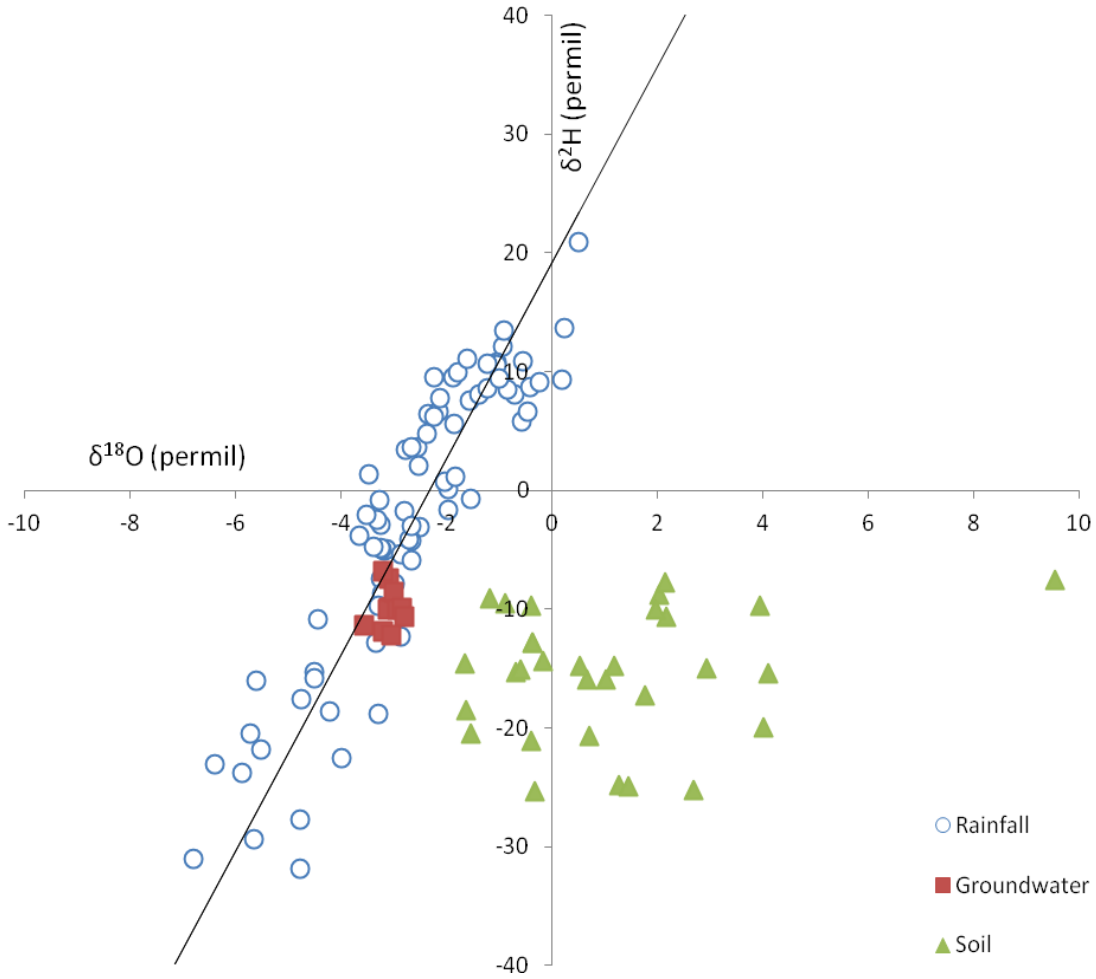

Figure 6.8 Combination of soil, rainfall and groundwater signatures

A possible reason that hydraulic lift or capillary rise has moved groundwater to the 4-5, 2, 2.4 and 1.6 m levels and that the isotope signature of deeper horizons does not match

that of groundwater, is that the existing soil isotope signature (infiltrated rainfall) mixed with that of groundwater (Figure 6.9) therefore making it hard to identify the groundwater signature.

Samples collected on 13/07/2013, 23/08/2013 and 11/09/2013 at the 2, 2.4, 1.6, 4-5 m soil horizons had a similar isotope composition to groundwater (Figure 6.9). There is a slight difference of ±1.0 between groundwater and soil water, although the accuracy of extraction using a water distillation unit is less when looking at the $\delta^{18}O$, than when looking at the $\delta^{2}H$. The accuracy of extraction of the $\delta^{2}H$ scale was 96%, while that of $\delta^{18}O$ was 86%, therefore the extraction of $\delta^{2}H$ is more accurate. Due to the upward fluxes mixing with downward fluxes, the isotope composition within the soil horizons varies significantly throughout the year. A trend line with soil depth was therefore not plotted. The soil $\delta^{2}H$ values between 2 and 3 m changed from -15 permil on the 17/07/2013 to -9 permil on 23/08/2013. There is little change in isotope composition between the 3 and 4 m soil horizon (-15 permil to -14 permil). The soil $\delta^{2}H$ value between 4 and 5 m changes in isotope composition from -20 permil on 23/08/2013 to -6 permil, -12 permil and -25 permil on 21/11/2013. Deep soil $\delta^{2}H$ signature values range from -15 permil to -25 permil. There is a relationship between groundwater and soil water, where groundwater is present in deep soil water during winter. During summer when there is more rainfall, the isotope composition of soil water is similar to rainfall.

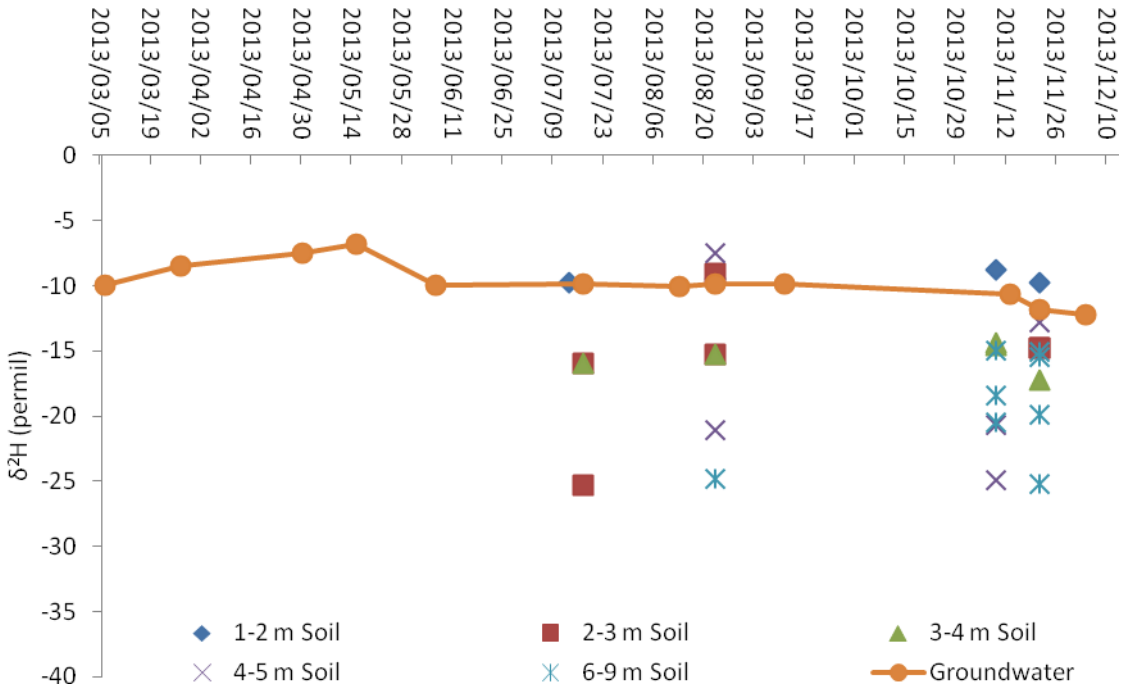

Figure 6.9 Time series of changes in soil $\delta^{2}H$ and groundwater $\delta^{2}H$

6.2 HYDRUS results

In the following section the results from HYDRUS that will be presented are:

- A validation to compare measured soil water content from CS616 and TDR 100 probes to simulated soil water content from HYDRUS.

- A comparison between potential root water uptake and actual root water uptake.

- A comparison between total evaporation measured using Eddy co-variance and simulated total evaporation.

6.2.1 Infiltration

The output data from HYDRUS suggested that all rainfall that was entered into the model infiltrated the soil surface, with no runoff. In a forested catchment it is understandable that the majority of rainfall received is allowed to infiltrate due to the large litter layer present below the canopy.

6.2.2 Validation

(Refer to CD Appendix IV, 1-4700;4700-8700, Output data, Obs_Node.out for raw data)
HYDRUS simulation was validated by comparing measured soil water from TDR 100 with those simulated by HYDRUS. The CS616 surface probe at 100 mm was used to compare with the surface observation node of HYDRUS (Figure 6.10). HYDRUS overestimated soil water content when there were small rainfall events and underestimated soil water content when there were large events (Figure 6.10). HYDRUS overestimated soil water content by < 20% to that of CS616 probe.

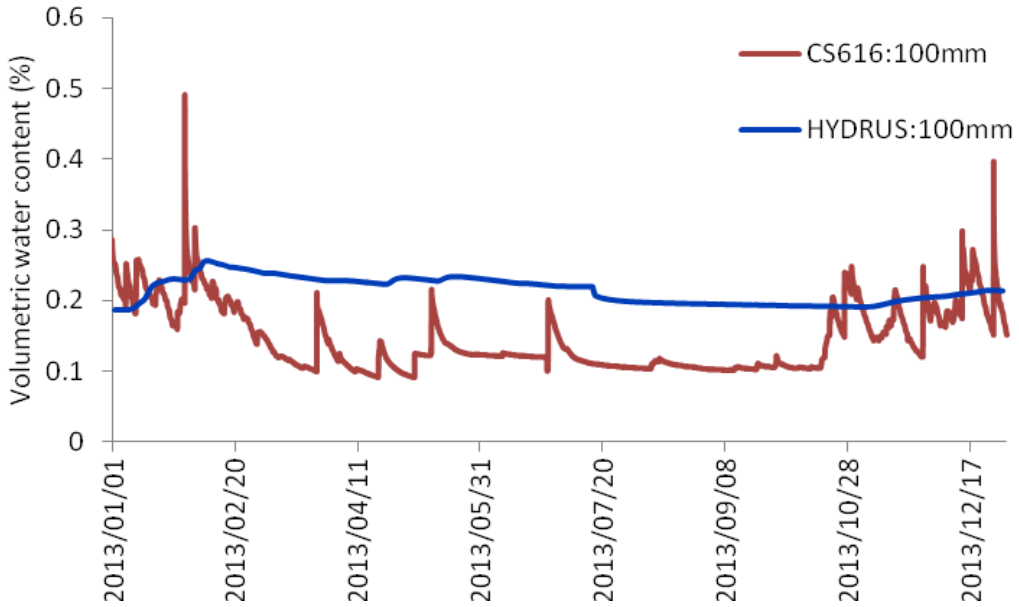

Figure 6.10 Comparison between CS616 surface probe 100 mm and HYDRUS simulation at 100 mm

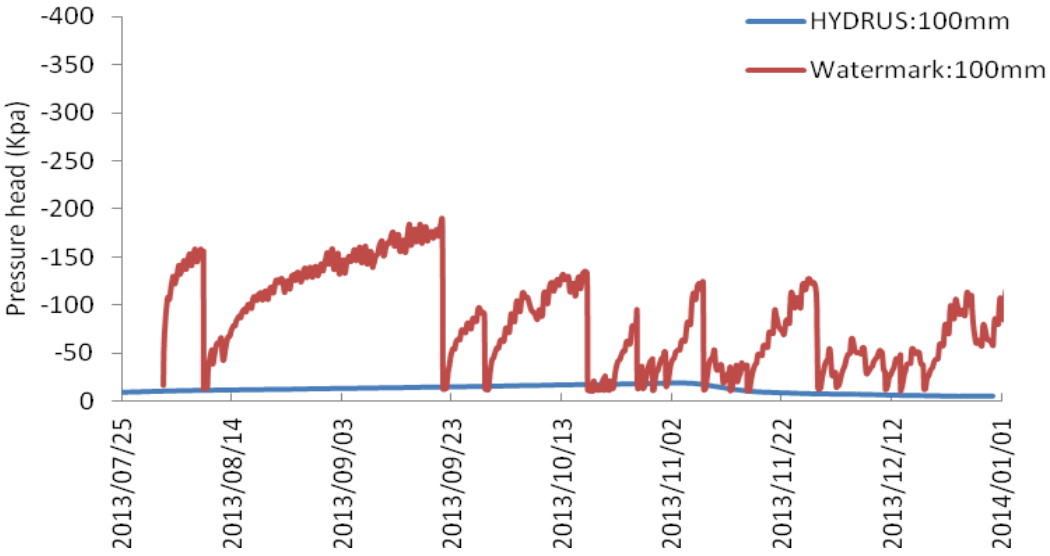

Figure 6.11 A comparison between a Watermark at 100 mm and HYDRUS simulation at 100 mm

At a depth of 400 mm, HYDRUS simulated no change in soil water potential (Figure 6.13). TDR 100 measurements were only available from late February. The initial soil water content of 0.19 was simulated for the entire period. Due to residual water content (Qr) (Van Genutchten curve) soil water content could not be lower than 0.19. TDR 100 at 400 mm demonstrated that there were fluctuations in soil water content when rainfall was received, but on average, the soil water content remained at 20% (Figure 6.12). The

HYDRUS simulation of soil water content at 400 mm did not change throughout the simulation, remaining at 19%, which is not far off the observed data.

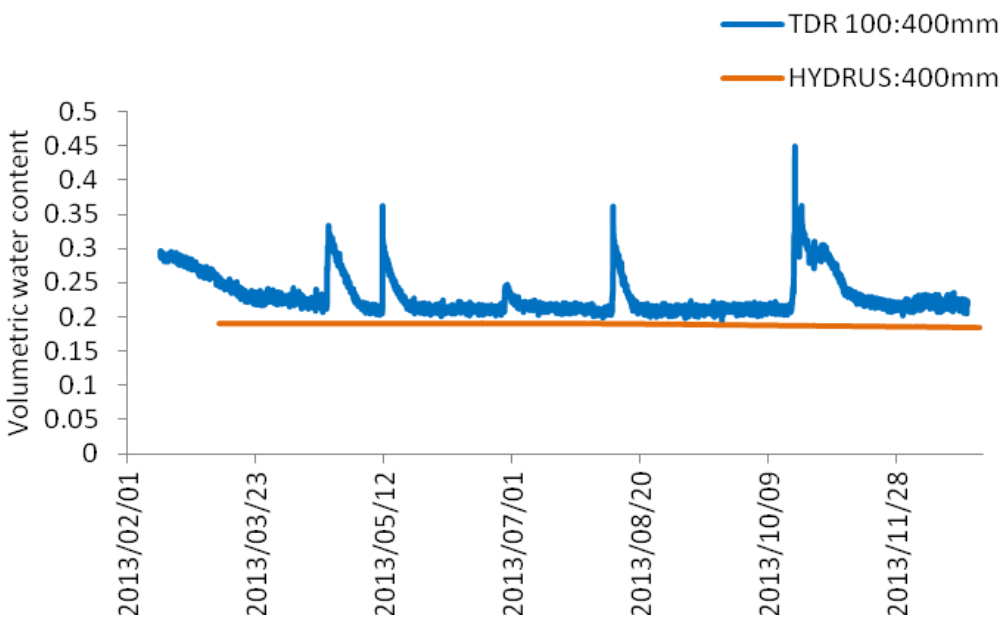

Figure 6.12A comparison between a TDR probe at 400 mm and HYDRUS simulation at 400 mm

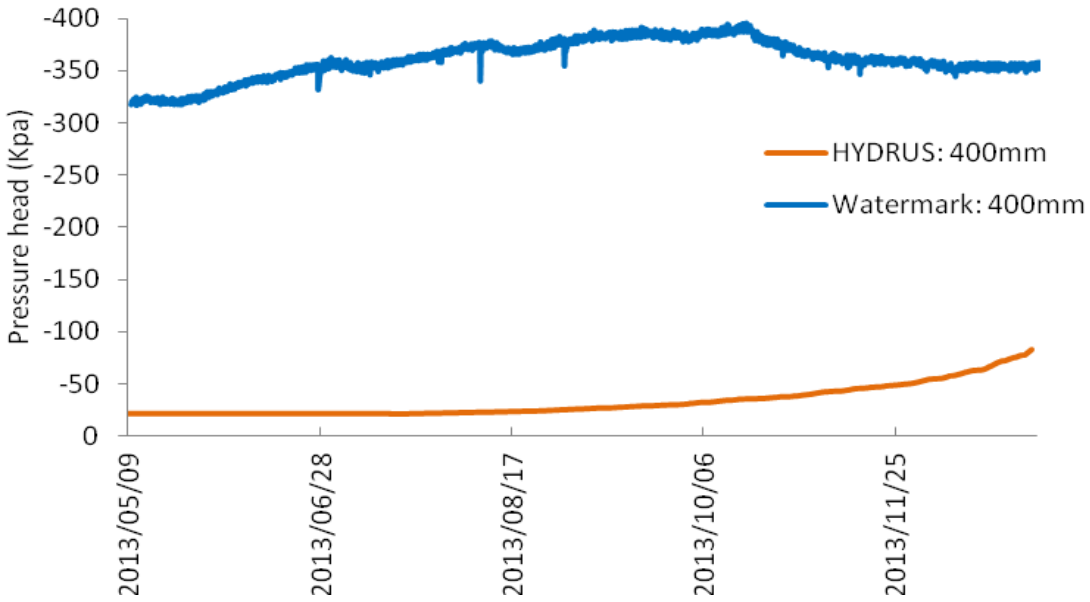

Figure 6.13A comparison between a Watermark sensor at 400 mm and HYDRUS simulation at 400 mm

There were slight fluctuations that were simulated by HYDRUS for soil water in the 0.3 m soil horizon. Changes in soil water content were evident during the wet season between January and February in 0.1 m horizon, where soil water content values peaked to 26%

and went down to 23% (Figure 6.14). During the wet season there were changes in the simulated 0.2 m soil horizon, where the peak soil water (23%) was observed at time step 2000. There was no change in simulated soil water content at the 0.3 m soil horizon. During the dry season 2013/07/01-2013/10/30), there was a decrease in simulated soil water content, where 0.1 m dropped to 0.19%, 0.2 m went down to 0.21% and 0.3 m remained the same. There were slight changes in soil water content and soil water potential for 0.2 m and 0.3 m depths, but due to slow infiltration there was a time lag from moisture received in the 0.1 m soil horizon (Figure 6.14 and Figure 6.15).

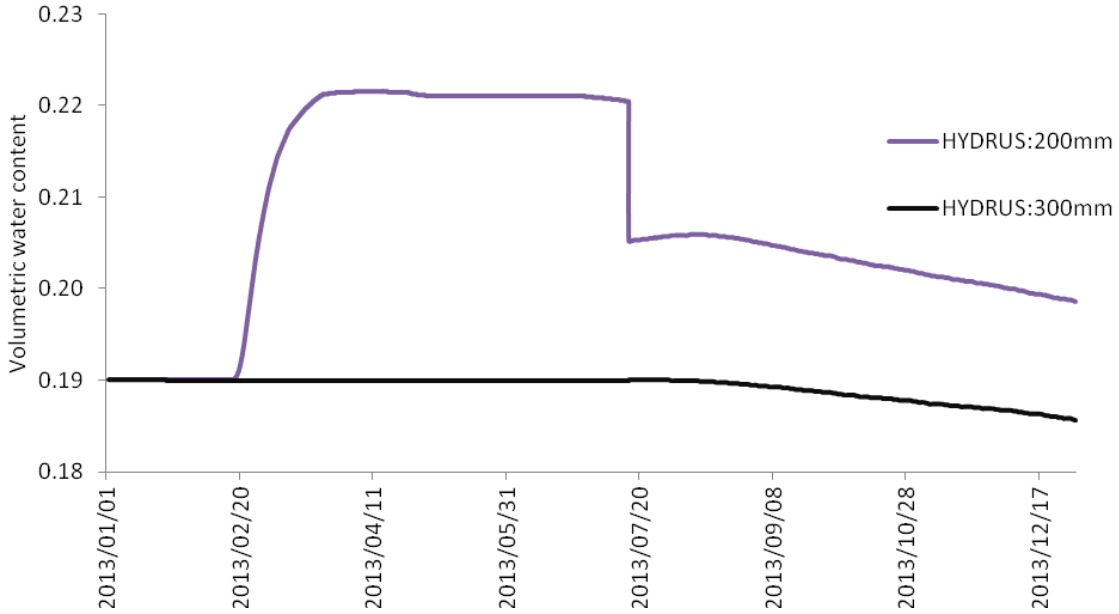

Figure 6.14 HYDRUS simulation of soil water content where no probes exist

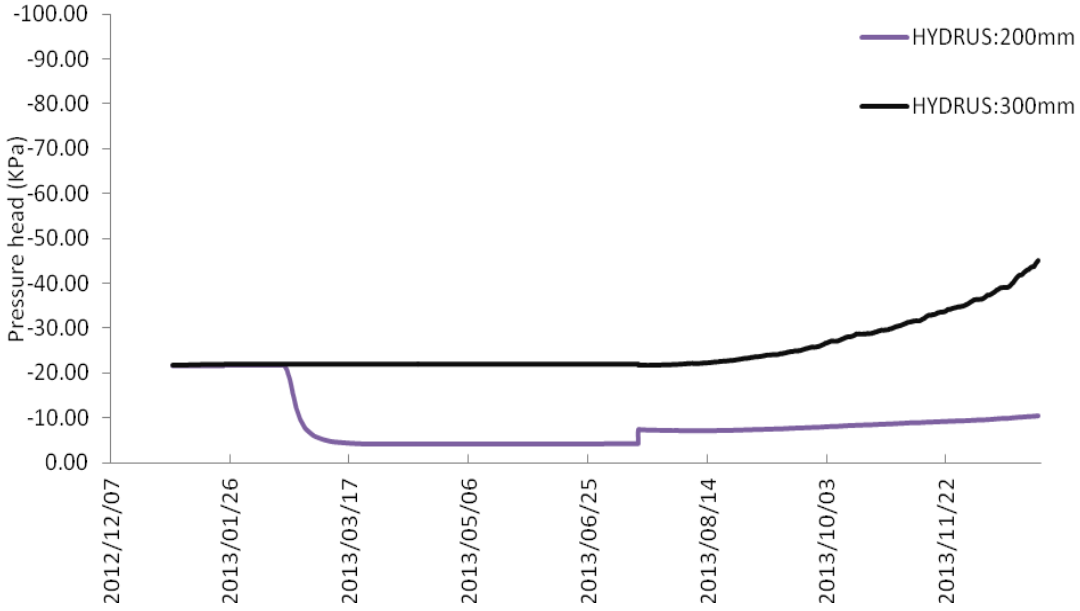

Figure 6.15 HYDRUS simulation of pressure heads where no probes exist

Simulated soil water content was different to that of measured soil water content. HYDRUS was able to account for the fluctuation and was unable to get simulated values (0.5-0.3) close to those of observed CS616 values (0.3-0.15). Simulated soil water content at 100 mm was generally wetter than that of observed 100 mm CS616 values. Although measured CS616 soil water probes do not take into account spatial resolution (measurement of a small area), HYDRUS was able to simulated the average soil water content at the 0.4 m depth, in that observed soil water content averaged around 20%, while HYDRUS simulated 0.19%.

Clulow *et al*. (2011) compared the WAVES (Water, Vegetation, Energy, Solute) model and ACRU (Agrohydrological Catchment Research Unit) with that of observed total soil water profile up to a depth of 2.4 m and found that the WAVES model was in good agreement and followed the trends that were measured, whereas ACRU was noticeably different. It was noted throughout the simulation that ACRU remained fairly constant throughout the year with small responses to large events. The WAVE model tended to overestimate the response to summer rainfall (Clulow *et al*., 2011).

The HYDRUS model tended to overestimate soil water at the surface, in a similar way to that of the WAVE model (Appendix II, Figure 10.3). The HYDRUS model response was similar to that of ACRU for the rest of the soil profile, by remaining constant. The overestimation of the HYDRUS model can be attributed to the insufficient parameterisation of the soil hydraulic model. There was a need for reverse modelling to re-estimate saturated hydraulic conductivity (ks), although there was concern that the model would not converge on a value.

6.2.3 Root water uptake

(Refer to CD Appendix IV, 1-4700;4700-8700, Output data, T_Level.out for raw data)
HYDRUS was able to simulate actual root water uptake almost identically to input potential root water uptake, therefore there was no water stress (Figure 6.16). There was therefore enough water in the soil for HYDRUS to simulate root water uptake to a depth of 5 m. Between, January and February there was higher potential and actual transpiration (0.45-0.20 mm hr^{-1}), as there was more reference evaporation due to the availability of sunlight during summer (Appendix III, Figure 10.4). From late February to July actual and potential evaporation (0.30-0.10 mm hr^{-1}) are lower due to less reference evaporation, as there was less radiation during winter (Figure 6.16).

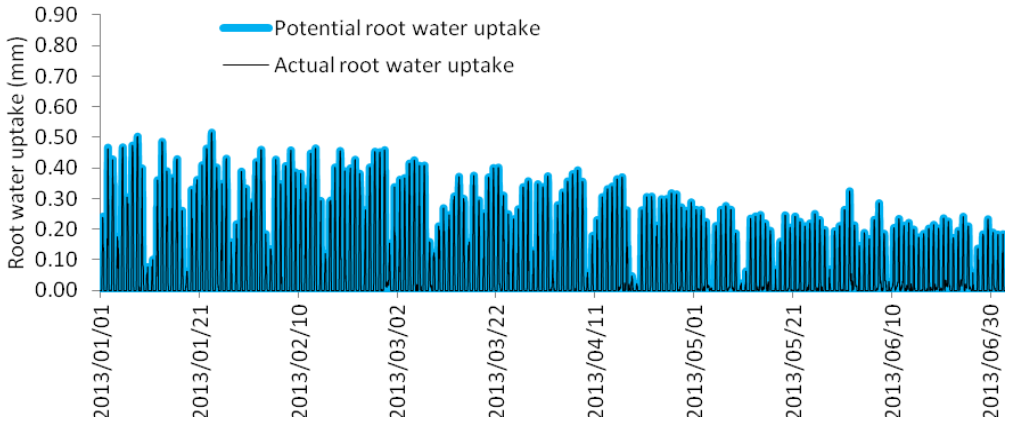

Figure 6.16 Potential and actual root water uptake to depth of 5 m (2013/01/01-2013/07/16)

Potential and actual transpiration of 2013/07/17-2013/12/31 and elsewhere is high, ranging from 0.30-0.60 mm hr^{-1}. Between, 2013/10-201/12 there is a large fluctuation in the amount of potential evaporation (0.05-0.75mm hr^{-1}) due to high temperature and rainfall (Appendix III, Figure 10.4), conditions that are experienced during summer (Figure 6.17). Towards the end of the simulation, 2013/11-2013/12 actual root water uptake is slightly less than potential transpiration, due to the unavailability of water when potential transpiration is high (0.60-70mm hr^{-1}) (Figure 6.17).

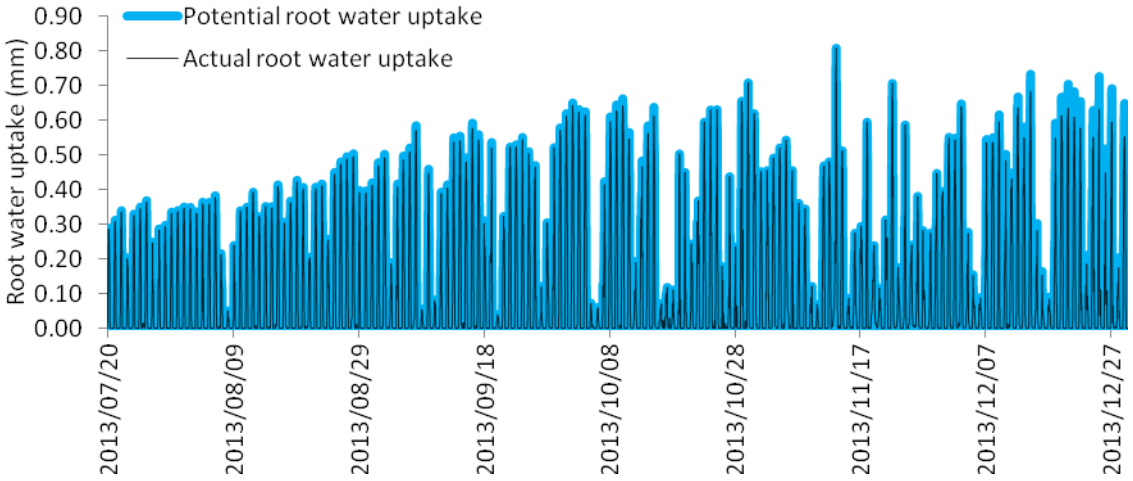

Figure 6.17 Potential and actual root water uptake to depth of 5 m (2013/07/17-2013/12/31)

The actual and potential root water uptakes are similar to one another, which suggests that there was enough water in the soil to allow for maximum uptake (Figure 6.18). Towards the end of the simulation (2013/12), potential root water uptake is less than that

of actual uptake (Figure 6.18), this is due to the water potential being too high and soil water content being too low.

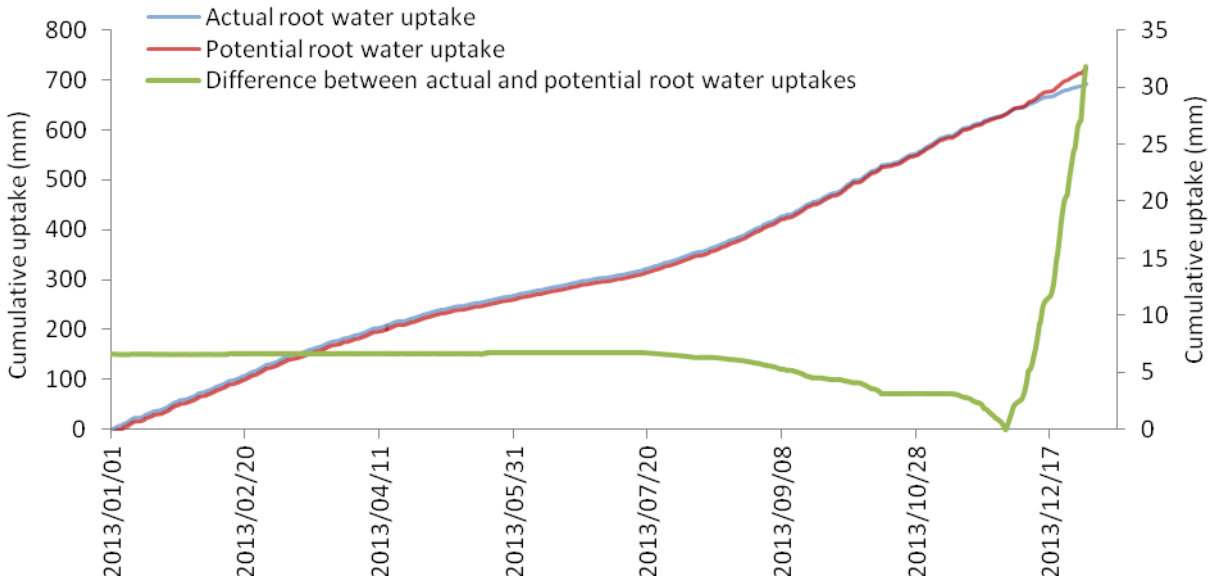

Figure 6.18 Difference between actual and potential root water uptake

Root water uptake totalled 691 mm in comparison to 306 mm of soil water evaporation (Jan-Dec, 2013). It is understandable that there should be little soil water evaporation in a forestry stand, due to the high leaf area index (LAI) which shades the soil surface and litter. HYDRUS simulated root water uptake as roughly double that of soil water evaporation, due to the high LAI of the trees. Potential soil water evaporation and potential root water uptake were separated using LAI. LAI should have accounted for evaporation potential, as groundcover was its driving factor. Root water uptake and soil water evaporation amounts were similar during the first few days of January , but deviated considerably after that (Figure 6.19). At the start of the simulation (2013/01-2013/06), rainfall was greater than root water uptake and soil water evaporation, but towards the end of the simulation (2013/07-2013/11), root water uptake was greater than that of rainfall. In forestry catchments it is assumed that root water uptake should be much higher than that of soil water evaporation due to shading of ground surface. The aim of the HYDRUS runs was to compare simulated total evaporation to actual evaporation, therefore the portioning of soil evaporation to transpiration was not changed. To provide for a better comparison between simulated total evaporation and measured total evaporation, research on portioning root water uptake to soil evaporation and the parameterization of the Feddes model for *Acacias mearnsii* is needed.

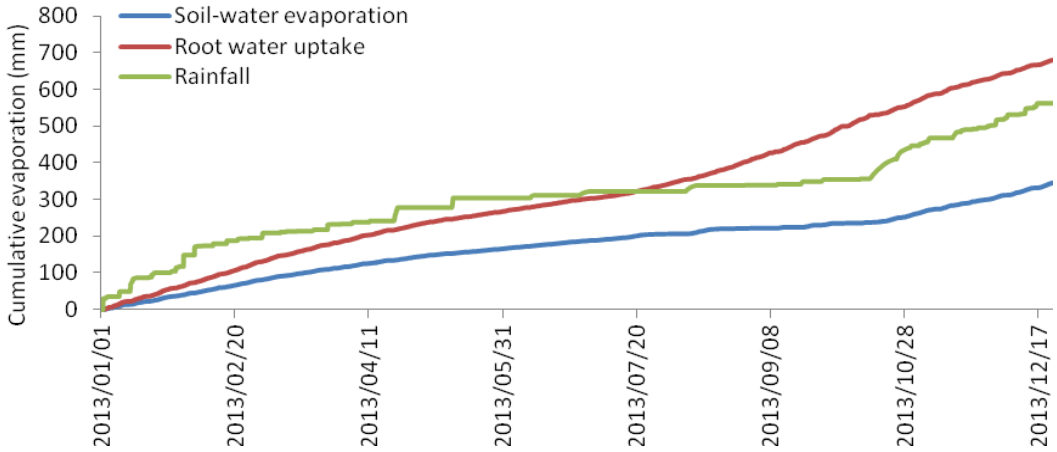

Figure 6.19 Cumulative evaporation with cumulative transpiration

6.2.4 Comparison between total evaporation estimates from Eddy co-variance and simulation total evaporation by HYDRUS

(Refer to CD Appendix IV, 1-4700;4700-8700, Output data, T_Level.out for raw data)

Total evaporation from HYDRUS was determined by adding soil water evaporation and actual transpiration. There was a difference between measured eddy co-variance total evaporation and simulated total evaporation from HYDRUS (Figure 6.20). From January to late February, it was evident that actual total evaporation (eddy co-variance) and simulated total evaporation (HYDRUS) were lower than the incoming rainfall. Rainfall was unable to contribute to simulated soil water content deeper than 0.3 m. Therefore, the model cannot simulate deep soil water content in winter (2013/04-2013/09) (Figure 6.20). HYDRUS simulated no runoff, thus it was presumed that from late January 2013 to late February 2013, water was stored in the top soil horizons. Actual total evaporation (1095 mm) and simulated total evaporation (1052 mm) were both greater than rainfall (571 mm). Simulated total evaporation and actual total evaporation measurements were in agreement with one another. A possible reason for HYDRUS simulating more evaporation than input rainfall might be the input soil water data. Due to the Qr parameter, the initial input soil water content could not be lower than 19%. The model was run from December 2013 to allow it to stabilise and to equilibrate soil water contents. Measurements from TDR 100, from 0.4-4.4 m, do not exceed 30% and usually did not drop below 8%.

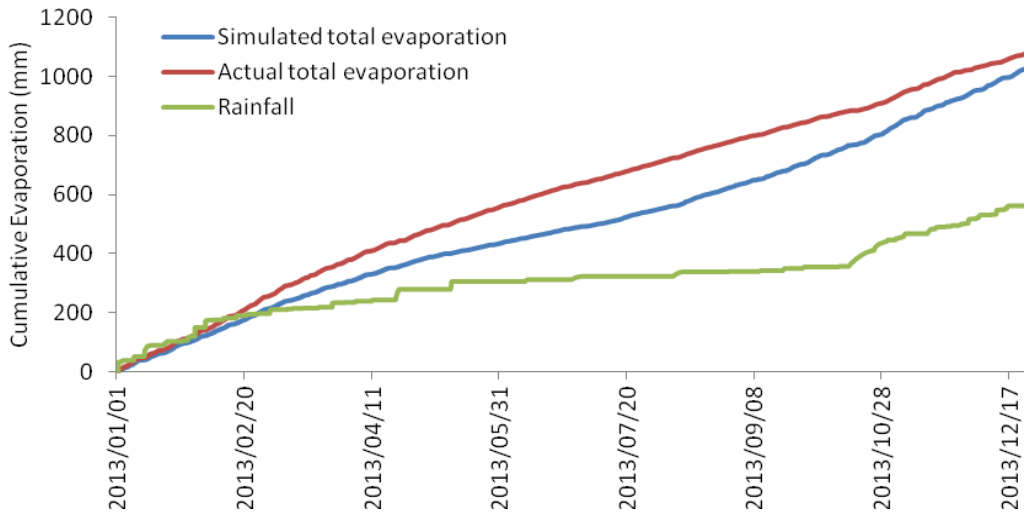

Figure 6.20 A comparison between simulated total evaporation (HYDRUS) and actual total evaporation (eddy co-variance)

Simulated total evaporation, actual total evaporation and rainfall are of the same magnitude from January to the end of February (Figure 6.20). The magnitude of simulated total evaporation and actual evaporation are greater than that of rainfall from end of February to December. It is possible that *Acacia mearnsii* are able to use groundwater during this period, although the isotope data that was collect does not confirm this as soil isotopes were only collected from July onwards (due to establishing a reliable extraction procedure).

HYDRUS 1D suggests that the simulated total evaporation was less than that of actual total evaporation (eddy co-variance) therefore, potential evaporation estimations (atmospheric demands) was too low. HYDRUS confirmed that using potential evaporation to simulate total evaporation would yield results less than that of the actual measured total evaporation, due to the trees using an extra source of groundwater that had not been accounted for in potential evaporation, and roots being able to extract water from groundwater. The simulated total evaporation measurement from HYDRUS provides for the amount of evaporation that can take place if rainfall is the only source. The portioning of root water uptake and soil water evaporation was done using LAI, although it is assumed that soil water evaporation is too high for a forested catchment. Therefore soil water evaporation and root water uptake needed to be partitioned, using a different method. The bottom flux boundary condition that was used in this study was free drainage, but by changing the bottom flux boundary condition to variable pressure head boundary, extending the soil profile to groundwater table, entering groundwater depth and

altering the Penman-FAO56 reference evaporation to actual eddy co-variance, HYDRUS may improve the simulation of deep groundwater uptake.

6.3 Soil water analysis

(Refer to CD Appendix V, Soil water analysis for raw data)

The soil survey done by Kuenene *et al*. (2013) suggest that the clay content of the soils at Two Stream increase from 11% at 0.4 m to 60% at 2.8 m and down to 40% at 4.4 m, suggesting that the soils at Two Streams between the horizons 0.4-0.8 m will be able to hold water more tightly (due to the higher cation exchange capacity) (higher soil water potential) than the soil at the surface and deeper than 2.8 m.

During the wet season (2013/01-2013/04/15 and 2013/10-2013/12), the CS 616 surface probe responded to rainfall events and generally the soil water content fluctuated between 18 and 25% (Figure 6.21). Xylem pressure potential readings (-40 to -45KPa) during the wet season suggested that the trees were under little stress (Figure 6.22). The 0.4 m TDR probe responded to rainfall events during the wet season, reaching a maximum soil water content of 45% and dropping down to 22% during times of little rainfall. The 0.8 m TDR probe showed little response to rainfall (0.15-0.22) (Figure 6.21). The Watermark sensor at 0.8 m responded to rainfall during the wet season (0 to -300 KPa), while at 0.4 m there was little response to rainfall (-300 to -350 KPa) and the soil layer was generally stressed during the wet season (Figure 6.22). The TDR and CS 616 readings suggest that the movement of water is downwards during the wet season, due to the deeper soil horizon (0.8 m) having a greater soil water content than that of the above horizon (0.4 m) (Figure 6.22), while the Watermark sensor suggests that movement is upwards due to the soil water potential of the deeper horizon (0.8 m) being greater (more dry) than that of the above horizon (0.4 m) . Due to little fluctuation of the Watermark sensor at 0.4 m, it is suggested that the sensor was not working properly (Figure 6.22).

During the dry season (2013/04/15-2013/09), the CS 616 probe responded to rainfall (0.15-0.22), but was dry when there was no rainfall (0.12) (Figure 6.21). Xylem pressure potential readings during the dry season suggested that the trees were stressed (-200KPa)(Figure 6.22). During the dry season the TDR readings at 0.4 m fluctuated when rainfall was received (0.22-0.35), but was generally dry when there was little rainfall (0.22-0.25). The TDR readings at 0.8 m did not fluctuate when rainfall was received and was dry during the season. The Watermark sensor at 0.4 m did not perform well during the dry season. However, the Watermark sensor at 0.8 m performed well during the dry season, showing fluctuation between -300KPa and -5KPa and responding to rainfall received.

Generally, the Watermark sensor at 0.8 m showed that there was some stress during the dry season. The Watermark sensors that were installed at 0.1, 0.4 and 0.8 operated out of their range (greater and -200KPa) for most of the year, therefore more emphasis is placed on the TDR results.

The TDR probe data suggested that the movement of water is downwards during the dry season, due to the fluctuation of water content and water potential with depth.

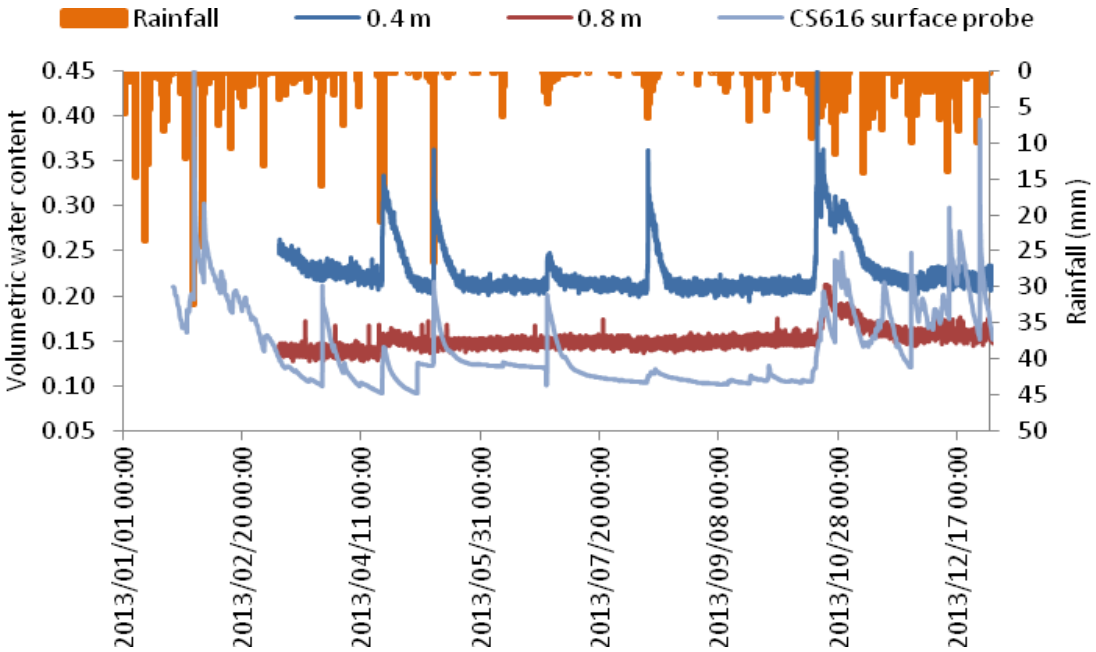

Figure 6.21 Shallow TDR sensor readings with rainfall

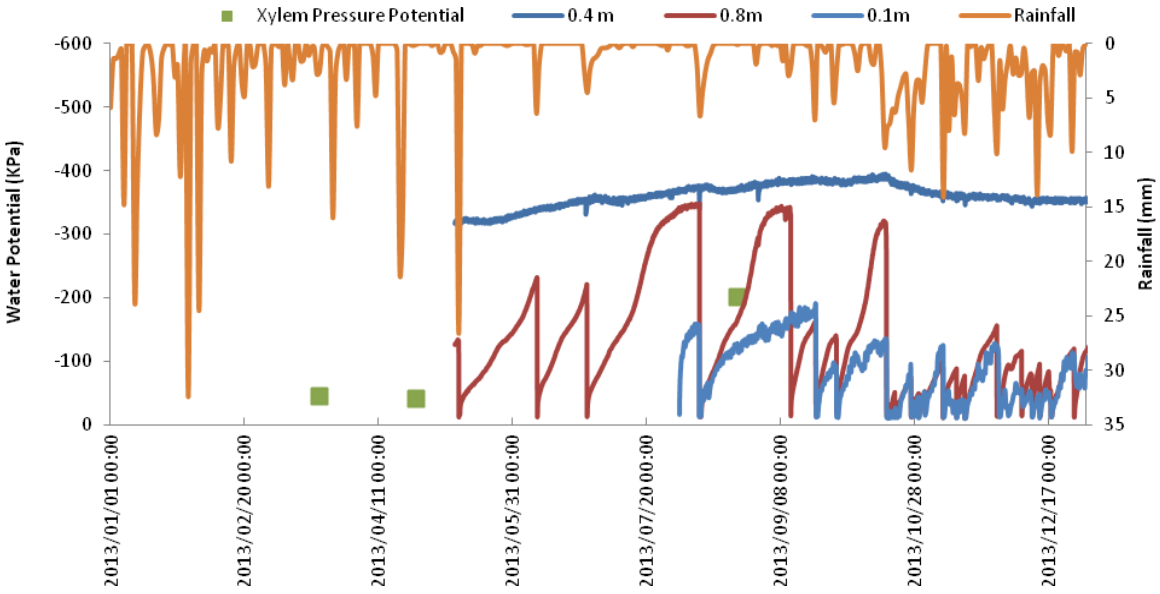

Figure 6.22 Shallow Watermark and Xylem pressure potential readings with rainfall

During the wet season (2013/01-2013/04/15 and 2013/10-2013/12), there was little fluctuation measured with the TDR probes at 1.2 and 1.6 m. However, during the large rainfall events that were received in 2013/11, the TDR reading fluctuated 20-30% at 1.2 m probe and 24-30% at 1.6 m probe (Figure 6.23). Generally the TDR probe at 1.2 m recorded soil water contents of 20-21%, while the probe at 1.6 m recorded soil water contents around 22-25% (Figure 6.23). The Watermark reading for 0.4 and 0.8 m fluctuated during the wet season (-5KPa to -100KPa) (-5KPa to -100KPa) (Figure 6.24). The TDR readings suggest that the general trend is a upward movement of water due to the deeper soil horizon being more dry than the above horizon. The Watermarks showed a downward movement due to the deeper horizon being more wet

During the dry season (2013/04/15-2013/09), the TDR reading at 1.2 and 1.6 m did not respond to rainfall and remained at 20-21% and 24-25%, respectively (Figure 6.23). During the dry season, the Watermark sensor at 1.2 and 1.6 m responded to rainfall and fluctuated from -100 to -400KPa and -300 to -500KPa (Figure 6.24). During the dry season, the TDR probes at 1.2 and 1.6 m suggested upward movement of water, although the Watermark sensors suggested a downward movement.

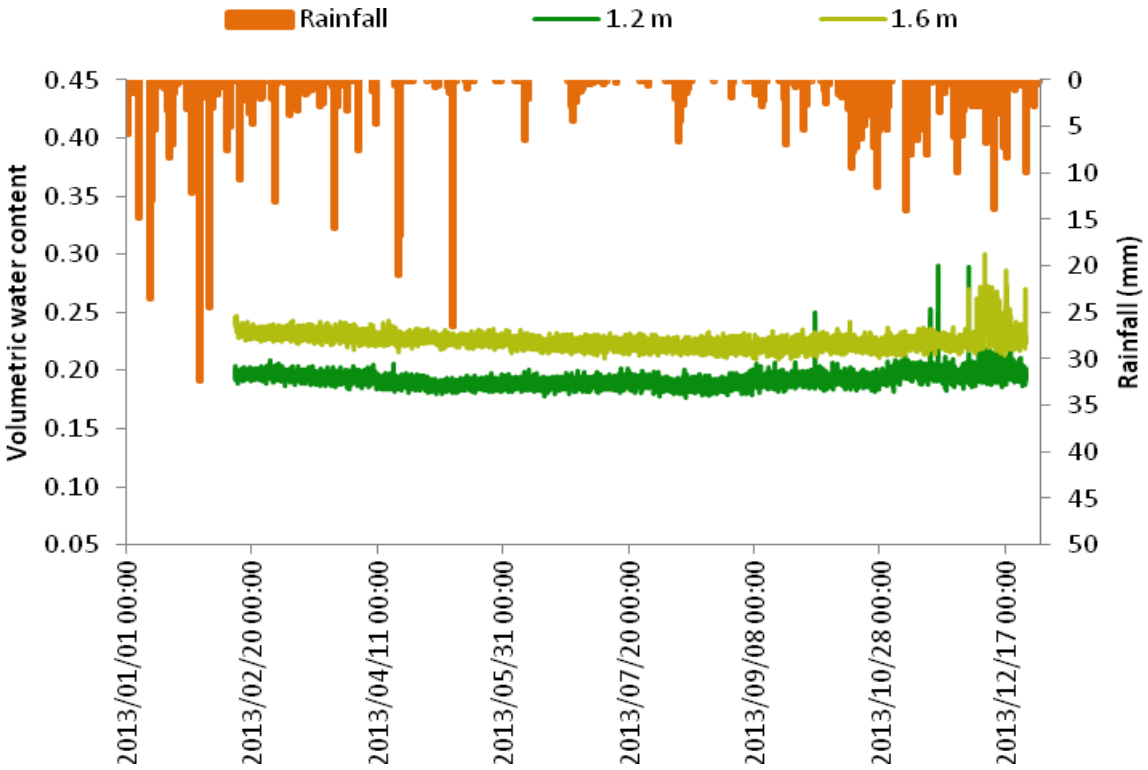

Figure 6.23 TDR and rainfall readings between 1 m and 2 m

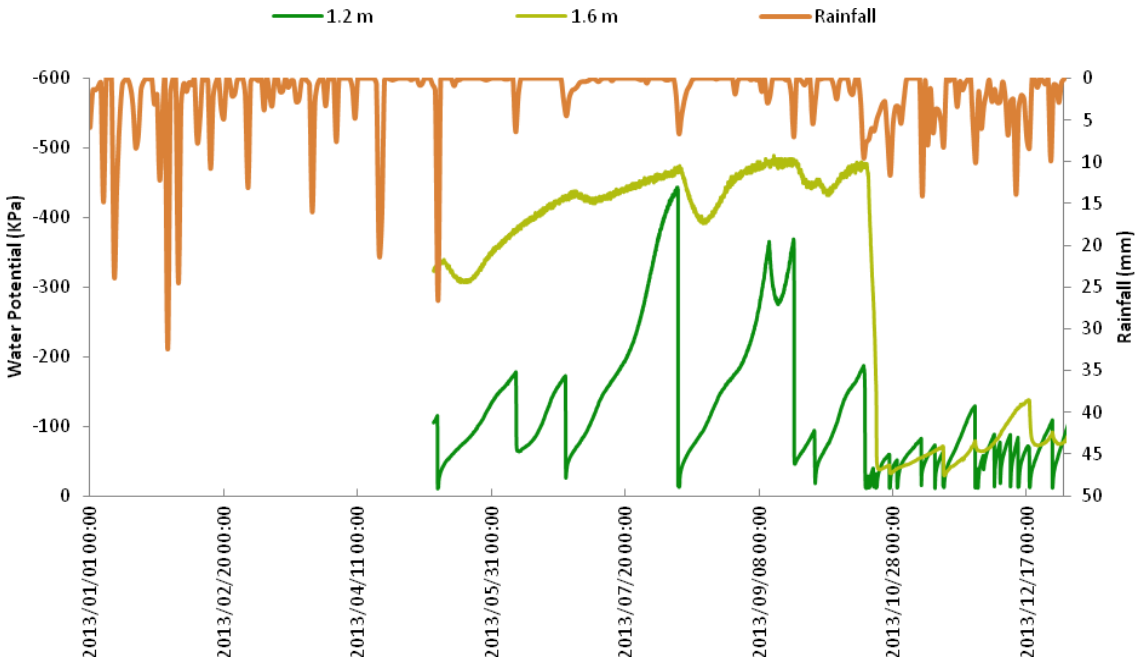

Figure 6.24 Watermark and rainfall readings between 1 m and 2 m

During the wet season (2013/01-2013/04/15 and 2013/10-2013/12), the TDR probes at 2.0, 2.4 and 2.8 m showed little response to rainfall. The soil water content measured at the 2.0 m TDR probe during the wet season ranged from 24-25%. The TDR probe at 2.4 m measured a reading of 10-12%, while the probe at 2.8 m measured a reading of 16-14% during the wet season (Figure 6.25). The Watermark sensors at 2.0, 2.4 and 2.8 m responded to rainfall that was received during the wet season, it is evident by the decrease in soil water potential from 2013/10/28-2013/12/17, where soil water potential dropped from -450 to -50KPa. The Watermark sensor at 2.0 m measured soil water potential ranging from -400KPa to -130KPa. The Watermark sensor at 2.4 m measured soil water potential ranging from -320KPa to -140KPa, while the Watermark sensor at 2.8 m measured soil water potential ranging from -500KPa to -320KPa (Figure 6.26). TDR probe measurements suggest that there is an upward movement of water from 2.8 to 2.4 m during the wet season. Watermark sensors suggest that there is a downward movement of water during the wet season as the soil water potential of the deeper soil horizon 1.6 m is greater (more wet) than that of the 1.2 m horizon.

During the dry season (2013/04/15-2013/09), the TDR probes at 2.0, 2.4, 2.8 m measurements of soil water content did not fluctuate much. The TDR probe at 2.0 m measured a soil water content of 24-25%. The TDR probe at 2.4 m measured a soil water content of 8-10% , while the TDR probe at 2.8 m measured a soil water content of 13-15%

(Figure 6.26). The Watermark sensor at 2.0 m measured a soil water potential from -250 to -420KPa. The Watermark sensor at 2.4 m measured a soil water potential of between -250 to -320KPa, while the Watermark sensor placed at 2.8 m ranges from -320 to -500KPa (Figure 6.27). TDR measurements suggest that there were upward movement between the 2.4 m and 2.8 m soil horizon, while downward movement were between 2.0 m and 2.4 m. Watermark sensors suggest that there were upward movement between the 2.0 m and 2.4 m as the 2.4 m horizon is more wet than the above horizon 2.0 m. The Watermarks that were installed at 2.0, 2.4 and 2.8 m operated out of their range of most of the year therefore their results are less significant.

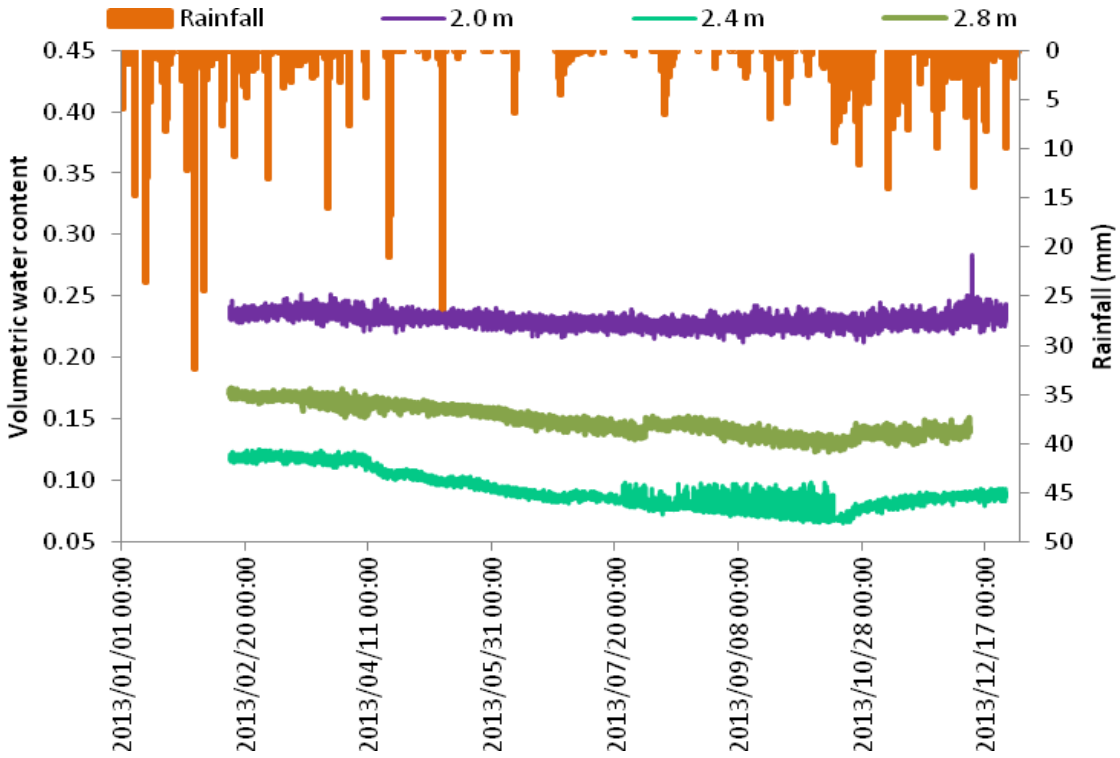

Figure 6.25 TDR and rainfall readings between 2 m and 3 m

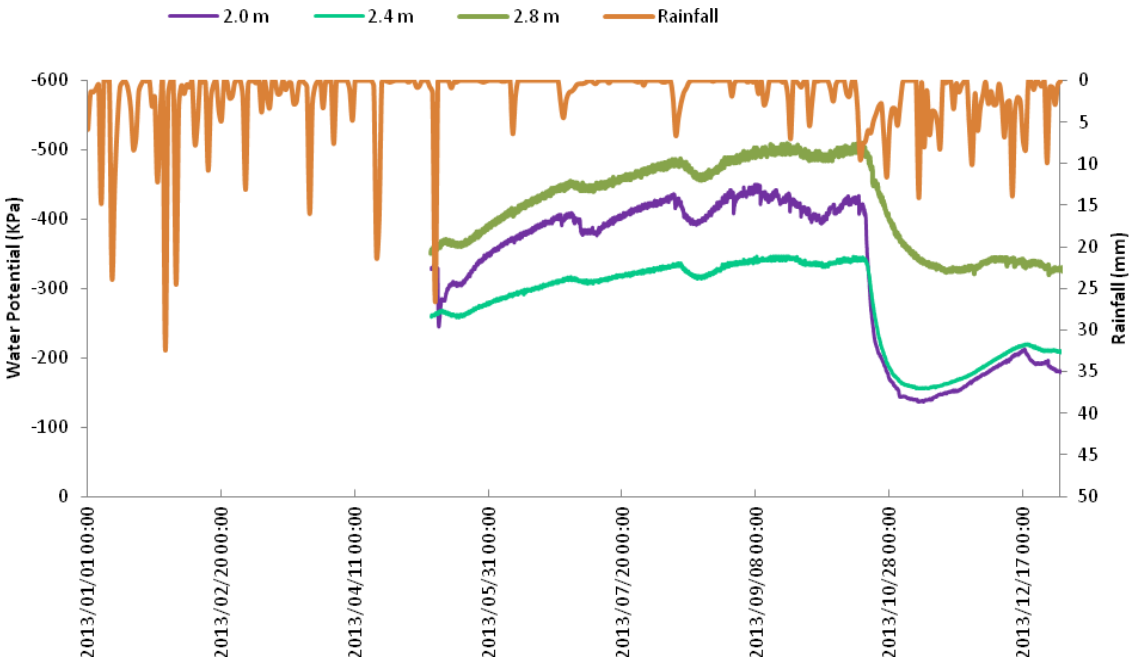

Figure 6.26 Watermark and rainfall readings between 2 m and 3 m

During the year, TDR probes at a depth of 3.2, 4.0, 4.4 and 4.8 m did not respond to received rainfall (Figure 6.27). The TDR readings at probe 3.2 m were between 8-10%, at 4.0 m they were 12-15%, at 4.4m they were 7-8% and at 4.8 m they were from 8-9%. Watermark sensors at depths of 3.2, 4.0, 4.4, 4.8 and 8.8 m responded to rainfall and experienced drying throughout the year. In the wet season (2013/01-2013/04/15 and 2013/10-2013/12), the Watermarks at 3.2 m were -430 to -350 KPa, at 4.0 m -430 to -270KPa, at 4.4 m -450 to -400KPa, at 4.8 m -430 to -400KPa and at 8.8 m -320 to -270KPa (Figure 6.28). TDR readings throughout the wet season suggested an upward movement from the 4.0 m to the 3.2 m soil profile as the 4.0 m soil horizon is more wet than the 3.2 m soil horizon during the year (Figure 6.27). Watermark readings throughout the wet season suggested an upward movement between the 4.0 m and the 3.2 m soil profiles as the 4.0 m horizon is more wet than the 3.2 m horizon, although this result is less significant as the probes are operating out of their range (greater than -200KPa) (Figure 6.28).

During the dry season (2013/04/15-2013/09), the Watermark sensors recorded soil drying due to little rainfall. The readings of the Watermark sensor at 3.2 m readings ranged from -320 to -400KPa, at 4.0 m -320 to -400KPa, at 4.4 m -340 to -500KPa, at 4.8 m -340 to -450KPa and at 8.8 m -270 to -300KPa (Figure 6.29). The TDR readings throughout the dry season suggested an upward movement between the 4.0 m to 3.2 m soil profiles as

the 4.0 m horizon is more wet than that of the 3.2 m horizon (Figure 6.27). The Watermark sensor readings suggested an upward movement of water from 4.8 m to 4.4 m and from 8.8 m to 3.2 m, since the deeper horizons are more wet than the shallow horizons, although these sensors are operating out of their range (Figure 6.28).

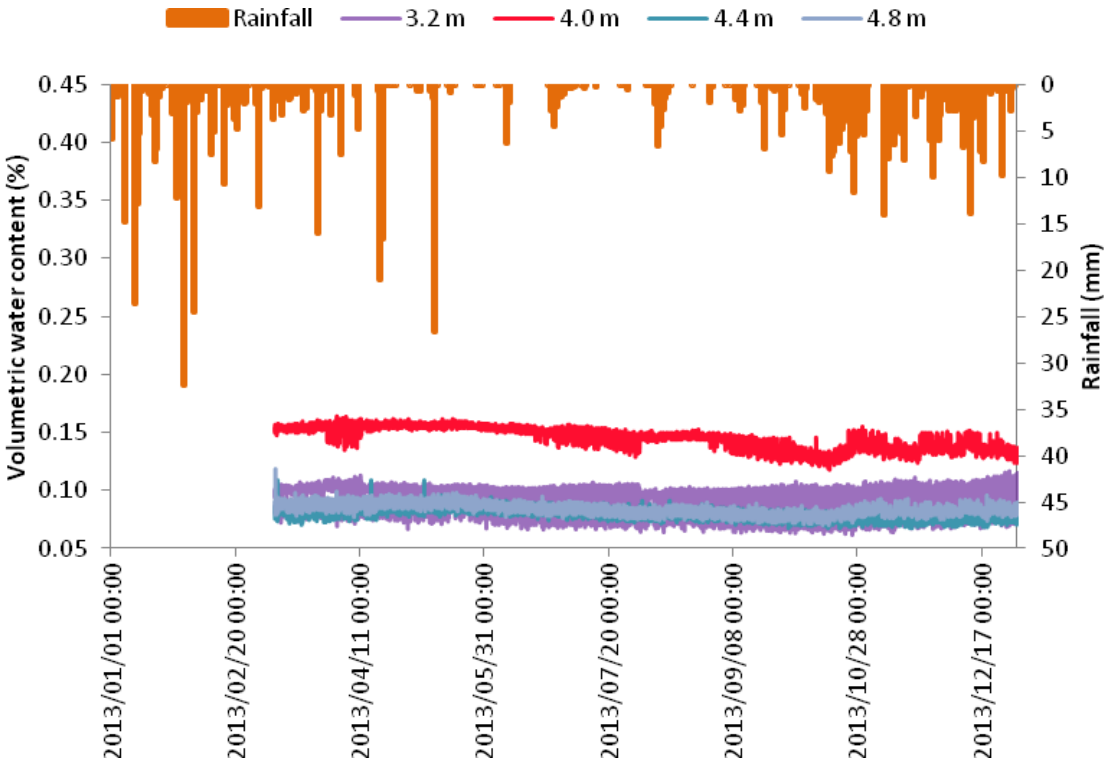

Figure 6.27 TDR and rainfall readings greater than 3 m

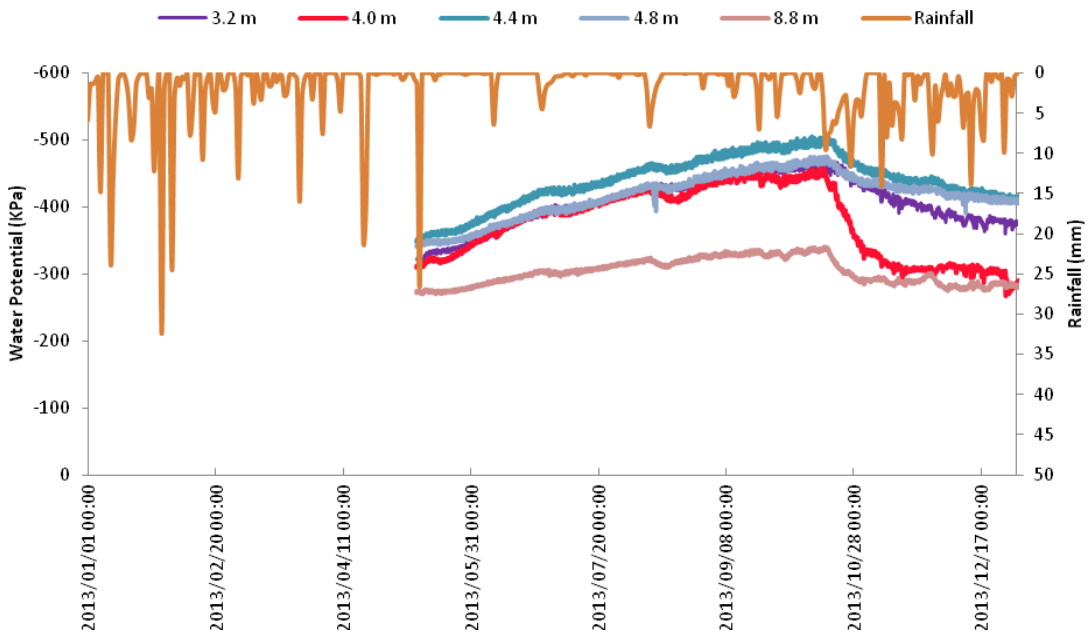

Figure 6.28 Watermark and rainfall readings greater than 3 m

Previous soil water measurements done by Everson *et al*. (2011) at Two Streams showed that the driest soil profile was at 1.6 m, which is different to these results as the 2.4, 3.2, 4.4 and 4.8 m are the driest horizons.

Conclusions made by Kuenene *et al*. (2013) on hillslopes free of trees were that soils in the top 7 metres drained rapidly after rainfall events and caused recharge of water in deep saprolite which then exited via valley bottom into streams. Kuenene *et al.* (2013) determined that water stored in hillslope saprolite amounted to 256620 m^3 for a 65.8 ha area, streamflow amounted to 4793 m^3 in 2005, where 251827 m^3 was available for usage during 2006. A comparison between the ratio of streamflow to that of rainfall from 2001-2004 was on average 0.03, where mature Wattle trees were drawing water from below 4.8 m. The storage of water in deep saprolite is important for streamflow generation during rainfree periods as well as providing water for growing trees (Kuenene *et al.,* 2013). The conclusions made by Kuenene *et al.* (2013) were that Wattle trees were able to access water deeper than 4.8 m, the same evidence was found in the isotope results and soil water measurement that have been presented here.

7. CONCLUSION AND RECOMMENDATIONS

The main aim of this project was to determine whether *Acacia mearnsii* is able to abstract groundwater. The soil isotope results showed that the groundwater isotope signature was similar to that of soil water at the depths of 2.0 and 2.4 m on 23/08/2013, 1.6 m on 13/07/2013 and 4-5 m on 09/11/2013, therefore suggesting that either capillary rise or hydraulic lift had moved groundwater to these horizons to allow for root water uptake. The evidence showing that the trees were using groundwater on the 23/08/2013, 13/07/2013 and 13/07/2013 supports the theory by Kuenene (2013) who suggested that there was a large amount of water stored in deep saprolite, which could supplement the water requirements of the trees during the dry season. The field measurements of total evaporation have confirmed simulations of total evaporation using HYDRUS to be correct, although simulated transpiration is significantly less than total evaporation due to soil water evaporation. The HYDRUS simulations suggested that soil water evaporation was roughly a third of total evaporation. Watermarks and soil water content trends suggest a downward movement of water from the soil surface to the 1.2 m soil horizon during the wet and dry season. Upward movement is evident in the dry season from 8.8 m to 1.2 m, 2.4 m to 1.6 m and 2.4 m to 2.0 m. Although the data suggests that there is some upward movement of water due to the above horizon being more wet than the deeper horizons, it was presumed that if there was to be upward movement there would be a steady drop in soil water content over time in the deeper TDR probes, while there would be a slight rise in soil water content in shallower TDR probes. The upward movement suggests that water is being removed from deeper horizons by means of hydraulic lift (root uptake) or capillary rise and being re-distributed to soil horizons that are accessible to plant roots. Therefore measurements from the TDR and Watermarks probes do not give conclusive evidence that there was upward movement (hydraulic lift or capillary rise) occurring at Two Streams during 2013. The quantification of mist interception was not done in this study and could still possibly be the extra source of moisture in the catchment.

Sub-hypothesis 2 was that if the isotope signature of soil water for a particular horizon is the same as groundwater and rooting matter has been found in this horizon, then the trees were accessing groundwater due to direct water uptake. From the research collected at Two Streams Research Catchment, rooting depth up to 4.8 m was evident (Appendix II, Table 10.3) and groundwater levels were noted to rise to 19 m. Therefore

trees are not able to extract water directly. The isotope signature of soil water and groundwater in the 2 m and 4 m soil horizons were similar, suggesting that hydraulic lift or capillary rise could be the mechanism for this movement. The hypothesis that the mechanism of root water uptake was capillary rise or hydraulic lift was not confirmed in this study due to the limited time, and funds.

Sub-hypothesis 3 was that if the stream water isotope signature is the same as groundwater during the dry period then most of the water leaving the catchment was from baseflow. Majority of water leaving the catchment was from baseflow and on only a few occasions did the groundwater and stream water signatures not match. It was concluded that during summer and winter most of the water leaving the catchment was from baseflow. Groundwater ridging pressure wave could be a possible cause for the occurrence of large amounts of groundwater in the stream.

Sub-hypothesis 4 was that if HYDRUS was able to simulate total evaporation greater that rainfall, then the trees were able to use summer stored water to transpire freely during winter. HYDRUS was able to simulate total evaporation greater than rainfall and a possible reason for this was that stored water or input soil water content was high. A possible reason for the model having a greater soil water content than of observed and therefore overestimating soil water content is due to the incorrect assignment of the van Genuchten parameters into the model. The results from the HYDRUS simulation confirm the need for accurate field measurements, especially those of soil surveys, and emphasize the need for inverse solution modelling to get better estimations of van Genuchten curves. There is also a great need to improve the Feddes model, to include tree species that are able to extract deep soil water.

The research questions that were asked during this study were:

Are the trees able to use groundwater and does their usage change between dry and wet season? During this study the groundwater isotope signature and the soil isotope signature at particular horizons were similar for a particular period, suggesting that the trees were using groundwater. No determination of usage amount during the dry and wet season was made with isotopes.

Is HYDRUS able to accurately model root water uptake and therefore transpiration? This study showed that HYDRUS simulated soil water content poorly and thus the validation was poor. The proportioning of soil water evaporation and transpiration was done using

Leaf Area Index, although from the results it was evident that soil water evaporation was too high due to the large surface shading in the catchment, thus the simulation of transpiration was too low.

Can the HYDRUS model allow for the identification of depth from which the trees are extracting water? From the HYDRUS results there was no clear indication to the depth with which trees were extracting water.

The techniques of samples and the design of new innovations were made in this project so that the accuracy of measurements could help with the determination of tree water use. The rainfall sampler functioned well and was able to separate samples from different rainfall events and separate samples during extended rainfall events. In addition, a glass funnel with a U-tube trap was inserted into the lids of the bottles to prevent the evaporation of samples, which would have altered the isotope signature of the sample. It was important to prevent evaporation of the rainfall samples, so that isotope tracing could be done. The innovation shown in the sampling of rainfall is likely to be beneficial to future isotope studies and was applied to an automatic streamflow sampling system, which was also installed at the weir during 2013, so that samples were collected during events to understand the rapid response mechanisms of the catchment and for possible hydrograph separation. The determination of a new cost effective technique for extracting isotopes from soil was made in this study. The water distillation technique worked well in extracting isotopes from soil and can be seen by the tests that were run using the standards. The accuracy of extraction of standards for $\delta^{2}H$ was 96%, while that of $\delta^{18}O$ was 86%. There is room for the improvement of the accuracy of extraction of the $\delta^{18}O$ isotopes, a possible cause of the extraction not being more accurate could be due to sample being left behind on the distillation coils (refer to Figure 4.11 for picture). The measurements that were collected from the TDR 100 probes that were installed using a hand auger were good and comparable to gravimetric water content measurements. Although, there was slight interference observed on a few of the probes and one of the probes did not work, the TDR probes performed well during the study. The Watermark sensors performed well during the course of the study, although the majority of the time they were out of their range of measurement (greater than -200 Kpa).

With regard to future water resources planning and the allocation of *Acacia mearnsii* plantation to water-stressed catchments, it needs to be clarified that this tree species is able to use all available precipitation and access groundwater for its growth. The trees therefore have a large detrimental impact on streamflow, groundwater and thereafter

downstream users. Further research that could be recommended is to determine the mechanism with which water is being lifted at Two Streams Research Catchment i.e. hydraulic lift or capillary rise. The extraction of plant isotope signature using Azeotropic distillation and comparing the plant signature to that of the groundwater and the average precipitation signature will help confirm the results from this study. The installation of sensitive deep soil water probes will help confirm the upward movement of water. Gypsum block sensors installed to 12 m will allow for the measurement of soil water up to -10 KPa and down to -400 KPa will help confirm when upward water movement is occurring.

8. REFERENCES

Aggarwal, P. K. 2002. Isotope hydrology at the International Atomic Energy Agency, *Hydrological Processes* 16(11):2257-2259.

Allen, RG, Pruitt, WO, Wright, JL, Howell, TA, Ventura, F, Snyder, R, Itenfisu, D, Steduto, P, Berengena, J, Yrisarry, JB, Smith, M, Pereira, LS, Raes, D, Perrier, A, Alves, I, Walter, I and Elliott, R. 2006. A recommendation on standardized surface resistance for hourly calculation of reference ET_o by the FAO56 Penman-Monteith method. *Agricultural Water Management*, 81(1-2):1-22.

Ameglio, T, Archer, P, Cohen, M, Valancogne, C, Daudet, F, Dayau, S and Cruizat, P. 1999. Significance and limits in the use of predawn leaf water potential for tree irrigation. *Plant and soil*. 207(2):155-167.

American Society of Civil Engineers (ASCE). 1996. Hydrology Handbook, Second Edition. Library of Congress Catalog Card No:96-41049. United States of America.

Anati, D and Gat, J. 1989. Restricted marine basins and marginal sea environments. In ed:. Baskaran M, *Handbook of Environmental Isotope Geochemistry,* Chapter 2. Elsevier Science, Detroit, United States of America

Ashkenas, L, Johnson, S, Gregory, S, Tank, J and Wollheim, W. 2004. A Stable Isotope Tracer Study of Nitrogen Uptake and Transformation in an Old-growth Forest Stream. *Ecology* 85(6):1725–1739.

Berman, E, Gupta, M, Gabrielli, C, Garland, T and McDonnell, J. 2009. High frequency field-deployable isotope analyzer for hydrological applications. *Water Resources Research* 45(10)

Boyer, JS. 1995. Measuring the water status of plants and soils. Academic Press, San Diego.

Brunel, J, Walker, G and Kennett-Smith, A. 1995. Field validation of isotope procedures for determining sources of water used by plants in a semi-arid environment. *Journal of Hydrology* 167(1-4):351-368.

Brunel, J, Walker, G, Walker, C, Dighton, C and Kennett-Smith, A. 1990. Using stable isotopes of water to trace plant water uptake. In: eds. Stable isotopes in plant nutrition, soil fertility and environmental studies. Proceedings of the International Conference, IAEA. Vienna,n543-551.

Bulcock, H and Jewitt, G. 2012. Field data collection and analysis of canopy and litter interception in commercial forest plantations in KwaZulu-Natal Midlands, South Africa. *Hydrology and Earth System Sciences* 16:3717-3728.

Burger, C. 1999. Comparative evaporation measurements above commercial forestry and sugarcane canopies in the KwaZulu-Natal midlands. Unpublished MSc thesis, Department of Agriculture, University of Natal, Pietermaritzburg, South Africa.

Busch, D, Ingraham, N and Smith, S. 1992. Water uptake in woody riparian phreatophytes of the south western United Stated: a stable isotope study. *Ecological Applications* 2(4):450–459.

Caldwell, MM, Dawson, TE and Richards, JH. 1998. Hydraulic lift: consequences of water efflux from the roots of plants. *Oecologia,* 131:151-161.

Campbell Scientific, 2010. TDR 100 Instruction Manual. Logan, Utah, United States

Clulow, AD. 2007. The long-term measurement of total evaporation over *Acacia mearnsii* using large aperture scintillometry. Unpublished, MSc thesis, School of Bioresources Engineering and Environmental Hydrology, University of KwaZulu-Natal, South Africa.

Clulow, A, Everson, C and Gush, M. 2011. *The long-term impact of Acacia mearnsii trees on evaporation, streamflow and ground water resources*. Report No. TT505/11. Water Research Commission, Pretoria, South Africa.

Cooper, L and DeNiro, M. 1989. Covariance of oxygen and hydrogen isotope compositions in plant water: species effects. *Ecology*. 70(6):1619–1628.

Craig, H. 1961. Standards for reporting concentrations of deuterium and oxygen-18 in natural waters. *Science*, 133(3467):1833-1834.

Craig, H and Gordon, L. 1965. Deuterium and oxygen-18 variations in the ocean and the marine atmosphere. *Stable Isotopes in Oceanographic Studies and Paleotemperature*. 9-130.

Dawson, T and Ehleringer, J. 1991. Streamside trees that do not use stream water. *Nature*. 350:335-337.

Dawson, T.E. 1993. Hydraulic lift and water use by plants implications for water balance, performance and plant-plant interactions. *Oecologia*. 95(4):565-574.

Dawson, T and Pate, J. 1996. Seasonal water uptake and movement in root systems of Australian phraeatophytic plants of dimorphic root morphology: a stable isotope investigation. *Oecologia*, 107(1):13-20.

Dansgaard, W. 1960. The content of heavy oxygen isotopes in the water masses of the Philippine Trench. *Deep Sea Research.* 6(1959-1960):346-350.

Dansgaard, W. 1964. Stable isotopes in precipitation. *Tellus*. 16(4):436-468.

Dahlman, R and Kucera, C. 1965. Root productivity and turnover in native prairie. *Ecology*. 46(1-2):84-89.

Doussan, C, Pierret, A, Garrigues, E and Pages, L. 2006. Water uptake by plant roots. II. Modelling of water transfer in the soil root-system with explicit account of flow within the root system comparison with experiments. *Plant and Soil*. 283 (1-2):99-117.

Dwyer, LM and Stewart, DW. 1984. Indicators of water stress in corn (*Zea mays* L.) *Canadian Journal of Plant Science*. 64:537-546.

Ehhalt, D, Munnich, K.O, Roether, W, Schölch, J and Stich, W. 1963. Artificially produced radioactive noble gases in the atmosphere. *Journal of Geophysical ResearchI. 68, 2817*

Ehleringer, J and Osmond, C. 1989. Stable isotopes, In eds: Pearcy, RW, Ehleringer, JR., Mooney, HA and Rundel, PW, *Plant Physiology Ecology,* Field Methods and instrumentation, Chapman and Hall Ltd., London, 281-300.

Epstein, S and Mayeda, T. 1953. Variations of the ^{18}O content of waters from natural sources. *Geochim. Cosmochim. Acta.* 4(5):213-224.

Everson, C.S, Dye, P.J, Gush, M.B, Everson, T.M. 2011.Water use of grasslands, agroforestry systems and indigenous forests. *Water Research Commission*.

Food and Agriculture Organization of the United Nations. 1998. Abstract of Forestry Facts for the year 1996/1997. Forestry Owners Association, Rivonia

Farrington, P, Turner, J and Gailitis, V. 1996. Tracing water uptake by jarrah (*Eucalyptus marginata*) trees using natural abundances of deuterium. *Trees.* 11(1):9-15.

Feddes, RA, and Raats, PAC. 2004. Parameterizing the soil water-plant root system. In eds: Feddes, RA, de Rooij, GH, and van Dam,JC., *Unsaturated-zone Modeling: Progress, Challenges*, Chapter 4, 95–141 vol. 6, Wageningen UR Frontis Series

Feddes, RA, Kowalik, PJ and Zaradny, H. 1978. Simulation of field water use and crop yield. John Wiley Sons. Wageningen.

Gat, J. 2010. Isotope Hydrology: A study of the Water cycle. *Imperial College Press*, Covent Garden, London.

Gardner, W. 1960. Dynamic aspects of water availability to plants. *Soil Science*. 89(2):63-73.

Giese, K, Tiemann, R. 1975. Determination of the complex permittivity from thin-sample time domain reflectometry improved analysis of the step response waveform. *Advances Molecular Relaxation Processes* 7: 45–59.

Gonfiantini, R, Gratziu, S and Tongiorgi, E. 1965. Oxygen isotope composition of water in leaves. Isotopes and Radiation in Soil Plant Nutrition Studies. Technical Report. Series No. 206. IAEA, Vienna, 405-410.

Grellier, S. 2011. Invasion ligneuse par l'*Acacia sieberiana* dans un pâturage raviné du KwaZulu-Natal (Afrique du Sud). Diplôme, Ecohydology, Academie de Paris. Universite Pierre et Marie Curie.

Hachmann, JW. 2011. Modelling water fluxes in savanna on granite hillslopes in the Kruger National Park, South Africa. Unpublished, MSc thesis, School of Bioresources Engineering and Environmental Hydrology, University of KwaZulu-Natal, South Africa.

Haitjema, H.M. 1995. Analytic Element Modeling of Groundwater Flow. *Academic Press*, San Diego, United States of America.

Harris, C, Burger, C, Miller, J and Rawoot, F. 2010. O-and H-Isotope record of Cape Town rainfall from 1996-2008, and its application to recharge studies of Table Mountain groundwater, South Africa. *South African Journal of Geology.*113(1):33-56.

Hopmans, J and Bristow, K. 2002. Current capabilities and future needs of root water and nutrient uptake modeling. *Advances in Argronomy*. 77(2002):104–175.

IAEA, 2004. International Atomic Energy Agency. Annual Report. GC (49)/5

Javaux, M, Schroder, T, Vanderborght, J and Vereecken, H. 2008. Use of a three-dimensional detailed modeling approach for predicting root water uptake. *Vadose Zone Journal*. 7(3):1079–1088.

Kebede, S, Travi, Y and Rozanski, K. 2009. The δ^{18} and δ^{2}H enrichment of Ethiopian Lakes. *Journal of Hydrology.* 365(3):173-182.

Kendall, C and McDonnell, J. 1998. *Isotope tracers in catchment hydrology*. Elsevier, Oxford. United Kingdom.

Kuenene, BT. 2013. Hillslope hydropedology of the Two Streams catchment in KwaZulu-Natal. Department of Soil, Crop and Climate Sciences, University of the Free State. South Africa.

Kulmatiski, A, Beard, K.H, Verweij, R.J and February, E.C. 2010. A depth-controlled tracer technique measures vertical, horizontal and temporal patterns of water use by trees and grasses in a subtropical savanna. *New Phytoloisgt*.188(1): 199-209

Lamb, L and Berthelot, M. 2002. Monitoring of water from the underground to the tree: first results with a new sap extractor on a riparian woodland. *Plant and Soil*. 241(2):197-207.

Ledieu, J, de Ridder, P, de Clerck, P and Dautrebande, S. 1986. A method of measuring soil moisture by time-domain reflectrometry. *Journal of Hydrology*. 88: 319-328.

LGR, 2010. Los Gatos Research: Liquid Water Isotope Analyser Manual. California, USA.

Lorentz, S, Bursey, K, Idowu, O. Pretorius, C, Ngeleka, K. 2008. Definition and upscaling of key hydrological processes for application in models. *Water Research Commission*. Pretoria, South Africa.

Lui, Z, Bowen, G and Welker, J. 2010. Atmospheric circulation is reflected in precipitation isotope gradients over the conterminous United States. *Journal of Geophysical Research.*115(D22): 1-14.

Mensforth, L, Thorburn, P, Tyerman, S, Walker, G. 1994. Sources of water used by riparian *Eucalyptus camaldulensis* overlying highly saline groundwater. *Oecologia*, 100(1-2):21–28.

Meyer, WS and Green, GC. 1980. Water use by wheat and plant indicators of available soil water. *Agronomy Journal*. 72(2):253-257.

Michener, R and Lajtha, K. 2007. *Stable Isotopes in Ecology and Environmental Science*. Blackwell Publishing. Oxford, United Kingdom

Mmolawa, K and Or, D. 2000. Root zone solute dynamics under drip irrigation: a review. *Plant and Soil*. 222(1-2):163-190.

Mook, W. 2001. Environmental Isotopes in the Hydrological Cycle: Principles and Applications. United Nations Educational, scientific and cultural organisation, Technical Document No. 39 Vol.iii. pp. 1-291.

Mucina, L and Rutherford, M.C. 2006. The Vegetation of South Africa, Lesotho and Swaziland. *Strelitzia 19*, South African National Biodiversity Institute, Pretoria, South Africa.

Mualem, Y. 1976. A new model for predicting the hydraulic conductivity of unsaturated porous media. *Water Resources Research*. 12(3):513-522.

National Water Act. 1998. RSA Government Gazette No. 36 of 1998: 26 August 1998, No. 19182. Cape Town, RSA.

Nier, A. 1950. A redetermination of the relative abundances of the isotopes of carbon, nitrogen, oxygen, argon and potassium. *Physical Review*. 77:789-793.

Pretorius, JJ. 2012. Isotope analysis report. School of Bioresources Engineering and Environmental Hydrology, University of KwaZulu-Natal. Pietermaritzburg, South Africa.

Priestley, CHB and Taylor, RJ. 1972. On the assessment of surface heat flux and evaporation using large scale parameters. *Monthly Weather Rev*. 100:81-92.

Rassam, D, Walker, G, Knight, J. 2004. Applicability of the Unit Response Equation to asses salinity impacts of irrigation development in the Mallee region. CSIRO Technical Report 35/04

Redfield, A and Friedman, I. 1965. Factors affecting the distribution of deuterium in the ocean. *Symposium on Marine Geochemistry.* University of Rhode Island, Occasional Publications. 3:149-168.

Revesz, K and Woods, P. 1990. A method to extract soil water for stable isotope analysis. *Journal of Hydrology*.115:397-406.

Rubio, C.M and Poyatos, R. 2012. Applicability of Hydrus-1D in a Mediterranean Mountain Area Submitted to Land Use Changes. *ISRN Soil Science*. 375842, 7.

Schlegel, P, Huwe, B and Teixeira, W.G. 2003. Modelling species and spacing effects on root zone water dynamics using Hydrus-2D in an Amazonian agroforestry system. *Agroforestry Systems*. 60:277-289

Savage, MJ. 2010. Soil-Plant-Atmosphere Research Unit, School of Environmental Sciences, University of KwaZulu-Natal, Pietermaritzburg, South Africa

Sato, T, Abdalla, O, Oweis, T and Tetsu, S. 2006. The validity of predawn leaf water potential as an irrigation-timing indicator for field-grow wheat in northern Syria. *Agricultural Water Management*. 82(1-2):223-236.

Schmidhalter, U. 1997. The gradient between pre-dawn rhizoplane and bulk soil matric potentials, and its relation to the predawn root and leaf water potentials of four species. *Plant Cell Environment*. 20:953-960.

Scholander, P, Hammel, H, Bradstreet, HE. 1965. Sap pressure in vascular plants. *Science*.148: (3668):339-345.

Schulze, R.E. 2009. Hydrological modelling: Concepts and Practice. School of Bioresources Engineering and Environmental Hydrology. University of KwaZulu-Natal, Pietermaritzburg, South Africa.

Scott, D, Prinsloo, F, Moses, G, Mehlomakulu, M, Simmers, A. 2000. A re-analysis of South African catchment afforestation experiment. Report No. 810/1/100. *Water Research Commission*, Pretoria, South Africa.

Šejna, M, J. Šimůnek, and van Genuchten, M. 2011. The HYDRUS software package for simulating two- and three dimensional movement of water, heat, and multiple solutes in variably saturated media. *PC Progress*, Prague, Czech Republic.

Singh, B and Kumar, B. 2005. Isotopes in Hydrology, Hydrogeology and Water Resources. *Narosa Publishing House*, Delhi, India.

Silva, M.S, Nachabe, M.H, Simunek, J and Carnahan, R. 2008. Simulating Root Water Uptake from a Heterogeneous Vegetation Cover. *Journal of Irrigation and Drainage Engineering*. 134(2):168-174

Šimůnek, J, van Genuchten, M and Sejna, M. 2011. HYDRUS: Model Use, Calibration and Validation. *American Society of Agricultural and Bilological Engineers*. 55(4):1261-1274.

Šimůnek, J and Sejna, M. 2011. Software Package for Simulating the Two-and Three-Dimensional Movement of Water, Heat and Multiple Solutes in Variably-Saturated Media. *PC-Progress* User Manual Version 2.

Šimůnek, J, Šejna, M, Saito, H Sakai, M and van Genuchten, M. 2012. The HYDRUS-1D software package for simulating the one-dimensional movement of water, heat, and multiple solutes in variably-saturated media, Department of Environmental Sciences, University of California Riverside, USA.

Šimůnek J, van Genuchten, M and Šejna, M. 2008. Development and applications of the HYDRUS and STANMOD software packages, and related codes, *Vadose Zone Journal*. 7(2):587-600.

Šimůnek J, Šejna M, Saito H, Sakai M, and Van Genuchten M. Th. 2009. The hydrus-1d software package for simulating the one-dimensional movement of water, heat, and multiple solutes in variably-saturated media. 4.08 ed

Šimůnek, J, and Hopmans, JW. 2009. Modeling compensated root water and nutrient uptake, *Ecological Modeling*. 220(4):505-521.

Smithers, J and Schulze, R. 1995. ACRU: Hydrological Modelling System user manual version 3rd edition. University of Natal, Pietermaritzburg, South Africa.

Stričević, R and Čaki, E. 1997. Relationships between available soil water and indicators of plant water status of sweet sorghum to be applied in irrigation scheduling. *Irrigation Science*.18(1): 17-21.

Sundaram, B, Feitz, A, de Caritat, P, Plazinska, A, Brodie, R, Coram, J and Ransley, T. 2009. Groundwater sampling and analysis - A field Guide. Record 2009/27. *Geoscience*, Canberra, Australia.

Thorburn, PJ, Walker, GR and Brunel, JP. 1993(a). Extraction of water from *Eucalyptus* trees for analysis of deuterium and oxygen-18: laboratory and field techniques. *Plant Cell Environment*. 16(3):269-277.

Thorburn, PJ, Hatton, TJ and Walker, GR .1993(b). Combining measurements of transpiration and stable isotopes of water to determine groundwater discharge from forests. *Journal of Hydrology.* 150(2-4):563-587.

Topp, G.C, Davis, J.L and Annan, A.P. 1982. Electromagnetic determination of soil water content: Measurements in coaxial transmission lines. *Water Resources Research*. 16(3):574-582.

Valancogne, C, Améglio, T, Ferreira, I, Cohen, M, Archer, P, Dayau, S, Daulet, FA. 1997. Relations between relative transpiration and predawn leaf water potential in different fruit trees species. In ed: Chartzoulakis KS. Proceedings of the 2nd International Symposium on Irrigation of Horticultural Crops. *Acta Horticulturae*. 449:423-430.

van Genuchten, MT. 1980. A closed-form equation for predicting the hydraulic conductivity of unsaturated soils. *Soil Science Society of America Journal*. 44 (5):892-898.

Verbist, K, Cornelis, W.M, Gabriels, D, Alaerts, K and Soto, G. 2009. Using an inverse modelling approach to evaluate the water retention in a simple water harvesting techique. *Journal of Hydrology and Earth Systems Sciences*. 13:1979-1992.

Wang, P, Song, X, Han, D, Zhang, Y, Liu, X. 2010. A study of root water uptake of crops indicated by hydrogen and oxygen stable isotopes: A case in Shanxi Province, China. *Agricultural Water Management*. 97(3):475-482.

Waswa, G.W, Clulow, A.D, Freese, C, Le Roux, P.AL, Lorenze, S.A. 2013. Transient pressure waves in the vadose zone and the rapid water table response. *Vadose Zone Journal.*Doi:10.213

Weaver, J and Talma, A. 2005. Cumulative rainfall collectors - A tool for assessing groundwater recharge. *Water SA.* 31(3):283-290.

West, A, Goldsmith, G, Matimati, I, Dawson, T. 2011. Spectral analysis software improves confidence in plant water stable isotope analysis performed by isotope ratio spectroscopy (IRIS). *Rapid Communications in Mass Spectrometry*. 25(16):2268-2274.

White, J.W.C, Cook, E.R, Lawrence ,J.R and. Broecker, W.S. 1985. The D/H ratios of sap in trees: implications for water sources and tree rings D/H ratios. Geochim. Cosmochim. Acta. 49:237-246.

Zimmermann, U, Ehhalt, D, Munnich, K. 1967. Soil water movement and evapotranspiration: changes in the isotope composition of the water. In: Proceedings of the IAEA Symposium on the Use of Isotopes in Hydrology, IAEA, Vienna, 567–584.

9. APPENDIX I

Rayleigh Equations can be used to describe an isotope fractionation process if: the material is removed from a mixed system that contains two or more of the same isotopic species, the fractionation process that is occurring simultaneously by the removal process is described by a fractionation factor α, α does not change during the process. Under these given conditions the evolution of the isotopic composition of the reactant material is described by:

$$(R / R_o) = (X_1 / X_{1o})^{\alpha-1} \quad (9.1)$$

Where: R is the ratio of the isotopes (e.g. $^{18}O/^{16}O$) in the reactant, R_o is the initial ratio, X_1 is the concentration of the more abundant lighter isotope (e.g. ^{16}O) and X_{1o} is the initial concentration (Kendall and McDonnel, 1998).

Table 9.1 Rainfall isotopes collected at Two Streams Research Catchment

Sample no	Sampling type	Name	Date (sampled)	Air T (°C)	Volume (mm)	Average δ2H	δ2H (permil)	δ2H std	δ18O (permil)	δ18O std
1	manual	bottle1	2012/02/29	n/a	n/a	n/a	8.120	1.323	-0.720	0.299
2	manual	bottle2	2012/02/29	n/a	n/a	n/a	8.715	1.223	-0.412	0.124
5	manual	bottle3	2012/02/29	n/a	n/a	n/a	6.685	0.942	-0.468	0.226
4	manual	bottle4	2012/02/29	n/a	n/a	n/a	5.826	1.478	-0.586	0.231
3	manual	bottle5	2012/02/29	n/a	n/a	n/a	9.119	1.212	-0.248	0.161
16	manual	Bottle 1	2012/03/07	n/a	n/a	n/a	-31.866	1.312	-4.793	0.273
14	manual	Bottle2	2012/03/07	n/a	n/a	n/a	-73.513	0.119	-9.076	0.144
13	manual	Bottle3	2012/03/07	n/a	n/a	n/a	-45.326	1.907	-6.489	0.083
9	manual	Bottle4	2012/03/07	n/a	n/a	n/a	-12.768	0.450	-3.346	0.165
23	manual	Bottle1	2012/03/16	n/a	n/a	n/a	-12.284	0.748	-2.877	0.081
26	manual	Bottle2	2012/03/16	n/a	n/a	n/a	-22.552	0.429	-4.001	0.064
22	manual	Bottle3	2012/03/16	n/a	n/a	n/a	-18.843	1.087	-3.290	0.068
16	manual	Bottle1	2012/03/23	n/a	n/a	n/a	9.340	0.703	0.191	0.075
23	manual	Collected during event	2012/03/29	n/a	n/a	n/a	20.925	2.591	0.502	0.280
25	manual	Bottle1	2012/03/29	n/a	n/a	n/a	13.711	1.611	0.221	0.148
27	manual	Bottle2	2012/03/29	n/a	n/a	n/a	10.921	0.736	-0.546	0.144
21	manual	Bottle1	2012/04/25	n/a	n/a	n/a	8.461	1.409	-0.856	0.260
29	manual	Bottle2	2012/04/25	n/a	n/a	n/a	3.601	0.714	-2.554	0.191
28	manual	Bottle3	2012/04/25	n/a	n/a	n/a	6.408	1.213	-2.361	0.149
30	manual	Bottle4	2012/04/25	n/a	n/a	n/a	6.690	0.610	-2.152	0.093

17	manual	Bottle1	2012/08/08	n/a	n/a	n/a	-144.636	0.860	-19.494	0.057
21	manual	Bottle2	2012/08/08	n/a	n/a	n/a	-141.616	2.720	-19.031	0.123
23	manual	Bottle3	2012/08/08	n/a	n/a	n/a	-113.404	1.588	-16.010	0.140
20	manual	Bottle4	2012/08/08	n/a	n/a	n/a	-73.010	0.794	-12.157	0.168
22	manual	Bottle5	2012/08/08	n/a	n/a	n/a	-23.063	1.139	-6.397	0.186
18	manual	Bottle6	2012/08/08	n/a	n/a	n/a	-15.959	2.420	-5.620	0.212
24	manual	Collected during event	2012/08/08	n/a	n/a	n/a	-87.877	1.453	-12.062	0.128
15	manual	Bottle1	2012/07/20	n/a	n/a	n/a	12.093	0.462	-0.930	0.223
6	manual	Bottle2	2012/07/20	n/a	n/a	n/a	9.538	1.005	-2.245	0.211
3	manual	Bottle3	2012/07/20	n/a	n/a	n/a	9.493	0.870	-1.887	0.064
26	manual	Bottle1	2012/10/08	n/a	n/a	n/a	5.590	1.390	-1.850	0.160
29	manual	Bottle2	2012/10/08	n/a	n/a	n/a	7.610	0.920	-1.570	0.020
27	manual	Bottle3	2012/10/08	n/a	n/a	n/a	-5.050	1.300	-3.190	0.150
30	manual	Bottle4	2012/10/08	n/a	n/a	n/a	-4.940	1.650	-3.140	0.240
9	manual	Bottle1	2012/11/01	n/a	n/a	n/a	-8.730	1.550	-3.200	0.120
10	manual	Bottle2	2012/11/01	n/a	n/a	n/a	-3.050	3.200	-2.510	0.130
3	auto	ALCO 2	n/a	n/a	n/a	n/a	0.157	0.791	-1.964	0.216
4	auto	ALCO 1	n/a	n/a	n/a	n/a	0.778	0.828	-2.036	0.120
5	auto	ALCO 1	n/a	n/a	n/a	n/a	-2.884	1.365	-3.259	0.155
22	auto	ALCO 1	2013/06/09 08:31	9.41	0.70	n/a	-27.667	1.227	-4.773	0.076
23	auto	ALCO 3	2013/06/09 11:39	7.77	5.20	n/a	6.241	1.507	-2.232	0.207
24	auto	ALCO4	2013/06/09 13:58	6.77	0.70	-4.555	7.760	1.727	-2.127	0.206
25	auto	ALCO5	2013/06/27 02:13	9.85	0.20	n/a	9.948	0.738	-1.798	0.192
26	auto	ALCO6	2013/06/27 04:28	9.35	0.30	6.017	2.087	0.545	-2.543	0.098
13	auto	ALCO 1	2013/05/17 00:00	13.53	1.00	8.09	8.088	0.716	-1.392	0.136
6	auto	ALCO 2	2013/05/11 06:20	8.21	11.80	n/a	-10.786	0.584	-4.440	0.083
7	auto	ALCO 3	2013/05/11 09:13	9.39	11.40	-17.291	-23.796	0.643	-5.885	0.036
21	auto	ALCO1	2013/06/27 09:11	9.86	0.10	n/a	1.182	0.954	-1.835	0.110
22	auto	ALCO2	2013/06/27 12:42	10.87	0.10	n/a	-4.240	0.666	-2.669	0.061
23	auto	ALCO3	2013/06/27 13:57	10.97	1.20	n/a	-1.583	0.520	-1.979	0.086
24	auto	ALCO4	2013/06/27 18:13	10.23	0.10	n/a	-5.345	1.093	-2.882	0.182
25	auto	ALCO 5	2013/06/27 18:54	9.86	0.10	n/a	-1.780	0.684	-2.815	0.041
26	auto	ALCO 6	2013/06/27 19:43	9.85	0.10	n/a	-4.892	0.511	-3.232	0.134
27	auto	ALCO7	2013/06/27 21:11	9.95	0.30	-3.070	-4.833	1.051	-3.247	0.120
28	auto	ALCO9	2013/06/28	4.84	0.10	-4.723	-4.723	0.540	-3.391	0.123

			06:14							
29	auto	ALCO10	2013/06/29 03:10	6.33	0.10	n/a	-4.147	0.670	-2.712	0.062
30	auto	ALCO11	2013/06/29 06:19	5.97	0.10	-2.438	-0.729	0.345	-1.549	0.130
16	auto	ALCO2	2013/07/01 19:45	11.78	0.20	-3.024	-3.024	0.846	-2.669	0.084
17	auto	ALCO8	2013/06/28 00:57	7.28	11.00	-21.808	-21.808	0.741	-5.524	0.040
7	auto	ALCO1	2013/07/04 00:55	9.86	0.10	n/a	-7.796	1.248	-2.988	0.036
8	auto	ALCO2	2013/07/04 10:04	10.01	0.70	n/a	-7.410	0.623	-3.265	0.174
9	auto	ALCO3	2013/07/04 10:40	10.57	0.10	n/a	-8.647	1.715	-3.229	0.063
10	auto	ALCO4	2013/07/04 11:46	10.69	0.10	n/a	-9.721	0.330	-3.289	0.122
22	auto	ALCO7	2013/07/04 17:07	11.01	0.30	-7.471	-3.780	1.240	-3.660	0.090
5	auto	ALCO16-20	2013/08/09 22:16	n/a	0.60	-17.589	-17.589	0.902	-4.768	0.164
6	auto	ALCO9	2013/08/08 22:53	9.09	7.10	4.833	4.833	0.583	-2.380	0.118
12	auto	ALCO10-11	2013/08/09 00:00	n/a	0.60	n/a	1.362	1.003	-3.479	0.270
7	auto	ALCO12	2013/08/09 04:58	9.04	3.80	n/a	-2.437	1.095	-3.313	0.078
2	auto	ALCO13	2013/08/09 07:20	7.92	8.90	n/a	-15.298	1.539	-4.523	0.072
23	auto	ALCO14	2013/08/09 09:15	6.34	1.90	n/a	-31.040	2.080	-6.810	0.210
10	auto	ALCO15	2013/08/09 10:50	6.81	1.00	-11.980	-29.301	0.608	-5.657	0.089
30	auto	ALCO2-6	n/a	n/a	2.80	n/a	3.457	1.005	-2.790	0.097
17	auto	ALCO1	2013/08/30 21:36	10.42	2.00	-5.9	-5.900	0.900	-2.660	0.120
20	auto	ALCO15	2013/09/11 09:00	n/a	0.20	8.64	8.640	1.940	-1.240	0.150
23	auto	ALCO6	2013/08/31 03:08	4.76	0.30	-18.56	-18.560	1.040	-4.230	0.280
25	auto	ALCO12	2013/09/09 16:46	8.98	0.60	n/a	10.790	1.640	-1.050	0.130
28	auto	ALCO13	2013/09/09 21:24	8.94	1.50	10.92	11.050	1.320	-1.610	0.270
7	auto	ALCO	n/a	n/a	n/a	n/a	-20.462	0.591	-5.719	0.080
10	auto	ALCO20	2013/07/11 01:04	n/a	0.10	n/a	10.544	1.903	-1.045	0.072
12	auto	ALCO 19	2013/07/10 13:02	n/a	0.30	n/a	13.474	1.877	-0.915	0.286
16	auto	ALCO7	2013/08/08 20:23	n/a	2.40	n/a	3.601	1.700	-2.666	0.253
18	auto	ALCO12-20	n/a	n/a	n/a	n/a	-15.766	0.400	-4.515	0.187
24	auto	ALCO1	2013/09/11 23:27	n/a	5.50	n/a	-0.784	0.561	-3.268	0.202
27	auto	ALCO6	2013/09/12 21:37	n/a	n/a	n/a	9.433	1.177	-0.998	0.146

23	auto	ALCO	n/a	n/a	n/a	n/a	-2.068	1.496	-3.526	0.194
25	auto	ALCO6	n/a	n/a	n/a	n/a	10.663	1.231	-1.219	0.132

Table 9.2 Groundwater isotopes collected at Two Streams Research Catchment

Sample no	Position	Date	δ2H (permil)	δ2H std	δ18O (permil)	δ18O std	Date analysed
6	Centre	2012/02/29	-5.739	1.556	-1.899	0.279	2012/02/12
7	North	2012/02/29	-5.745	0.878	-2.290	0.239	2012/02/13
10	Centre	2012/03/07	-4.700	1.441	-2.041	0.250	2012/03/07
12	North	2012/03/07	-5.478	1.694	-2.421	0.263	2012/03/08
19	North	2012/03/12	-7.853	1.145	-2.025	0.042	2012/03/23
20	Centre	2012/03/12	-7.485	0.486	-2.378	0.057	2012/03/29
25	Centre	2012/03/16	-8.943	0.466	-2.092	0.027	2012/03/16
27	North	2012/03/16	-7.737	0.571	-2.531	0.102	2012/03/16
17	North	2012/03/23	-7.782	0.917	-2.449	0.131	2012/03/23
18	Centre	2012/03/23	-7.785	0.186	-2.338	0.193	2012/03/23
22	North	2012/04/25	-6.839	0.967	-2.487	0.214	2012/04/25
25	Centre	2012/04/25	-8.774	0.901	-2.630	0.222	2012/04/25
2	Centre	2012/07/20	-11.415	0.495	-3.785	0.091	2012/07/20
4	North	2012/07/20	-10.452	0.701	-3.279	0.186	2012/07/20
19	North	2012/08/08	-11.950	0.433	-4.068	0.121	2012/08/08
n/a	Centre	2012/08/08	-31.970	1.100	-5.430	0.120	2012/08/08
1	North	2012/08/16	-10.861	1.462	-3.563	0.134	2012/08/16
3	Centre	2012/08/16	-12.461	1.055	-3.720	0.088	2012/08/16
2	North	2012/08/30	-11.653	1.308	-3.401	0.240	2012/08/30
3	Centre	2012/08/30	-10.965	0.148	-3.651	0.088	2012/08/30
1	Centre	2013/03/06	-9.976	1.498	-3.119	0.227	11-09-2013
6	Centre	2013/03/27	-8.517	1.462	-3.009	0.194	30-01-2014
2	Centre	2013/04/11	-9.035	0.318	-2.634	0.137	18-06-2013
15	Centre	2013/04/30	-9.602	1.163	-2.655	0.131	18-06-2013
2	Centre	2013/04/30	-7.447	0.927	-3.100	0.125	30-01-2014
8	Centre	2013/05/15	-10.167	1.333	-3.261	0.198	25-06-2013
4	Centre	2013/05/15	-6.840	0.538	-3.210	0.179	30-01-2014
14	Centre	2013/05/29	-8.376	1.692	-2.871	0.046	25-06-2013
23	Centre	2013/06/06	-9.933	1.396	-3.088	0.137	25-06-2013
29	Centre	2013/06/27	-10.356	1.363	-2.970	0.195	04-07-2013
20	Centre	2013/07/17	-8.436	0.852	-2.949	0.116	18-07-2013
11	Centre	2013/07/17	-11.396	1.505	-3.578	0.103	30-01-2014
17	Centre	2013/08/23	-10.003	1.682	-2.948	0.168	30-01-2014
25	Centre	2013/09/11	-9.856	1.935	-2.844	0.168	30-01-2014
n/a	Centre	2013/09/11	-10.633	0.953	-2.810	0.062	30-01-2014
n/a	Centre	2013/11/21	-11.850	0.311	-3.209	0.131	n/a
n/a	Centre	2013/12/04	-12.193	1.044	-3.053	0.073	n/a

Table 9.3 Stream samples collect at Two Streams Research Catchment

Sample no	Date sampled	Volume (m^3)	δ2H (permil)	δ2H std	δ18O (permil)	δ18O std	Date analysed
1	2013/04/04 00:00	n/a	-7.128	1.070	-2.325	0.145	18-06-2013
2	2013/04/11 15:32	0.0460	-2.127	0.675	-2.434	0.041	18-06-2013
3	2013/04/15 12:00	0.0432	-7.472	0.727	-2.628	0.158	18-06-2013
4	2013/04/18 06:52	0.0382	-7.542	0.311	-2.560	0.073	18-06-2013
5	2013/04/18 12:00	0.0378	-7.555	0.622	-2.449	0.145	18-06-2013
6	2013/04/19 22:33	0.0429	-8.301	0.303	-2.577	0.067	18-06-2013
7	2013/04/20 11:51	0.0480	-7.398	1.498	-2.581	0.111	18-06-2013
8	2013/04/20 18:05	0.0530	-8.604	0.417	-2.850	0.044	18-06-2013
9	2013/04/21 20:42	0.0476	-8.254	0.480	-2.716	0.126	18-06-2013
10	2013/04/22 12:00	0.0468	-8.121	0.548	-2.689	0.046	18-06-2013
11	2013/04/29 12:00	0.0515	-6.404	0.404	-2.407	0.140	18-06-2013
12	2013/05/02 12:00	0.0480	-7.151	0.819	-2.964	0.162	18-06-2013
13	2013/05/06 12:00	0.0453	-7.050	0.556	-2.990	0.149	18-06-2013
14	2013/05/11 04:51	0.0495	-5.822	1.356	-2.588	0.230	18-06-2013
15	2013/05/11 07:56	0.0547	-6.863	1.167	-3.096	0.143	18-06-2013
16	2013/05/11 08:27	0.0599	-7.623	0.767	-2.842	0.108	18-06-2013
17	2013/05/11 09:01	0.0650	-8.353	1.328	-3.296	0.115	18-06-2013
18	2013/05/11 09:03	0.0701	-6.666	0.564	-3.498	0.240	18-06-2013
19	2013/05/11 09:05	0.0752	-8.416	0.517	-3.607	0.100	18-06-2013
20	2013/05/11 09:07	0.0807	-8.814	1.562	-3.519	0.062	18-06-2013
21	2013/05/11 09:10	0.0857	-3.382	0.551	-3.152	0.285	18-06-2013
22	2013/05/11 09:13	0.0907	-0.398	1.662	-3.126	0.096	18-06-2013

23	2013/05/11 09:39	0.0857	-0.855	1.989	-2.976	0.271	18-06-2013
24	2013/05/11 09:48	0.0804	-4.944	1.756	-3.673	0.243	18-06-2013
25	2013/05/11 10:24	0.0651	-9.418	0.727	-3.293	0.098	25-06-2013
26	2013/05/11 10:47	0.0600	-9.132	1.031	-3.023	0.100	25-06-2013
27	2013/05/11 12:13	0.0550	-8.971	0.744	-2.996	0.095	25-06-2013
28	2013/05/13 12:00	0.0529	-8.618	0.742	-3.082	0.171	25-06-2013
29	2013/05/16 12:00	0.0489	-8.237	0.735	-3.211	0.073	25-06-2013
30	2013/05/20 12:00	0.0461	-6.994	1.001	-2.818	0.067	25-06-2013
31	2013/05/23 12:00	0.0443	-6.901	0.948	-2.654	0.111	25-06-2013
32	2013/05/27 12:00	0.0432	-6.024	1.142	-2.743	0.126	25-06-2013
33	2013/05/30 12:00	0.0503	-8.278	0.570	-2.768	0.160	18-07-2013
34	2013/06/02 00:00	0.5063	-9.720	1.480	-3.110	0.130	28-08-2013
35	2013/06/02 00:00	0.5063	-8.620	1.140	-3.000	0.200	28-08-2013
36	2013/06/02 00:00	0.5063	-7.320	1.870	-3.070	0.090	28-08-2013
37	2013/06/02 00:00	0.5063	-9.080	1.020	-2.900	0.110	28-08-2013
38	2013/06/02 00:00	0.5063	-4.770	0.950	-2.390	0.100	28-08-2013
39	2013/06/02 00:00	0.5063	-12.270	1.050	-3.280	0.130	28-08-2013
40	2013/06/02 00:00	0.5063	-9.930	1.290	-3.540	0.220	28-08-2013
41	2013/06/02 00:00	0.5063	-7.480	0.560	-2.980	0.100	28-08-2013
42	2013/06/02 00:00	0.5063	-10.702	1.878	-4.155	0.242	18-07-2013
43	2013/06/02 00:00	0.5063	-14.927	0.687	-3.927	0.034	18-07-2013
44	2013/06/02 00:00	0.5063	-16.161	0.315	-3.968	0.063	18-07-2013
45	2013/06/02 00:00	0.5063	-15.635	1.092	-4.216	0.073	18-07-2013
46	2013/06/06 12:00	0.0470	-7.110	0.791	-2.835	0.091	25-06-2013
47	2013/06/02 00:00	0.5041	-8.012	1.205	-2.564	0.042	25-06-2013
48	2013/06/02 00:00	0.5041	-7.468	0.734	-2.804	0.161	25-06-

							2013
49	2013/06/02 00:00	0.5041	-7.622	1.699	-2.860	0.219	25-06-2013
50	2013/06/02 00:00	0.5041	-7.250	1.653	-2.997	0.167	25-06-2013
51	2013/06/02 00:00	0.5041	-7.255	0.760	-3.080	0.095	25-06-2013
52	2013/06/02 00:00	0.5041	-7.799	1.728	-3.295	0.241	25-06-2013
53	2013/06/02 00:00	0.5041	-7.217	1.390	-3.063	0.149	25-06-2013
54	2013/06/06 12:00	0.0470	-7.103	1.265	-3.008	0.158	04-07-2013
55	2013/06/09 09:53	0.0520	-6.452	0.412	-3.006	0.191	04-07-2013
56	2013/06/09 12:36	0.0469	-7.019	0.709	-2.955	0.064	04-07-2013
57	2013/06/10 12:00	0.0475	-6.612	0.964	-2.960	0.097	04-07-2013
58	2013/06/13 12:00	0.0462	-6.119	0.765	-3.068	0.121	04-07-2013
59	2013/06/17 12:00	0.0420	-7.313	0.640	-3.109	0.128	04-07-2013
60	2013/06/20 12:00	0.0417	-7.522	0.829	-2.895	0.171	04-07-2013
61	2013/06/22 18:06	0.4994	-6.954	1.380	-3.095	0.269	04-07-2013
62	2013/06/22 18:06	0.0423	-5.987	1.598	-2.931	0.199	04-07-2013
63	2013/06/24 12:00	0.0401	0.150	1.120	-1.493	0.202	04-07-2013
64	2013/06/27 12:00	0.0399	-7.395	1.740	-2.881	0.181	04-07-2013
65	2013/06/27 00:00	0.5495	-8.421	1.740	-2.779	0.166	04-07-2013
66	2013/06/27 00:00	0.5495	-8.551	0.973	-2.827	0.158	04-07-2013
67	2013/06/28 00:00	0.5037	-7.852	0.361	-3.155	0.177	18-07-2013
68	2013/07/01 00:00	0.5037	-7.746	0.935	-2.805	0.066	18-07-2013
69	2013/07/04 00:00	0.4963	-7.975	0.862	-2.848	0.081	18-07-2013
70	2013/07/15 00:00	n/a	-7.975	0.862	-2.848	0.081	
71	2013/08/01 12:00	0.0379	-9.110	0.750	-3.390	0.160	28-08-2013
72	2013/08/05 12:00	0.0346	-16.850	1.310	-4.060	0.090	28-08-2013
73	2013/08/08 12:00	0.0348	-7.808	1.176	-2.667	0.110	11-09-2013

74	2013/08/08 21:32	0.0399	-7.500	1.450	-3.440	0.100	28-08-2014
75	2013/08/09 03:14	0.0349	-6.998	1.230	-2.683	0.119	11-09-2013
76	2013/08/09 04:05	0.0399	-8.910	1.240	-3.580	0.120	28-08-2013
77	2013/08/09 06:03	0.0450	-9.401	0.783	-3.350	0.128	11-09-2013
78	2013/08/09 07:44	0.0399	-15.490	1.020	-4.290	0.110	28-08-2013
79	2013/08/12 12:00	0.0423	-7.275	1.772	-2.749	0.112	11-09-2013
80	2013/08/15 12:00	0.0400	-16.460	1.450	-3.950	0.110	28-08-2013
81	2013/08/19 12:00	0.0374	-8.435	1.105	-2.924	0.155	11-09-2013
82	2013/08/22 12:00	0.0357	-7.010	0.750	-3.230	0.080	28-08-2013
83	2013/08/26 12:00	0.0342	-5.920	1.130	-2.920	0.160	26-09-2013
84	2013/08/29 12:00	0.0313	-7.750	1.510	-3.090	0.080	26-09-2013
85	2013/09/02 12:00	0.0314	-9.460	0.990	-2.930	0.180	26-09-2013
86	2013/09/05 12:00	0.0308	-5.730	0.750	-2.660	0.060	26-09-2013
87	2013/09/09 12:00	0.0315	-8.130	1.470	-3.040	0.250	26-09-2013
88	2013/09/16 10:59	0.4856	-12.200	1.000	-3.000	0.100	26-09-2013
89	2013/12/04 00:00	n/a	-6.879	1.388	-2.968	0.122	
90	2013/12/12 12:00	0.0463	-9.037	1.738	-2.964	0.130	05-02-2014
91	2013/12/13 17:42	0.0564	-7.058	1.137	-2.738	0.080	05-02-2014
92	2013/12/13 17:47	0.0667	-6.612	0.760	-2.677	0.082	05-02-2014
93	2013/12/13 18:21	0.0567	-10.848	0.322	-3.074	0.174	05-02-2014
94	2013/12/13 19:17	0.0669	-10.851	1.479	-3.371	0.224	05-02-2014
95	2013/12/13 19:19	0.0779	-10.537	0.726	-3.240	0.058	05-02-2014
96	2013/12/13 19:21	0.0881	-9.705	0.387	-3.020	0.042	05-02-2014
97	2013/12/13 19:23	0.0983	-9.986	0.812	-3.203	0.153	05-02-2014
98	2013/12/13 19:50	0.0881	-9.977	0.555	-2.891	0.093	05-02-2014
99	2013/12/13 20:01	0.0780	-10.428	0.641	-3.381	0.099	05-02-2014

100	2013/12/13 20:13	0.0679	-9.794	0.813	-3.287	0.220	05-02-2014
101	2013/12/13 20:34	0.0579	-9.933	1.235	-3.449	0.132	05-02-2014
102	2013/12/16 12:00	0.0530	-9.584	0.817	-3.310	0.075	05-02-2014
103	2013/12/19 12:00	0.0569	-8.077	0.418	-3.209	0.112	05-02-2014
104	2013/12/23 12:00	0.0501	-7.663	1.326	-2.976	0.185	31-01-2014
105	2013/12/26 12:00	0.0478	-6.088	0.518	-3.053	0.107	31-01-2014
106	2013/12/26 13:29	0.0582	-8.379	1.511	-3.398	0.232	31-01-2014
107	n/a	n/a	-7.712	1.643	-3.242	0.086	31-01-2014
108	2013/12/30 12:00	0.0486	-7.320	0.270	-3.304	0.080	31-01-2014
109	2014/01/02 12:00	0.0454	-9.058	1.641	-2.788	0.178	31-01-2014
110	2014/01/02 12:00	0.0454	-6.557	1.948	-3.149	0.296	31-01-2014
111	2014/01/06 12:00	0.0419	-7.119	0.753	-2.877	0.097	31-01-2014
112	2014/01/09 12:00	0.0394	-7.302	1.622	-2.708	0.170	31-01-2014
113	2014/01/09 18:30	0.0498	-5.725	1.800	-2.588	0.249	31-01-2014
114	2014/01/09 18:33	0.0603	-8.388	0.367	-2.897	0.061	31-01-2014
115	2014/01/09 18:36	0.0703	-8.115	1.109	-3.102	0.066	31-01-2014
116	2014/01/09 18:39	0.0804	-9.459	1.616	-2.863	0.204	31-01-2014
117	2014/01/09 18:41	0.0905	-8.416	2.490	-3.138	0.226	31-01-2014
118	2014/01/09 18:59	0.0804	-9.811	0.808	-2.801	0.069	31-01-2014
119	2014/01/09 19:06	0.0703	-12.570	1.650	-3.249	0.149	31-01-2014
120	2014/01/09 19:19	0.0602	-10.578	1.606	-3.226	0.186	31-01-2014
121	2014/01/09 19:35	0.0800	-9.029	1.949	-2.694	0.227	31-01-2014
122	2014/01/09 19:35	0.0928	-8.943	1.630	-2.690	0.263	31-01-2014
123	2014/01/09 19:35	0.1076	-8.994	1.646	-3.071	0.123	31-01-2014
124	2014/01/09 19:35	0.1232	-8.289	1.018	-2.576	0.156	31-01-2014
125	n/a	n/a	-8.463	1.400	-2.669	0.265	31-01-

							2014
126	2014/01/09 19:36	0.1550	-9.317	0.609	-2.933	0.199	31-01-2014
127	n/a	n/a	-11.524	1.078	-3.324	0.147	31-01-2014
128	2014/01/09 19:36	0.1702	-10.597	0.613	-3.423	0.153	31-01-2014

Table 9.4 Isotopes extracted from soil samples at Two Streams Research Catchment

Sample No	Soil Depth (m)	Date	δ2H (permil)	δ2H std	δ18O (permil)	δ18O std	Date analysed
1	2.8	2013/07/17	-25.287	0.748	-0.326	0.083	14-08-2013
2	3.6	2013/07/17	-15.940	0.660	0.650	0.140	28-08-2013
3	2.4	2013/07/17	-15.913	0.982	1.027	0.096	11-09-2013
4	1.6	2013/07/13	-9.733	0.797	-0.396	0.121	n/a
5	4	2013/08/23	-21.095	1.181	-0.401	0.261	11-09-2013
6	6	2013/08/23	-20.487	1.399	-1.539	0.131	11-09-2013
7	5	2013/08/23	-7.488	0.240	9.551	0.205	11-09-2013
8	3	2013/08/23	-15.271	0.820	-0.686	0.111	11-09-2013
9	2.8	2013/08/23	-9.065	1.184	-1.193	0.238	29-10-2013
10	2	2013/08/23	-9.501	1.324	-0.895	0.187	29-10-2013
11	9	2013/11/21	-18.449	1.841	-1.630	0.165	n/a
12	8	2013/11/21	-14.988	1.783	2.929	0.142	30-01-2014
13	7	2013/11/21	-25.206	2.080	2.678	0.114	30-01-2014
14	6	2013/11/21	-15.050	0.604	-0.607	0.297	n/a
15	4.8	2013/11/21	-12.818	1.118	-0.384	0.064	30-01-2014
16	2.8	2013/11/21	-14.756	1.415	0.515	0.180	22-04-2014
17	1.6	2013/11/21	-9.742	1.180	3.944	0.151	22-04-2014
18	2.4	2013/11/21	-14.815	1.150	1.182	0.184	22-04-2014
19	3.2	2013/11/21	-17.274	1.755	1.759	0.233	22-04-2014
20	8	2013/11/09	-15.425	2.096	4.110	0.206	29-10-2013
21	7	2013/11/09	-19.937	1.273	4.015	0.276	29-10-2013
22	6	2013/11/09	-24.790	1.290	1.270	0.280	26-09-2013
23	4.4	2013/11/09	-24.920	1.690	1.450	0.150	26-09-2013
24	4.8	2013/11/09	-20.654	1.317	0.711	0.212	30-01-2014
25	3.2	2013/11/09	-14.583	1.645	-1.660	0.108	30-01-2014
26	3.6	2013/11/09	-14.384	1.565	-0.183	0.077	22-04-2014
27	1.6	2013/11/09	-8.783	1.172	2.036	0.183	22-04-2014
28	1.6	2013/11/09	-7.754	1.640	2.154	0.198	22-04-2014
29	5.2	2013/11/09	-10.633	1.892	2.167	0.051	22-04-2014
30	5.2	2013/11/09	-10.040	1.521	1.959	0.077	22-04-2014

10. APPENDIX II

10.1 Hydraulic input parameters

Stationary Boundary Flux conditions for Two Streams Research Catchment: South Facing Slope, Oakleaf (Orthic A-400mm, Neocutanic B-2000mm) (Kuenene *et al*., 2013)

Table 10.1 van Genuchten parameters (Kuenene *et al*., 2013)

Material	Qr	Qs	Alpha (1/cm)	n (-)	Ks (cm/hour)	l(-)	Depth (cm)
1	0.173	0.599	0.027	1.491	21.0637	0.5	100
2	0.181	0.028	0.028	1.921	37.3884	0.5	2000
3	0.181	0.028	0.028	1.921	37.3884	0.5	5000

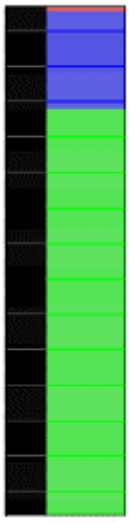

Figure 10.1 van Genuchten parameters for the soil column that were used in HYDRUS (Kuenene *et al*., 2013)

The Feddes' root water uptake model was selected for the HYDRUS simulations. Due to the limited information on *Acacia mearnsii* the parameters were estimated.

Table 10.2 Feddes' parameters

PO(cm)	0
Popt(cm)	-25
P2H(cm)	-10000
P2L(cm)	-10000
P3(cm)	-20000
r2H(cm/hour)	0.020833
r2L(cm/hour)	0.004167

Where PO is the pressure head below which roots start to extract water from the soil, Popt is the pressure head below which roots extract water at the maximum possible rate, P2H is the limiting pressure head below which roots cannot extract water at the maximum rate (assuming a potential transpiration rate of *r2H*), P2L is the same as P2H but for a potential transpiration rate of *r2L*, P3 is the pressure head below which root water uptake ceases (wilting point), r2H is potential transpiration rate [LT^{-1}] (currently set at 0.5 cm/day) and r2L is potential transpiration rate [LT^{-1}] (currently set at 0.1 cm/day) (Simunek and Sejna, 2011)

Table 10.3 Rooting masses with soil depth

Depth (m)	Rooting
0.1	0.825682
3	0.054526
3.8	0.091031
4.6	0.017843

Figure 10.2 Root water uptake model used for the soil column in HYDRUS

10.2 Comparison between WAVE, ACRU and HYDRUS

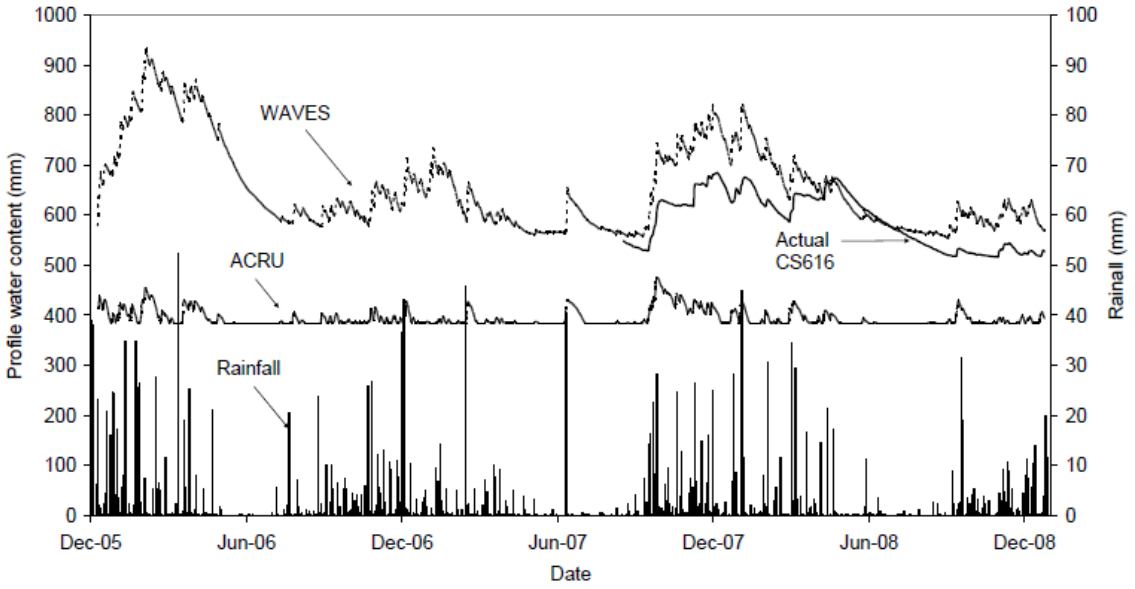

Figure 10.3 Comparison between soil water profile results obtained from WAVE, ACRU and measured CS616 probes installed at Two Streams Research Catchment

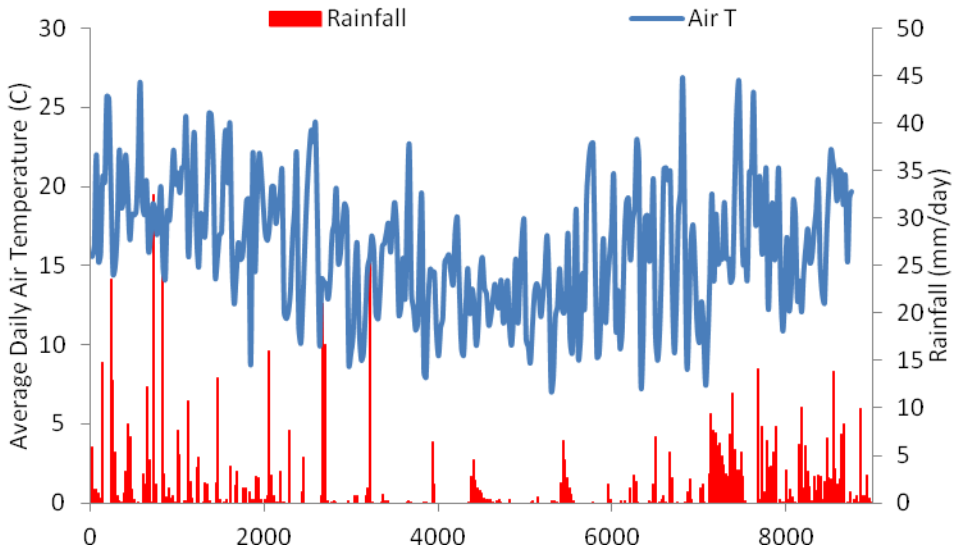

Figure 10.4 Averaged Daily Air Temperature with rainfall over the simulation period

11. APPENDIX III

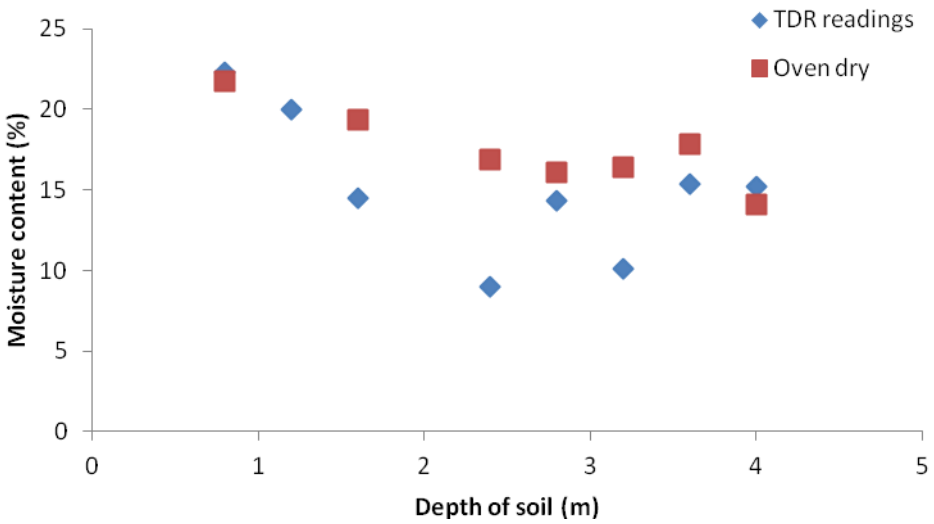

Figure 11.1 Comparison between TDR readings and oven dry mass